Bacterial Oxidases of the Cytochrome *bd* Family: Redox Enzymes of Unique Structure, Function, and Utility As Drug Targets

Vitaliy B. Borisov,[1] Sergey A. Siletsky,[1] Alessandro Paiardini,[2] David Hoogewijs,[3] Elena Forte,[2] Alessandro Giuffrè,[4] and Robert K. Poole[5]

Abstract

Significance: Cytochrome *bd* is a ubiquinol:oxygen oxidoreductase of many prokaryotic respiratory chains with a unique structure and functional characteristics. Its primary role is to couple the reduction of molecular oxygen, even at submicromolar concentrations, to water with the generation of a proton motive force used for adenosine triphosphate production. Cytochrome *bd* is found in many bacterial pathogens and, surprisingly, in bacteria formally denoted as anaerobes. It endows bacteria with resistance to various stressors and is a potential drug target.
Recent Advances: We summarize recent advances in the biochemistry, structure, and physiological functions of cytochrome *bd* in the light of exciting new three-dimensional structures of the oxidase. The newly discovered roles of cytochrome *bd* in contributing to bacterial protection against hydrogen peroxide, nitric oxide, peroxynitrite, and hydrogen sulfide are assessed.
Critical Issues: Fundamental questions remain regarding the precise delineation of electron flow within this multihaem oxidase and how the extraordinarily high affinity for oxygen is accomplished, while endowing bacteria with resistance to other small ligands.
Future Directions: It is clear that cytochrome *bd* is unique in its ability to confer resistance to toxic small molecules, a property that is significant for understanding the propensity of pathogens to possess this oxidase. Since cytochrome *bd* is a uniquely bacterial enzyme, future research should focus on harnessing fundamental knowledge of its structure and function to the development of novel and effective antibacterial agents. *Antioxid. Redox Signal.* 00, 000–000.

Keywords: respiratory chain, terminal oxidase, cytochrome *bd*, bacterial cytochromes

Table of Contents

[1]Belozersky Institute of Physico-Chemical Biology, Lomonosov Moscow State University, Moscow, Russian Federation.
[2]Department of Biochemical Sciences, Sapienza University of Rome, Rome, Italy.
[3]Department of Medicine/Physiology, University of Fribourg, Fribourg, Switzerland.
[4]CNR Institute of Molecular Biology and Pathology, Rome, Italy.
[5]Department of Molecular Biology and Biotechnology, The University of Sheffield, Sheffield, United Kingdom.

I. Introduction

CYTOCHROME *BD*, FIRST described in 1928 [(345), see also Cook and Poole (75) and references therein], is a respiratory terminal oxidase thus far uniquely identified in the electron transport chain of prokaryotic organisms (36, 48, 151, 163, 252). As it promotes virulence in a number of pathogenic bacteria, it is currently recognized as a prospective drug target for the development of new antibacterial drugs.

Phylogenetically unrelated to the more extensively investigated haem/copper oxidases, such as mitochondrial cytochrome aa_3 (53, 58, 59, 243, 274, 301, 336), cytochrome *bd* catalyzes the reduction of O_2 to H_2O with remarkably high affinity, using quinols as physiological reducing substrates (55, 163). The reaction, although not associated with a proton pumping activity (267), is electrogenic (19, 20, 38, 51, 155, 267) and thus contributes to generating a proton motive force (PMF) and sustaining bacterial energy conservation.

Cytochrome *bd* displays distinct biochemical features with respect to haem/copper oxidases, including a *d*-type O_2-reactive haem and no copper atoms, which, on the contrary, are invariantly present in haem/copper oxidases (see Fig. 1 for haem types). The three-dimensional structure of cytochrome *bd* has remained a mystery for a long time, but it was recently solved for two members of this protein family, the enzymes from *Geobacillus thermodenitrificans* (281) and, more recently, from *Escherichia coli* (280, 317), re-

vealing unexpected structural differences between the two proteins, most likely of evolutionary significance.

A large body of evidence suggests that cytochrome *bd* enables bacterial O_2 consumption, either for bioenergetic purposes, to drive specific metabolic pathways and/or to afford protection from O_2 toxicity and a variety of stress conditions, including hypoxia, medium alkalinization, high temperature, and exposure to toxic compounds, such as uncouplers, antibiotics, or classical respiratory inhibitors, for example, nitric oxide (NO), cyanide, and hydrogen sulfide (H_2S) [see Borisov *et al.* (46), Borisov *et al.* (48), Forte *et al.* (115), Giuffre *et al.* (124), Giuffre *et al.* (125), Korshunov *et al.* (192), Poole and Cook (252) and references therein].

Furthermore, cytochrome *bd* was shown to facilitate degradation of harmful reactive oxygen and nitrogen species (ROS and RNS), such as hydrogen peroxide (H_2O_2) or peroxynitrite ($ONOO^-$) [reviewed in Forte *et al.* (117)], produced by the host immune system to control microbial infections.

The growing attention that is being paid by the scientific community toward *bd*-type bacterial terminal oxidases as potential drug targets prompted us to present here a comprehensive update on the information currently available about these enzymes and their impact on bacterial physiology.

A prelude on nomenclature is in order. The accepted name for the subject of this review is "quinol oxidase (electrogenic, proton-motive force generating), EC 7.1.1.7", product of the *cydAB* (and other) genes." It is generally called cytochrome
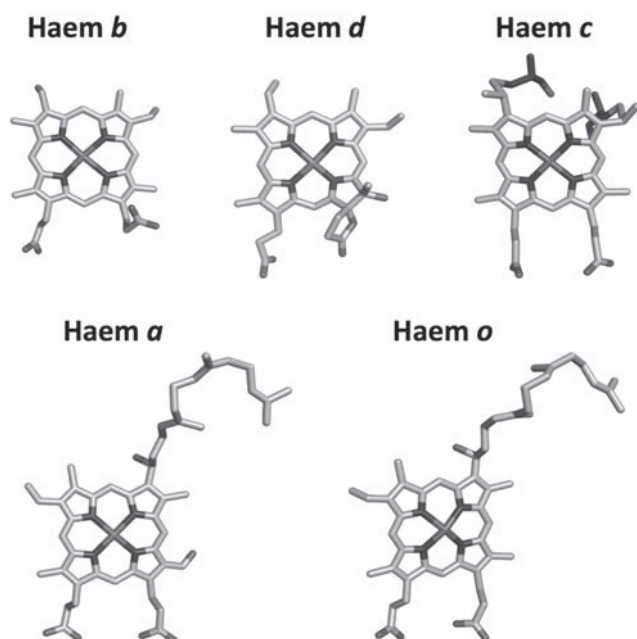
FIG. 1. Haem types in respiratory oxidases. Haem *b* (haem b_{595} of *Geobacillus thermodenitrificans* cytochrome *bd*, PDB entry 5DOQ); haem *d* (from *G. thermodenitrificans* cytochrome *bd*, PDB entry 5DOQ); haem *c* (from mitochondrial cytochrome *c* in complex with bovine cytochrome *c* oxidase, PDB entry 5IY5); haem *a* (haem a_3 of bovine cytochrome *c* oxidase, PDB entry 5B1A); haem *o* (from *Escherichia coli* cytochrome bo_3, PDB entry 1FFT). PDB, Protein Data Bank. Reprinted by permission from Forte *et al.* (117).

bd and, less logically, "cytochrome *bd* oxidase." The latter is unfortunate because the complex does not oxidize cytochrome *bd* but *is* cytochrome *bd*! However, there have been more uncertainty and debate on the correct nomenclature of the other major oxidase in *E. coli* and many other bacteria, to which we refer, namely cytochrome bo_3, *bo* oxidase, or *bo'*. The last name was proposed (251) because some years ago the IUB Enzyme Nomenclature "rules" proposed that ligand-binding haems should be designated with the suffix '. Hence *aa'* (for cytochrome aa_3) and *bo'* appeared correct.

The term cytochrome bo_3, emphasising the correlation with aa_3 did not, and still does not, appear logical, because there is, and never was, a bo_1 or bo_2, whereas the names a_1 and a_2 were both once common currency (for cytochromes b_{595} and *d*, respectively). However, bo_3 has been so widely adopted to describe EC 7.1.1.3 ubiquinol oxidase (H^+-transporting), product of *cyoABCD* in *E. coli* (219), that we have adopted it here.

II. Distribution, Evolution, and Regulation of Gene Expression

A. Distribution

Cytochrome *bd* is a membrane-integrated complex comprising two to four subunits (see later, sections II.B and II.C). The two largest and omnipresent subunits are subunits I and II, which are encoded by the chromosomal *cydA* and *cydB* genes. In *E. coli*, two different cytochrome *bd*-type oxidases have been described, the best studied cytochrome *bd*-I

and the more recently discovered cytochrome *bd*-II (93). Whereas *bd*-I is encoded by the *cydAB* operon, *bd*-II is encoded by the *cyxAB* operon (55). The *bd*-family of oxygen reductases has a very broad taxonomic distribution with orthologs found in various bacterial phyla. These include diverse groups of Eubacteria, from gram-positive Firmicutes and Actinomycetes to the whole phylum of Proteobacteria.

A number of Archaea also encode *bd*-family homologues, with members of the family found in Crenarchaeota (*Thermoproeus tenax*, *Pyrobaculum neutrophilum*, *Vulcanisaeta moutnovskia*), Euryarchaeota (*Methanosarcina barkeri*, *Archaeoglobus sulfaticallidus*) (57), and Korarchaeota (*Korarchaeum cryptofilum*) (96). Cytochrome *bd*-type oxygen reductases are very common in some phyla, such as the Proteobacteria and Actinobacteria, and sporadically distributed in others. Intriguingly, homologues of cytochrome *bd* have been detected in many species described as strict anaerobes such as *Methanosarcina barkeri*, *Methanosarcina acetivorans* (57), *Bacteroides fragilis* (13), *Desulfovibrio gigas* (202), *Desulfovibrio vulgaris* Hildenborough (288), *Geobacter metallireducens* (141), *Moorella thermoacetica* (92), and *Chlorobaculum tepidum* (204).

A more recent survey of cytochrome *bd* sequences highlighted the diversity of molecular forms of cytochrome *bd* (96). Although no clear pattern could be discerned in the distribution of the two types of cytochrome *bd* among the classes of Alpha-, Beta-, and Gammaproteobacteria, Epsilonproteobacteria possess only the *bd*-I type. In contrast, the majority of Deltaproteobacteria has short CydA and CydB proteins that are evidently related to the catalytic subunits of ancestral cytochromes *bd* of *Bacillus subtilis* (337).

In addition, a phylogenetically isolated group of Deltaproteobacteria such as *Desulfobulbus propionicus* contains *cydA* sequences that are longer than those of the rest of the class, due to Q loop extensions similar to those of *bd*-I type oxidases. Furthermore, the genomes of over 50 Deltaproteobacteria contain atypical chimeric forms of *cydA* that are fused with genes encoding multiple *c*-type cytochromes but not associated with a *cydB* gene.

The recent discovery of the small subunit CydX (68, 102, 144, 145, 314, 324) provided the opportunity for multiple taxonomic coverage studies. Using the previously characterized *E. coli* CydX protein as a query sequence, Allen *et al.* conducted a survey for orthologs using multiple homology-based *in silico* tools in completed genomes from 1095 taxa spanning the major Eubacterial divisions (111). Their comprehensive approach resulted in the identification of over 300 CydX homologues that are restricted to the phylum of Proteobacteria and more specifically to its Alpha, Beta, and Gamma classes (3). Only two orthologs were identified using refined methods in the species *Leptospirillum ferrooxidans C2–3* and *Leptospirillum ferriphilum ML-04*, both members of the *Nitrospiraceae* family in the phylum *Nitrospirae*. A more recent analysis (96) identified a class of remote orthologs of CydX, termed CydX-like proteins. Their function remains currently unknown.

B. Phylogeny

Previous studies suggested that the *bd*-family of oxygen reductases is an ancient innovation, already present in the ancestor of both Bacteria and Archaea (63). However, it has

been reported that the family may have originated in Bacteria and was later acquired by Archaea *via* lateral gene transfer (57, 135). Phylogenetic reconstructions of the *bd*-family showed that lateral gene transfer plays a substantial role in the distribution of the family, with many phyla acquiring cytochrome *bd* genes multiple times independently. A representative phylogenetic tree is shown in Figure 2. Sequence analysis has demonstrated that CydA and CydB have different rates of evolution, with CydB evolving 1.2 times faster than CydA (135). The biological relevance of this asymmetrical evolution remains essentially unknown.

More recently, Degli Esposti *et al.* specifically studied proteobacterial cytochromes *bd* using integrated approaches of genomic and protein analysis (96). Their work generated a molecular classification of diverse types of cytochrome *bd*, allowing reinterpretation of their evolution and substantiating the occurrence of multiple lateral gene transfer events. Specifically, their findings provided insights on basal taxa of Alphaproteobacteria from which the Gammaproteobacterial lineage probably emerged. A duplication of the original gene cluster of a cytochrome *bd* might have occurred in the ancestors of extant Alphaproteobacteria of the *Rhodospirillales* order, such as *Acidocella*, from which the *bd*-I type of oxidase might have diffused to other proteobacterial lineages.

This conclusion derives from the robust clustering of the Gammaproteobacterium *Salinisphaera hydrothermalis* with *Acidocella sp. MX-AZ02 and Acidocella facilis*. As *Acidocella* lives in strongly acidic environments of wetlands and lakes, a transfer of the cytochrome *bd* operon from *Acidocella* to the halophilic *Salinisphaera* must have occurred in ancient evolutionary times, when both organisms shared common marine environments, or ancestors. The cyanide-insensitive oxidase type, on the contrary, may have differentiated into recognizable subtypes after another gene cluster duplication. These subtypes are widespread in the genomes of Alpha-, Beta-, and Gammaproteobacteria, with occasional instances of lateral gene transfer.

The small size of CydX proteins makes it difficult to robustly resolve phylogenetic inferences and requires critical interpretation. Similar challenges have been encountered with relatively small globin proteins, particularly in invertebrates (147) and simpler species (325). The comparative bioinformatic approaches by Allen *et al.* (3) to examine the distribution of the CydX protein across bacterial species resulted in a predominant association with the Proteobacter phylum and identified two orthologs in the *Nitrospiraceae* family. Given the phylogenetic distance between these *Leptospirillum* species and the other CydX-containing species, of which all are contained in the Proteobacter phylum, it is likely that these bacteria gained the *cydABX* operon through horizontal gene transfer.

Furthermore, in contrast to the CydA and CydB genes, with orthologs in a broad range of phyla, the CydX-containing

FIG. 2. Representative phylogenetic tree of 5000 cytochrome *bd* sequences. The neighbor-joining tree was obtained with all the results of a broad DELTA-BLAST search using *cydA* of *Bacillus subtilis* as a query against 5000 species of proteobacteria excluding most δ-proteobacteria and all ε-proteobacteria, as well as Enterobacterales. Potential lateral gene transfers are indicated. COI sequences are defined in subtypes A, B, and C according to the classification proposed by Degli Esposti *et al.* (96) with subtype A indicating their likely ancestral nature, subtype B for the predominance of betaproteobacteria, and subtype C for the inclusion of *bona fide* CIO oxidases. CIO, cyanide-insensitive oxidase Reprinted by permission from Degli Esposti *et al.* (96).

species were found to be members of the Alpha, Beta, and Gamma classes of the Proteobacteria. This distribution difference is consistent with a model in which CydA and CydB evolved earlier than the CydX small subunit. Since the Alpha, Beta, and Gamma classes have been suggested to be diverged after the earlier branching of Delta- and Epsilon-proteobacteria (70), the distribution of CydX suggests that it may have evolved in association with the *cydAB* operon in a progenitor of the Alpha-, Beta-, and Gammaproteobacteria clades (3).
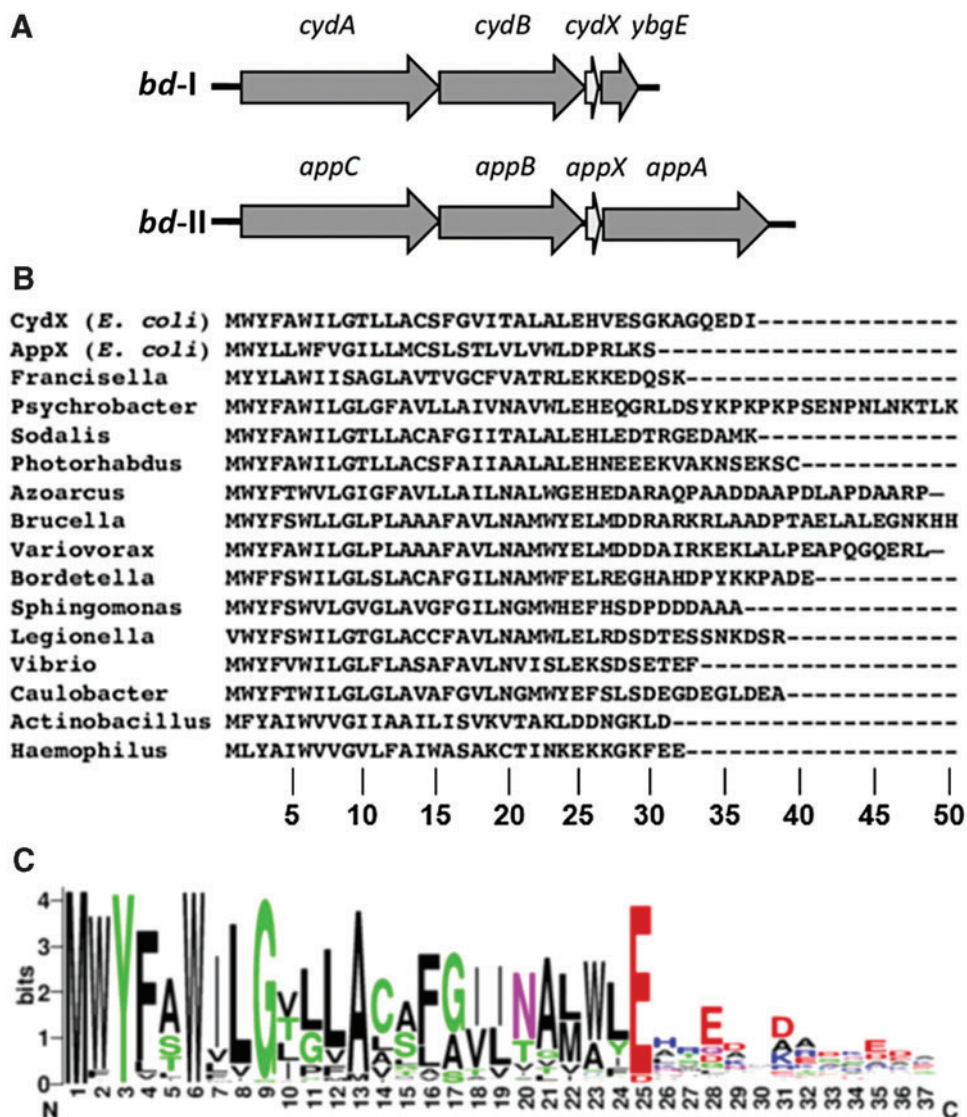
Intriguingly, the early diverging group, lacking CydX orthologs, contains anaerobic organisms, whereas the other includes predominantly aerobic and facultative anaerobic organisms. Additional evidence for horizontal gene transfer of CydX genes was found by superimposing a phylogenetic tree based on CydX on a reference phylogenetic tree of all investigated taxa, suggesting that *Rhodospirillum photometricum DSM 122* gained its *cydABX* operon through horizontal gene transfer (3). It is very likely that the *cydABX* operon has been transferred numerous times between closely related and divergent bacterial species.

C. CydX and CydH subunits

1. CydX. Until recently, it was generally accepted that cytochrome *bd* consists of two subunits. These are CydA (~ 52–$57\,kDa$) and CydB (~ 40–$43\,kDa$) encoded by *cydA* and *cydB* genes, respectively (131, 183, 222, 283). CydA carries the quinol oxidation site and all haems, b_{558}, b_{595}, and *d* (see section III). However, recent studies (68, 102, 144, 145, 314, 324) showed that in Proteobacteria, including *E. coli*, *Brucella abortus*, *Shewanella oneidensis*, and *Salmonella enterica* serovar *Typhimurium*, there is a short gene, *cydX*, located at the 3′-end of the *cydAB* operons that encodes a small protein essential for the function of the oxidase (Fig. 3A).

The CydX protein appeared to be a third subunit of cytochrome *bd*. Deletion of *cydX* in *B. abortus* leads to impaired intracellular growth, loss of viability in stationary phase, increased sensitivity to H_2O_2, and to the combination of the respiratory chain inhibitor sodium azide and the uncoupling agent nickel sulfate (314). Accordingly, $\Delta cydX$ *E. coli* mutants also reveal phenotypes associated with reduced cytochrome *bd*-I

FIG. 3. Cytochrome *bd* operons in *E. coli* and conservation of CydX throughout Eubacteria. (A) Diagram of operons of cytochrome *bd*-I and cytochrome *bd*-II in *E. coli*. Note, that gene *ynhF* encoding the fourth CydH subunit of cytochrome *bd*-I is not part of the operon (280). **(B)** Alignment of selected CydX homologues with indication of amino acid position. The alignment was produced by MUSCLE (105). **(C)** Alignment of 294 CydX homologues in which amino acid size correlates with degree of conservation. The sequence logo was generated by WebLogo. Reprinted from Hobson *et al.* (144) under the terms of the Creative Commons Attribution License. Color images are available online.

activity (324). Phenotypes of Δ*cydX E. coli* cells show slow growth in liquid culture, mixed-colony formation, and sensitivity to *β*-mercaptoethanol. Membrane extracts from Δ*cydX E. coli* cells have reduced *N,N,N′,N′*-tetramethyl-*p*-phenylenediamine oxidase activity. Interestingly, overexpression of *appX*, paralog of *cydX*, compensates the *cydX* deletion in *E. coli* (324). Upon isolation of *E. coli* cytochrome *bd*-I, CydX copurifies with CydAB (145).

The lack of CydX correlates with the absence of the high-spin haems b_{595} and *d*, while the low-spin haem b_{558} is retained (Fig. 4). The loss of the high-spin haems results in the loss of enzymatic activity. Hoeser *et al.* (145) suggested that CydX is essential for the assembly and/or the stability of the high-spin haem site. In contrast to CydX in *E. coli*, its counterpart in *S. oneidensis* does not seem to be essential to the oxidase activity (68). Although markedly impaired in function, CydX-lacking cytochrome *bd* from *S. oneidensis* can still confer a high level of resistance to nitrite.

This suggests that a functional protein complex can be assembled by the two large subunits only. Chen *et al.* (68) concluded that complexation of CydA and CydB is independent of CydX. Furthermore, CydX does not rely on the CydA-CydB complex for its translocation and integration into the membrane. Nonetheless, as in *E. coli*, CydX in *S. oneidensis* is apparently critical to positioning and stabilization of the haems, especially haem *d*.

CydX is conserved in over 200 species of Proteobacteria (3, 96, 144) (Fig. 3B) (see also sections II.A and II.B). There are *cydAB* operons that encode CydX-like proteins denoted CydY and CydZ, possibly performing similar functions (3).
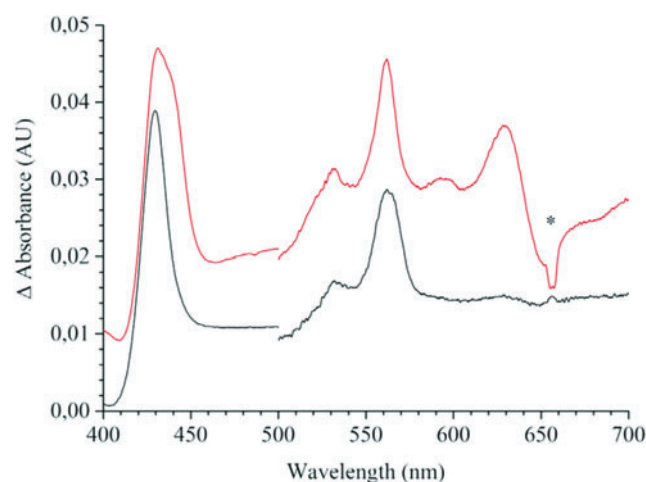

FIG. 4. **Different absorption spectra (dithionite-reduced minus air-oxidized) of purified *E. coli* cytochrome *bd*-I containing (*red*) or lacking (*black*) CydX.** The absorbance difference between 400 and 500 nm is scaled down to one-fifth of intensity. The *black spectrum* shows the peaks at 429.5, 531, and 562 nm corresponding to haem b_{558}. The signals from haem b_{558} are also present in the *red spectrum*. In addition, the *red* spectrum displays a shoulder at about 440 nm and a peak at 594 nm corresponding to haem b_{595}, and a peak at 629 nm corresponding to haem *d*. The Soret signal from haem *d* in the *red spectrum* is superimposed with that of haem b_{558} at 430 nm. The 655-nm signal (*) is an artifact of the spectrometer. Reprinted by permission from Hoeser *et al.* (145). Color images are available online.

CydX is a 30- to 50-amino-acid protein containing a single hydrophobic α-helix. The protein has the conserved N-terminal region and the less conserved C-terminal region (3, 68, 144) (Fig. 3C). The N-terminal region contains the completely conserved W6, and the highly conserved Y3 (all but one homologue), G9 (all but seven homologues), and E/D25 (all but one homologue). The analysis predicts that Y3, W6, and G9 are part of the transmembrane α-helix (3). The N-terminal region of CydX is probably important for function (68). Interaction of CydX with the cytochrome complex may be coordinated through a combination of interactions between multiple residues rather than being dependent on individual residues (144).

A third subunit, denoted CydS, was identified in the structure of cytochrome *bd* from *G. thermodenitrificans K1041* and is thought to stabilize haem b_{558} (281) (see section III). CydS is conserved in Bacillales but shows no sequence similarity to its proteobacterial counterparts. Surprisingly, although the solved structure of the *E. coli* cytochrome *bd*-I shows the similar location of CydX (280), the CydX-lacking *bd*-I protein still retains haem b_{558} (145) (Fig. 4).

In summary, it seems likely that all cytochromes *bd* possess a third, small subunit. The CydX or CydX-like component could be overlooked in cytochrome *bd* of some microbes using standard biochemical and genomic methods. It is indeed difficult to identify such a small-size protein in cytochrome *bd* complex preparations, as well as the corresponding short gene out of many short open reading frames. One more possible reason for the apparent absence of *cydX* in some *cydAB* operons is that the gene could have migrated to another part of the genome. For instance, 4 of 20 CydS in Bacillales are encoded at gene loci far apart from their *cydAB* operons (281).

2. CydH. The structure of the *E. coli* cytochrome *bd*-I reveals a fourth, previously unknown subunit called CydH (280) [or CydY (317)]. Like CydX, CydH is a small non-catalytic accessory single transmembrane subunit (see section III). The subunit is encoded by the orphan gene *ynhF*, which is not part of the *cydAB* operon. Only members of the proteobacterial clade with cytochromes *bd* belonging to subfamily L (one of the two subfamilies of the *bd* enzymes, see section III) seem to have CydH homologues (280). The role of CydH appears to be more than just ''structural.'' The subunit blocks the O_2 entry route to haem b_{595} in the *E. coli* cytochrome *bd*-I (317). In the *G. thermodenitrificans* enzyme, CydH is absent, and therefore, this channel is open and provides O_2 access to haem *d* located in place of haem b_{595} at this site (281) (see also section III).

D. Regulation of expression

Regulatory mechanisms underpinning the expression of cytochrome *bd* have long been the subject of intense study, driven by the extraordinary features of this oxidase and its physiological significance. For example, the earliest studies on bacterial respiration revealed that cytochrome *bd*, recognizable initially by its distinctive optical properties, was maximally expressed in *E. coli* under conditions of low oxygen supply (252, 272). This is now considered to be a reflection of the very high oxygen affinity of this oxidase (88). Expression is also increased in the presence of cyanide (8),

NO (217), carbon monoxide (CO) (332), and Ru- and Mn-containing CO-releasing molecules (CORMs) (94, 333).

By far, the best-studied systems are in *E. coli*, where regulation has proven to be extremely complex, intricate, and responsive. Although we focus on the mechanisms in *E. coli*, which involve multiple promoters and at least three classes of transcriptional regulators, the identity of the regulators and their modes of action differ among genera, but are outside the scope of the present review. For example, in *Shewanella*, the two cytochrome *bd* subunit genes are cotranscribed with a third gene, *cydE*, that encodes a GbsR regulator that represses *cydAB* expression (340).

In several gram-positive genera, the transcription factor Rex is implicated in the regulation of genes important for fermentation and growth at low oxygen tensions, sensing the cellular redox poise in the form of NADH/NAD$^+$ ratios. Examples of the role of Rex in regulating cytochrome *bd* expression are found in *Streptomyces* (56, 207), *Saccharopolyspora spinosa* (348), and *Bacillus subtilis* (200, 266, 291, 331).

In *Rickettsia conorii*, a small regulatory RNA is implicated as a potential regulator of *cydA* (234). OxyR is a master regulator in a wide range of bacteria, but its role in regulating cytochrome *bd* appears limited: an OxyR binding site has been identified in the promoter region of *cydA* in *Corynebacterium glutamicum* (225, 316) and it plays a role in regulating electron flux to cytochrome *bd* in *S. oneidensis* (330).

Here we focus on the complex systems involved in regulating cytochrome *bd*-I of *E. coli*. Control of cytochrome *bd* expression in *E. coli* is achieved primarily through the combined and complex actions of ''fumarate nitrate reduction'' regulator (FNR) and the ArcB/ArcA two-component system. A regulatory complex of five promoters initiates the transcription of *cydAB*: four of them (P1–P4) are coordinately regulated by oxygen (*via* ArcA and FNR). ArcA binds at three sites at this promoter (214), but only one is essential for transcriptional activation (82). Also, two distinct sites for binding FNR are discernable (82): the downstream FNR-2 site is critical for FNR-mediated repression *in vivo*, whereas the upstream site (FNR-1) plays an ancillary role in regulation of the *cydAB* operon by oxygen (129). Detailed discussion of the biochemistry of these oxygen-sensing global regulators is beyond the scope of this review but a summary follows.

FNR is a protein of the CPR-FNR superfamily of transcription factors, which all possess an N-terminal sensory domain and a C-terminal DNA-binding domain (132). FNR regulates transcription of target genes (its regulon) under anaerobic conditions by assembly of an oxygen-labile [4Fe-4S] cluster into the N-terminus. Assembly of this cluster facilitates formation of an FNR dimer with enhanced DNA-binding activity. It targets specific nucleotide sequences in selected promoters, where it acts as an activator of ''anaerobic genes'' and a repressor of ''aerobic genes.'' As oxygen availability increases, the [4Fe-4S] cluster is degraded to a [2Fe-2S] cluster so that site-specific inhibition is inhibited. The details of how O$_2$ interacts with FNR are described elsewhere (83) and the effects of NO on the cluster are given in Crack *et al.* (84) and Cruz-Ramos *et al.* (87).

In *Azotobacter vinelandii*, CydR is an FNR-like protein, encoded adjacent to *cydAB* (180), that represses *cydAB* expression (339). Interestingly, FNR is structurally and functionally related to the cAMP receptor protein (CRP) [for a review see Green *et al.* (132)]. In *Mycobacterium smegmatis*, CRP directly regulates the expression of *cydAB* in response to hypoxia (9). No CRP site is present in the *M. smegmatis* cydDC promoter.

While FNR is a direct sensor of oxygen (and NO), ArcBA is a representative of the two-component regulators and is an indirect oxygen sensor. The ArcB protein is a membrane-integral sensor kinase and ArcA is its cognate response regulator. Two key cysteine residues in the cytosolic domain of ArcB must be reduced for the protein to be functional. It is generally accepted that it is the redox poise of respiratory chain quinones, such as those transferring electrons to the oxidase itself that is key to Arc function. Both the ubiquinone and menaquinone (MQ) pools are thought to be involved in regulating ArcBA (15). Fermentation products act as allosteric effectors (121, 122).

When oxygen is available, ArcB transits from being an autokinase to a phosphatase, *via* formation of two intermolecular disulfide bonds, resulting in the formation of a covalently linked ArcB dimer. Ultimately [for references see Bettenbrock *et al.* (30)], a phosphate group is transferred to ArcA, which assumes the role of a sequence-specific DNA-binding protein. In this form, it controls expression of several target promoters including *cydAB* (284). The system is switched off by the phosphatase activity of the oxidized (disulfide) form of ArcB, *via* dephosphorylation of ArcA (120).

When the oxygen tension drops, ArcA is phosphorylated by ArcB and activates *cydAB* transcription (81, 153). In early experiments, cytochrome *bd* expression was shown to reach a maximum at <2% oxygen tension (320) but more deliberate control of oxygen availability (2) questions this. When oxygen is decreased further, FNR becomes active and represses *cydAB* transcription (82, 320). A unique feature of the *cydAB* operon is the fact that FNR repression requires the presence of a functional ArcA protein (81, 82, 130). FNR has been proposed to act as an antiactivator by counteracting ArcA-mediated activation rather than directly repressing transcription (82, 130).

A role for the histone-like protein H-NS has also been reported (130). H-NS binds to an extended region within the *cydAB* promoter element, including sequences upstream from, and overlapping, the four regulated promoters. Oxygen control of *cydAB* transcription is thought to be mediated by three alternative protein-DNA complexes that are assembled sequentially on the promoter region as the cells are shifted from aerobic to microaerobic and to anaerobic conditions.

A recent systems approach to the oxygen response of cytochrome *bd*-I and the two other oxidases of *E. coli* (30, 104) has adopted a rigorous chemostat methodology, transcriptome profiling, and powerful mathematical modeling tools (287). In chemostats poised at quantified and constant oxygen provision rates, 89 genes exhibited expression changes when oxygen availability was modulated experimentally (276). O$_2$ availability in the chemostats was expressed as ''% aerobiosis'' (2), defined by the converse relationship between declining $q_{acetate}$ (a measure of ''overflow'' metabolism) and increasing oxygen transfer rate. Steady-state simulation results of the three oxidase activities in comparison with measurement data showed good correlations with measured oxidase levels (104).

Cytochrome *bd*-I levels were very low at the highest and lowest rates of O_2 transport and highest at 56% aerobiosis. Expression of this operon was 6.4-fold enhanced compared with anoxia (where acetate flux is maximal).

The expression of the second cytochrome *bd*-type oxidase of *E. coli*, cytochrome *bd*-II, is subject to less extreme regulation and has been studied less intensively; the function of this oxidase is unclear. Our current knowledge of the structures of cytochromes *bd*-I and *bd*-II suggests that their functions should be similar and perhaps interchangeable, yet they appear to be differentially regulated. Whereas *cydAB* is maximally expressed at O_2 tensions between microaerobic and oxygen-rich conditions (320), *appCB*, encoding cytochrome *bd*-II, is maximally expressed at 0% aerobiosis (using the acetate criterion). Spectroscopic assays of oxidase levels confirm these conclusions (276, 319). In contrast, the *cyoABCDE* operon, encoding cytochrome *bo₃*, was maximally induced under fully aerobic conditions.

Thus, shifts in oxidase expression are consistent with a progressive switch from fermentation to microaerobic respiration (where cytochrome *bd*-I acts as the dominant oxidase) and then to aerobic respiration (where cytochrome *bo₃*

is the prevailing terminal oxidase. Posttranscriptional regulation appears not to play a major role in oxidase expression.

III. Structure and Assembly

A. Structure

To date, cytochrome *bd* structures from two bacteria have been reported. In 2016, the first crystal structure of cytochrome *bd*, from the thermophile *G. thermodenitrificans K1041*, was determined at 3.1 Å (Protein Data Bank [PDB]: 5DOQ) and 3.80 Å (PDB: 5IR6) resolutions (281). The structure shows that this is a three-subunit enzyme. Both main subunits, CydA ($\sim$52 kDa) and CydB ($\sim$40 kDa) (283), are integral membrane proteins, each consisting of nine transmembrane helices, with the N-terminus and the C-terminus in the periplasmic and cytoplasmic sites, respectively (Fig. 5A). CydA and CydB are encoded by paralogous genes, which resulted from a duplication of a single ancestral unit codifying for a homodimeric oxidase (75). The heterodimeric structure is stabilized by hydrophobic interactions involving residues coming from the paired α3, α4, and α9 of CydA and CydB. The CydA and CydB subunits are structurally similar (root mean

FIG. 5. **(A) Ribbon model of the *bd* oxidase from *G. thermodenitrificans*.** The subunits CydA (*green*), CydB (*cyan*), and CydS (*brown*) are shown. The haem groups b_{558}, b_{595}, and *d* are represented by stick models (*pink*). Helices a3, a4, a5, a6, and a9 reported in the main text are labeled. **(B)** Ribbon model of the *bd*-I oxidase from *E. coli*. The subunits CydA (*green*), CydB (*cyan*), CydX (*yellow*), and CydH (*magenta*) are shown. The haem groups b_{558}, b_{595}, and *d* are represented by stick models (*pink*). UQ8, ubiquinone-8. Color images are available online.
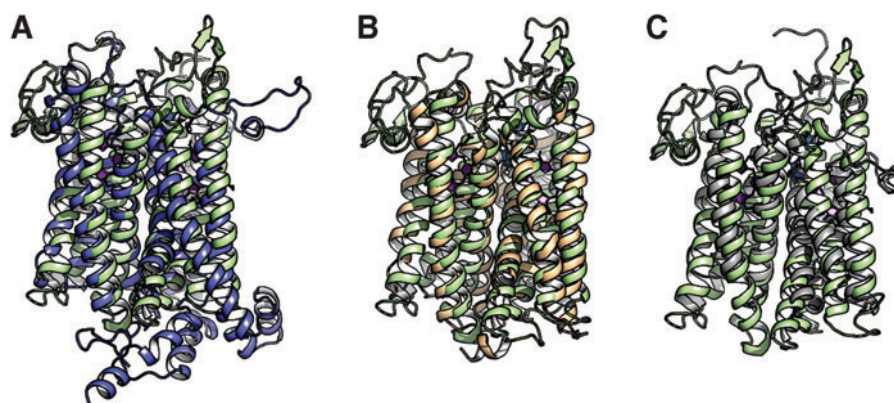
FIG. 6. Structurally similar subunits of *G. thermodenitrificans bd* oxidase. Structural superposition of *G. thermodenitrificans bd* oxidase (*green*) with **(A)** Complex III (Cytochrome bc_1) from *Flavobacterium johnsoniae* (*blue*; PDB:6BTM; RMSD: 3.4 Å); **(B)** Complex III (Cytochrome bc_1) from *Rhodothermus marinus* (*orange*; PDB:6F0K; RMSD: 3.4 Å; and **(C)** polysulfide reductase from *Thermus thermophilus* (*gray*; PDB:2VPX; RMSD: 3.2 Å). Superposition was carried out using PyMOL (Version 2.0; Schrödinger, LLC). RMSD, root mean square deviation. Color images are available online.

square deviation [RMSD]: 3.1 Å). A search for structurally similar subunits in PDB yielded a relatively low similarity with Complex III (cytochrome bc_1) from *Flavobacterium johnsoniae* (PDB:6BTM; RMSD: 3.4 Å; Fig. 6A) (311) and *Rhodothermus marinus* (PDB:6F0K; RMSD: 3.4 Å; Fig. 6B) (307), and polysulfide reductase from *Thermus thermophilus* (PDB:2VPX; RMSD: 3.2 Å; Fig. 6C) (162). CydS, in turn, is a single transmembrane helix of 33 amino acid residues ($\sim 4\,\mathrm{kDa}$), which is positioned at the peripheral interface formed by helices α5 and α6 of CydA. CydS is proposed to stabilize haem b_{558} during potential structural rearrangements of the CydA upon binding and oxidation of quinol (281).

In 2019, using single-particle cryoelectron microscopy (cryo-EM), two structures of the *E. coli* cytochrome *bd*-I, in lipid nanodiscs with a bound Fab fragment (280) and in the presence of aurachin C (317), were determined at 2.68 Å (PDB: 6RKO) and 3.3 Å (PDB: 6RX4) resolutions, respectively. The results of the two articles (280, 317) are consistent. It turns out that cytochrome *bd*-I is a four-subunit enzyme (Fig. 5B). The arrangement and architectures of subunits CydA, CydB, and CydX are similar to the overall structure of the cytochrome *bd* from *G. thermodenitrificans K1041* (Fig. 7). A fourth, previously unknown, subunit, absent in the *G. thermodenitrificans* oxidase, was named CydH (280) [or CydY (317)]. CydH appears to be a single transmembrane subunit that binds in the cleft between transmembrane helices α1 and α9 of CydA.

Cytochrome *bd* displays a unique binding domain for the oxidation of quinol called the Q-loop (218, 226). This is the loop connecting the α6 and α7 helices of CydA, facing the outside of the prokaryotic cell (Fig. 8A). The Q-loop is of variable length within the family (239, 282). Based on its size, the *bd*-type oxidases are divided into two subfamilies: L (long Q-loop) and S (short Q-loop) (7, 48). Cytochromes *bd* from *G. thermodenitrificans* and *E. coli* belong to S and L subfamilies, respectively. The quinone-analogue aurachin D is a powerful and relatively selective inhibitor of the *E. coli* cytochrome *bd*-I (221). Duroquinol:O_2 oxido-reductase activity of the isolated *bd*-I oxidase is inhibited by aurachin D with IC_{50} of 35 nM (317). In accord with

these data, aurachin D inhibits O_2 consumption of cytochrome *bd* in inverted membrane vesicles of *M. smegmatis* with an IC_{50} of ~ 400 nM (212).

An *in silico* docking model of the complex between aurachin D and cytochrome *bd* (Paiardini, unpublished data) suggests that indeed aurachin D binds at the cytochrome *bd* quinol oxidation site (Fig. 8B), in close proximity to the Q-loop. The docking data (Fig. 8B; Paiardini, unpublished data) are consistent with the fact that, in the structure reported by Theßeling *et al.* (317), there is a small but significantly
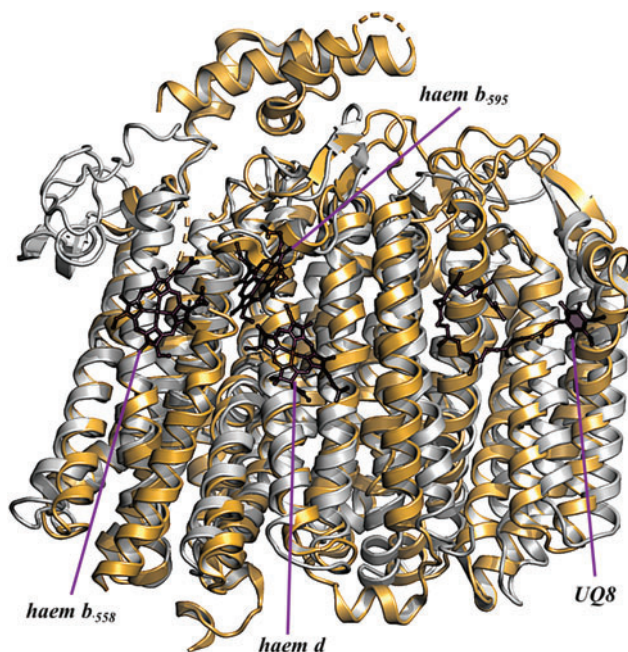

FIG. 7. Superposition of *G. thermodenitrificans bd* oxidase (PDB:5DOQ; silver) and *E. coli bd*-I oxidase (PDB:6RKO; gold). The positions of haems b_{558}, b_{595}, *d*, and UQ8 in 6RKO are shown as reference. The measured RMSD is 4.7 Å. Superposition was carried out using PyMOL (Version 2.0; Schrödinger, LLC). Color images are available online.
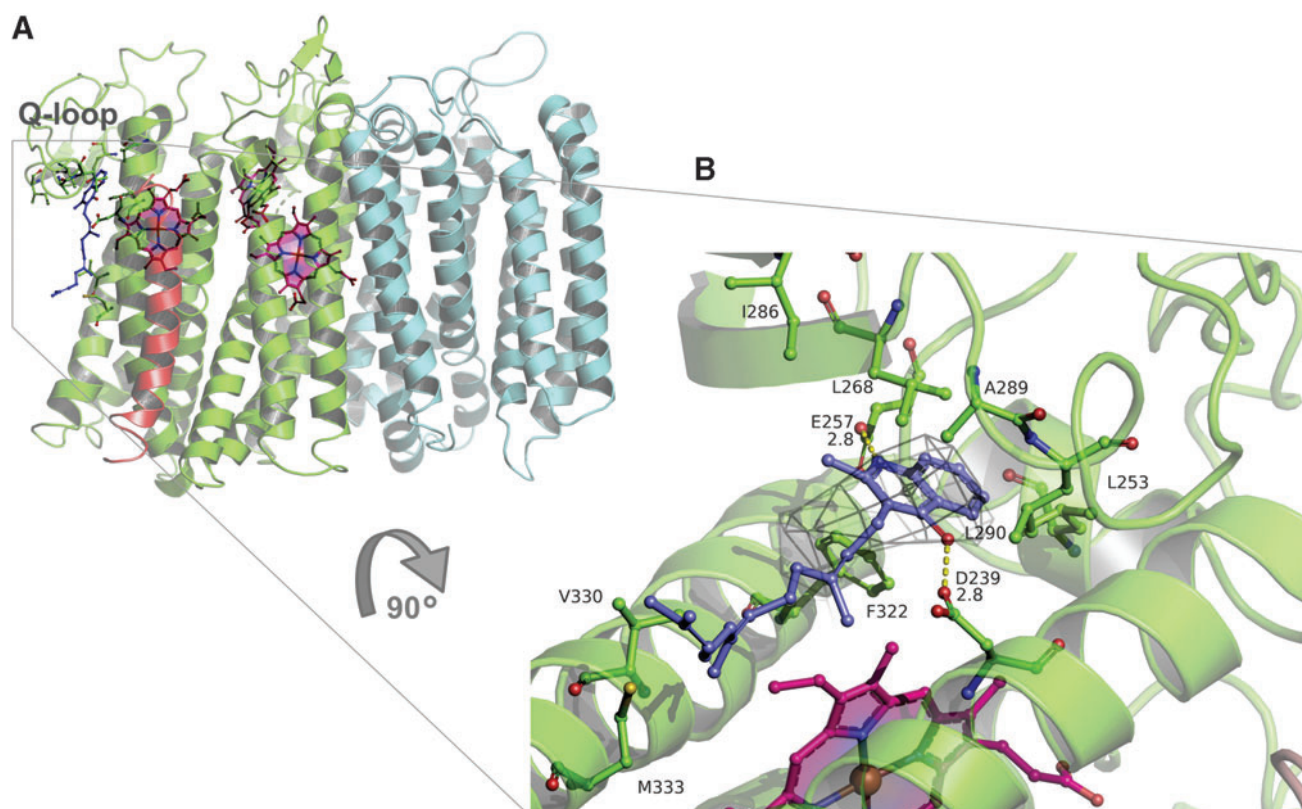
FIG. 8. Cytochrome _bd_ displays a unique binding domain for the oxidation of quinol. (A) Ribbon model of *G. thermodenitrificans bd* oxidase with aurachin D bound (slate sticks). **(B)** Detailed representation of the interaction between aurachin D and *G. thermodenitrificans bd* oxidase. The residues at less than 4 Å from aurachin D are represented as sticks, and labeled according to the crystal structure of *bd* oxidase from *G. thermodenitrificans* (PDB 5DOQ). Haem b_{558} is represented as *purple* sticks. The key polar interactions of aurachin D with residues E257 and D239 are represented as *yellow dashed lines*, and the distance between the involved atoms is reported (**Å**). The approximate position of the density of aurachin C as found in *bd* oxidase from *E. coli* (PDB: 6RX4) is reported as mesh. Docking was done using MVD (CLC Bio©) starting from the energy minimized structure of aurachin D and PDB file 5DOQ and considering search space a sphere of 12 Å centered on the Fe atom of haem b_{558}. The best docked pose, as assessed by the energy of interaction score (−128.2), is shown. MVD, Molegro Virtual Docker. Color images are available online.

unexplained electron density in a pocket comprising E257 and K252, possibly due to a bound aurachin C. The role of the Q-loop in the as-isolated cytochrome *bd* from *E. coli* without substrate, in the presence of ubiquinone-1 (substrate analogue), and a quinolone-type inhibitor AD3–11 was investigated (280). The Q loop is divided into two domains: a flexible, disordered Q_N (N-terminal part) and a rigid, well-ordered Q_C (C-terminal part). The Q_C domain that defines the L-subfamily does not appear to be involved in substrate binding.

A feature that emerged from the crystal structure of the cytochrome *bd* from *G. thermodenitrificans* was the unexpected triangular arrangement of the three haems located on CydA. This suggests a direct electron transfer from haem b_{558} to haem *d*, followed by equilibration with haem b_{595} (Fig. 9A and section V). The evolutionarily conserved W374 could participate in the electron transfer between haem b_{558} and haem *d* (281).

The *E. coli* cytochrome *bd*-I preserves triangular organization of the haems (Fig. 9B). The location and coordination of haem b_{558} are equivalent in both enzymes. It is coordinated by H186 and M325 (M393 in *E. coli*). Surprisingly, however, haem b_{595} and haem *d* in the *E. coli* structure are interchanged with respect to the *G. thermodenitrificans* enzyme (Figs. 5 and 9). In the latter structure, haem b_{595} is hexacoordinate

having H21 and E101 (H19 and E99 in *E. coli*) as axial ligands. It is buried in the protein interior deeper than haem *d*. Haem *d* has E378 (E445 in *E. coli*) as the axial ligand. In the *E. coli* structure, conversely, haem b_{595} is pentacoordinate with E445 as the axial ligand. Furthermore, haem b_{595}, rather than haem *d*, is located near the periplasmic surface.

There is a discrepancy in the nature of the axial ligand to haem *d* between the two *E. coli bd*-I structures. Safarian *et al.* (280) claim that this is H19, whereas Theßeling *et al.* (317) report that the ligand is E99. The difference in the haem *d* axial ligand observed in the two static structures may indicate flexibility in the haem iron/ligand coordination bond, assuming that the haem *d* iron may coordinate no more than one protein axial ligand at a time. In line with this suggestion, lability (transient formation/breaking) of the haem *d* iron bond to a protein ligand in one of the states of the catalytic cycle (the one-electron reduced "mixed-valence" state) was noted earlier in time-resolved experiments (304). This implies the possible functional significance of the intraprotein axial ligand exchange in the haem *d* coordination sphere during catalysis.

The short edge-to-edge distance (6.7 Å) between haem b_{558} and haem b_{595} and the interchanged positions of the high-spin haems suggest a sequential interhaem electron
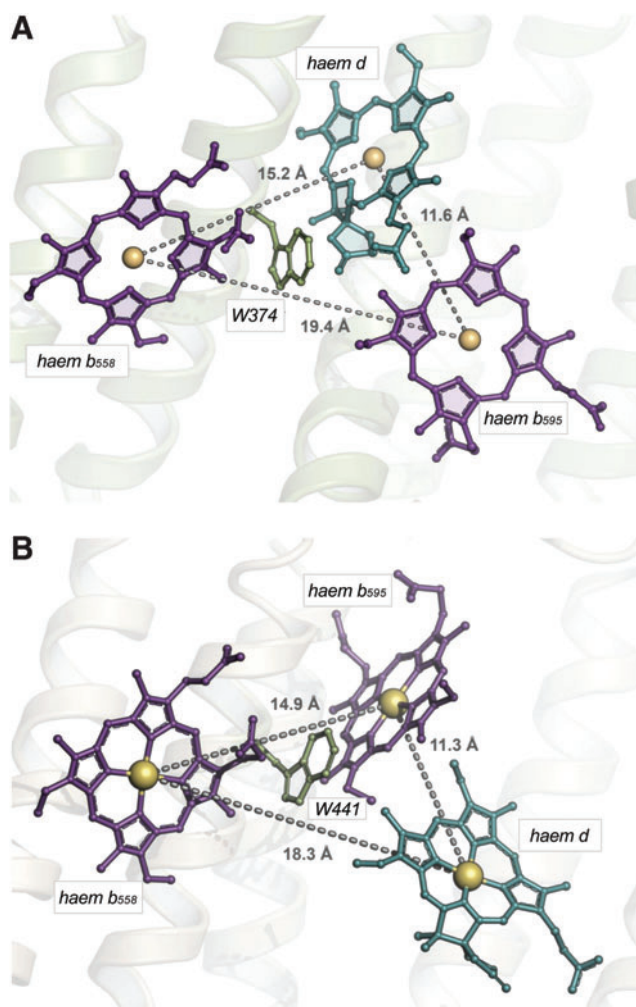
10

FIG. 9. Representation of the triangular arrangement of the three haems, in stick models, bound to CydA in (A) *G. thermodenitrificans bd* oxidase and (B) *E. coli bd*-I oxidase. Haems b_{558} and b_{595} are depicted in *violet* and haem *d* in *cyan*. The distance between Fe atoms is represented as dashed *gray lines* and labeled. In *G. thermodenitrificans bd* oxidase, this arrangement suggests a direct electron transfer from haem b_{558} to haem *d*, followed by equilibration with haem b_{595}. The evolutionarily conserved W374 (W441 in *E. coli bd*-I oxidase) could mediate electron transfer between haem b_{558} and haem *d*. Surprisingly, haem b_{595} and haem *d* in the *E. coli bd*-I oxidase structure are interchanged with respect to the *G. thermodenitrificans* enzyme. Adapted from Safarian *et al.* (280, 281). Color images are available online.

transfer in the *E. coli* oxidase, $b_{558} \rightarrow b_{595} \rightarrow d$, as proposed earlier (48, 258) (Fig. 9B and section V). The totally conserved W441 possibly mediates electron transfer between b_{558} and b_{595}. It is worth noting that the plane of haem b_{558} is organized more-or-less at right angles to the membrane plane in both the *E. coli* and *G. thermodenitrificans* oxidases, whereas either *d* or b_{595} is oriented at about 45° to the membrane plane in the two oxidases; these two high-spin haems are interchanged in the two species (280, 281, 317). Such an arrangement was predicted by electron paramagnetic resonance analyses of membrane multilayers rotated within the instrument cavity in 1980 before any structural data were available (250).

CydB contains a tightly bound ubiquinone-8 (UQ8; Fig. 5B). The molecule is located at a hydrophobic pocket, about 3.5 nm from haem *d*, in a near-symmetric conformation relative to haems b_{558} and b_{595}. The significant distance from the haems makes its direct participation in electron transfer to/from the haems or oxygen reduction unlikely. The bound UQ8 possibly plays a structural role (280, 317).

Cytochrome *bd* is not active as a transmembrane pump, but a net proton flux results from quinol oxidation and consequent proton ejection at the periplasmic side of the membrane and uptake of cytoplasmic protons during oxygen reduction. Two alternative proton pathways in the *G. thermodenitrificans* structure have been indicated, one in CydA and the other in CydB, which converge on haem b_{595} (Fig. 10) (281). In the *E. coli* enzyme, there is a hydrophilic, water-filled H-channel that connects the cytoplasm to haem *d* by the CydA pathway (Fig. 11). A chain of water molecules runs until D58 of CydB, and then, the conserved S108, E107, and S140 of CydA continue the pathway to haem *d*. Near D58, the H-channel branches and runs along the WDGNQ motif of CydB forming the CydB pathway branch (not shown). Surprisingly, in the center of CydB at W63, the hydrophilic branch merges with the hydrophobic oxygen-conducting channel (O$_2$ channel, Fig. 11).

The O$_2$ channel that goes parallel to the membrane plane connects the lipid interface to haem *d* (280, 317). In the *G. thermodenitrificans* structure, due to the lack of voluminous pathways there, O$_2$ may gain access to haem *d* via a potential O$_2$ entry site located laterally at a short distance from haem *d*.

FIG. 10. Potential proton transfer pathways in the *bd* oxidase from *G. thermodenitrificans* (PDB 5DOQ). The side chains of the residues that are involved in CydA and Cyd B proton transfer pathway are shown. Proton transfer pathways are crucial for protons to gain access to the oxygen-binding site. Two potential proton transfer routes, named the CydA pathway and CydB pathway respectively, have been identified: the former is located inside of the four-helix bundle α1–4 of CydA and the latter in the symmetry-related α1–4 four-helix bundle of CydB. HDD, haem *d*; HEB, haem b_{595}. Adapted from Safarian *et al.* (281). Color images are available online.

FIG. 11. Oxygen and proton channels in *E. coli* cytochrome *bd*-I (PDB: 6RKO). Adapted from Safarian *et al.* (280). The proton channel (*cyan spheres*) connects haem *d* directly to the cytoplasm *via* the CydA pathway. The oxygen channel (O_2 channel, *green spheres*) connects the UQ8 interface with heme *d*. Color images are available online.

Thus, for the *G. thermodenitrificans* cytochrome *bd*, O_2 present within the membrane could bind to haem *d* without the need for any functionally conserved protein cavity (281). The *E. coli* CydH occupies the O_2 entry site in the *G. thermodenitrificans* enzyme, where CydH is absent, thereby preventing access of O_2 to haem b_{595} from the hydrophobic lipid bilayer (280, 317).

B. Assembly—the role of CydDC

Understandably, when molecular genetic tools were brought to bear on cytochrome *bd*, the structural genes (*i.e.*, encoding the oxidase subuni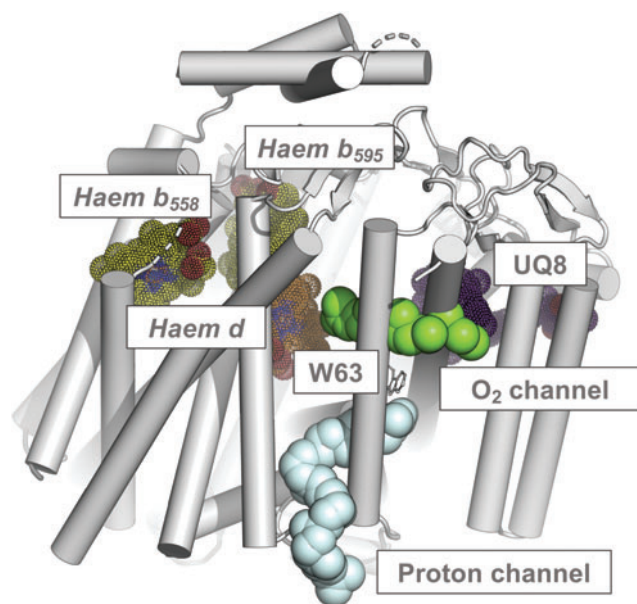ts) were the earliest focus. Mutants lacking the oxidase could be isolated and the encoding genes were cloned, sequenced, and analyzed, thus laying the foundations for studies on oxidase organization and function. However, other genes, involved in assembly of the oxidase complex in *E. coli*, were quickly found and these too have generated new information and hypotheses.

In *E. coli*, the *cydDC* genes are distant from the structural genes on the chromosomal map (123), but in certain bacteria they occur in a single operon with *cydAB* thus being expressed on one continuous transcript, as occurs in *Bacillus subtilis* (337). Other bacteria have oxidases that resemble cytochrome *bd*-I, yet have no spectrally detectable high-spin haems (b_{595} and the *d*-type haem) as in *Campylobacter jejuni*; nevertheless, two genes (cj0081, cj0082) that encode proteins similar to the CydAB proteins in *E. coli* were identified from genome sequences (241). These issues are discussed in Poole *et al.* (253).

Neither *cydD* nor *cydC* is an essential gene in *E. coli*, as evidenced by the strategies that identified *cydC* and *cydD* mutants. However, Eng *et al.* (108) describe *E. coli* *cydC* as an essential gene and suggest that cytochrome *bd*-I (*i.e.*,

CydABX) and CydDC do not always co-occur: among the 1965 genomes analyzed, 407 species exhibited highly conserved *cydC* genes, but only 53 showed a *cydB* homologue. It is puzzling that *cydDC* genes appear to be found in so many genomes that do not encode cytochrome *bd*-I; Kranz *et al.*, in the 33 bacterial genomes analyzed, found none (197), although six species encode the oxidase but not CydDC, namely *Rickettsia prowazekii*, *Chlamydia tracomatis*, *C. jejuni*, *Porphyromonas ginigivalis*, *Aquifex aeolicus*, and *Thermotoga maritima*. All were claimed to lack both CydDC and cytochrome *bd*-I by Eng *et al.* (108).

Furthermore, neither *Geobacillus* nor *Mycobacterium* species were found by Eng *et al.* to encode cytochrome *bd*-I, despite the fact that other authors report functional or structural studies on cytochrome *bd*-I from these bacteria (23, 114, 281). Caution is urged when deducing the apparent *absence* of genes from a genome, particularly genes such as *cydDC* that are members of a very large and diverse family—the adenosine triphosphate (ATP)-binding cassette (ABC)-type transporters.

1. *The cydDC genes.* In addition to the structural genes that encode the cytochrome *bd* complex, detailed above, it is now clear that, in many bacteria, two additional genes function in proper assembly of the oxidase. In *E. coli*, where information is most comprehensive, and most bacteria, they are named *cydC* and *cydD*. These genes encode a transport system in the ABC class and are widely thought to be the sole two components of a membrane-integrated export system.

By the early 1990s, *cydA* and *cydB* encoding the cytochrome *bd*-type terminal oxidase (*bd*-I) (61) were mapped to an operon at 16.6 min (188) on the chromosomal map. Remote from the *cydAB* locus and located at 19.2 min (123), a further gene, implicated in "cytochrome *d* assembly," was also identified. Mutants in this gene (named *cydC*) were devoid of absorbance bands in the visible spectrum that could be attributed to cytochrome *bd*-I; however, the spectrum was returned to wild-type (WT) characteristics by introducing the cloned *cydC*⁺ gene on an episome.

Transcription/translation experiments and Western immunoblotting of membranes from a *cydC* strain showed that the CydA and CydB subunits were present but diminished in membranes from a *cydC* strain relative to the isogenic *cydC*⁺ strain (123). Expression of the oxidase subunits in a *cydC* strain demonstrated that the b_{595} and b_{558} haems were overproduced, but the haem *d* component was absent. Thus, a plausible hypothesis was that CydC is involved in biosynthesis of haem *d*; in the absence of this haem, the oxidase subunits are largely absent and destabilized (123). Note that Siegele *et al.* independently described the *cydC* gene but named it *surB*, because its gene product was required for *E. coli* cells to exit (*i.e.*, survive) in a stationary phase aerobically (299).

In 1989, we identified a fourth *cyd* locus by adopting a markedly different strategy (260): survivors of a classical nitrosoguanidine mutagenesis were screened using a hand spectroscope (on samples held at 77 K) for loss of the characteristic absorbance at 630 nm of reduced cytochrome *bd*. The mutant gene in one such isolate was mapped to 19.3 min (260). Furthermore, a gene implicated in the ability to survive at elevated temperatures, *htrD*, was shown, after correcting a missing G in the earlier sequence, to be identical to *cydD* (98).

Cloning of the *cydC* and *cydD* genes (255) resulted in a fragment of chromosome originating in the 19-min region of the Kohara map, and thus consistent with earlier P1 mapping data (260). When such plasmids were used as templates for *in vivo* protein synthesis, two proteins identified as CydD (61 kDa), calculated to be 63 kDa, and CydC (59 *vs.* 63 kDa) (255) were generated. CydD and CydC were similar: the deduced amino acid sequences revealed 50% similarity and 27% identity. Hydropathy profiles predicted that the CydDC complex comprises two similar membrane proteins, and it was identified as the first documented example of a bacterial heterodimeric ABC transporter, probably an exporter, by comparison with known ABC family members.

2. The CydDC proteins: structure and function. Based on analysis of hydrophobicity of CydD and CydC, it was predicted that both subunits would have six transmembrane helices, the C-terminal portion of each polypeptide being hydrophilic and containing an ATP-binding site (255). A membrane topology model for CydDC predicted both subunits to have six transmembrane regions separated by two major cytoplasmic loops; both ends of each polypeptide chain were predicted to be located in the cytoplasm (86). Subsequent modeling of topography (253) was consistent with those models, and used to highlight the Walker A motif (which binds ATP), the Walker B motif (which interacts with Mg(II)), and conserved amino acids (histidine, glutamate, aspartic acid) that are part of the H-, Q-, and D-loops, respectively.

The periplasm of an *E. coli cydDC* knockout mutant is "overoxidizing" (126) indicating that CydDC may catalyze cell export of reductant(s). Indeed, loss of CydDC diminishes the level of reduced thiol detected in the extracytoplasmic compartment, while overexpression of CydDC decreases the cytoplasmic reduced thiol pool (146). These observations are consistent with *in vitro* studies that measured import of ^{35}S-labeled cysteine into everted membrane vesicles and demonstrated that, *in vivo*, CydDC mediates energy-linked export of cysteine (247).

CydDC also transports outward, and thus presumably into the periplasm, the tripeptide glutathione (L-γ-glutamyl-cysteinylglycine [GSH]), a major regulator of cellular redox poise (248). The transport rate for GSH by CydDC was fivefold higher than for cysteine; therefore, given the abundance of GSH in the bacterial cytoplasm (248), GSH is likely to be a major substrate for CydDC. Addition of GSH and cysteine both stimulated the ATPase activity of purified CydDC (342), supporting an enzymic role in the export of reductant. The complexity of the process is probably not fully understood: Eser *et al.* (110) studied the effects of mutating three genes (*cydD*, *ggt*—encoding periplasmic γ-glutamyl transpeptidase—and *mdhA*—encoding a multidrug-resistant-like ABC transporter) that might influence periplasmic GSH pools, but none affected the ability of glutaredoxin-3 (GrxCp) to catalyze the formation of disulfide bonds, suggesting the existence of other routes for GSH export in *E. coli*.

Because CydDC is an exporter and is required for haem assembly into the oxidase, it was hypothesized that CydDC might export haem, a proposal tested experimentally. However, use of everted vesicles and radiolabeled haem *in vitro* failed to demonstrate this function for CydDC (74). Later work exploited a purified form of CydDC with an absorption peak at

410–412 nm; pyridine haemochrome analyses indicated the presence of a bound *b*-type haem with a CydDC:haem ratio of 5:1 (342). This bound haem was reducible and oxidizable, and bound CO. Haemin and GSH/cysteine had synergistic and stimulatory effects on the ATPase activity of the complex. This suggests that the haem cofactor has a significant but obscure role in CydDC function.

Certain other reduced thiols (including homocysteine and methionine) also activated CydDC. Control experiments with *S*-substituted/nonthiol analogues and haem lacking the central iron (protoporphyrin) did not stimulate rates of ATPase activity, and inclusion of nonthiol reductants decreased the ATPase rate. These experiments suggest the need for either thiols or an iron-containing tetrapyrrole in CydDC function. Histidine was an intriguing exception: it gave a twofold increase in ATPase activity, which increased to eightfold on additional inclusion of 1 μM haemin. Since axial ligands to haem include both histidine and reduced thiol compounds, this suggests that the haem-ligating capacity of reduced thiols contributes to the enhancements in ATPase activity observed for GSH and cysteine (342).

3. Structural investigations into the CydDC complex. Two-dimensional crystals have been obtained by incorporating purified CydDC into *E. coli* lipids, thus permitting cryo-EM (342). The electron densities reveal arrays of dimeric units in "up" and "down" orientations, indicating CydDC heterodimers in the crystal lattice. Although no three-dimensional crystal structure has been reported, Shepherd and colleagues used a structural modeling approach to study the roles of individual residues in catalysis and cofactor binding (253).

The two-point mutations in the earliest *cydD1* allele are G319D and G429E (86). Based on homology modeling, the G429 residue is close to a conserved aspartate residue; it is postulated that substitution for a glutamate (also negatively charged) could disrupt the Walker A motif and abolish function. Mutation of G319, which was found to be buried at the bottom of the hydrophobic pocked, may also impact upon conformational changes during the catalytic cycle [see Poole *et al.* (253)].

4. Physiological impacts of CydDC function. Based on the above data on the effects of CydDC on periplasmic physiology, the pleiotropic phenotype of *cydDC* strains may result predominantly from the disruption of disulfide folding in that compartment (248). Indeed, sensitivity of the *cydDC* mutant to benzylpenicillin was attributed to misfolding of the disulfide-containing penicillin-binding protein 4. The observed loss of cell motility in *cydDC* strains may result, for example, from a defective P-ring motor protein (247), since exogenous cystine (*i.e.*, oxidized cysteine) corrects a motility defect in a *dsbB* mutant (89). Complementation of *cydDC* strains with exogenous reductant largely complemented the phenotypes associated with defective disulfide folding (248).

It is important to differentiate between deficiencies of oxidase *per se* and the additional defects in *cydDC* mutants, which do not assemble cytochrome *bd*. This distinction is difficult because both *cydDC* and *cydAB* mutants display diverse and sometimes overlapping phenotypes (252). All *cydAB* mutants (i) appear to lack spectroscopically detectable cytochrome *bd*, (ii) fail to survive as robustly as WT cells in

13

stationary phase (299), (iii) are sensitive to inhibitors (cyanide, azide, Zn(II) ions) (260), and (iv) intolerant of oxidative and nitrosative stresses (117, 124, 146, 295). *cydDC* mutants also exhibit low levels of other cytochromes, particularly those haemproteins in the periplasm (254), and have a more oxidized periplasm. The failure of *cydDC* mutants to export to the periplasm GSH and cysteine results in a more oxidized periplasm. However, we do not understand why *bd*-type oxidase assembly is inhibited by these defects. Among plausible hypotheses are the following:

- The haems exported by CydDC to the periplasm (74) may be assembled onto outward-facing domains of the oxidase subunits. The finding that haem stimulates the ATPase activity of purified CydDC is intriguing (Section III.B.2).
- The haems exported by CydDC to the periplasm CydDC occupy there critical sites such as on chaperones required for oxidase assembly.
- The processing and assembling processes of the periplasm are intolerant of the oxidized nature of the periplasm in *cydDC* mutants.
- In addition to GSH and cysteine, which were identified as substrates for CydDC in transport studies, CydDC may export other thus-far unidentified metabolites.

We discuss the implications of cytochrome *bd* deficiency (and by extension of *cydDC* mutations) in Sections VI to VIII and in Poole *et al.* (253).

5. Conclusions. CydDC is of great interest for its profound impact on oxidase assembly and also because it was the first heterodimeric ABC-type exporter to be described in prokaryotes. The genes may or may not be found in an operon with the structural oxidase genes. The loss of *bd*-type oxidase assembly and function in *cydDC* mutants reveals CydDC to be crucial for this respiratory complex. The CydDC system transports to the periplasm reducing molecules, notably GSH and cysteine, which stimulate the ATPase activity of the isolated CydDC complex. We lack information on other potential substrates for CydDC and unambiguous evidence that haem is transported outward to the periplasm where it may be assembled into the oxidase. A direct involvement of haem with CydDC function is, however, suggested by studies *in vitro* of the ATPase activity of CydDC.

IV. Spectral and Redox Properties

The absorption spectra of the three haems, b_{558} and b_{595} (which are protohaems IX) and *d* (which is a *cis*-haem *d* hydroxychlorin γ-spirolactone) constitute the overall absorption spectrum of cytochrome *bd*. To date, the *E. coli* cytochrome *bd*-I is the only cytochrome *bd* for which, by means of spectroelectrochemical redox titrations, the difference (reduced minus oxidized) in spectra of all three haems in the α-, β- (32, 185, 210), and Soret (32) regions was resolved (Fig. 12). The position of the Soret band maximum for haem b_{595} is consistent with that unveiled before by femtosecond spectroscopy (50, 328) and by investigations on the E445A mutant (6, 269). The spectral contribution of haem *d* to the aggregated Soret band is much smaller than those of either *b*-type haems.

Upper asymptotic redox potentials of haems b_{558}, b_{595}, and *d* in the *E. coli* cytochrome *bd*-I in sucrose monolaurate at pH 7.0 are +172, +182, and +256 mV, respectively (32). These values are consistent with those for apparent redox potentials of the haems in *bd*-type oxidases from *E. coli* and *A. vinelandii* reported earlier (17, 169, 185, 211, 220, 264, 277). The detergent's nature affects the apparent redox potentials for haems *b*, particularly haem b_{558}, but has virtually no effect on the haem *d* potential (32, 211). In the absence of haem *d*

FIG. 12. Resolved different absorption spectra (reduced minus oxidized) of haems b_{558}, b_{595}, and *d* in the WT *E. coli* cytochrome *bd*-I in the presence of 50 m*M n*-octyl-β-D-glucoside at pH 7.0. Haem b_{558} has an α-band at 561 nm, β-band at 531.5 nm, and the Soret band with $\lambda_{max} = 429.5$ nm and $\lambda_{min} = 413$ nm. Haem b_{595} shows an α-band at 594 nm, β-band at 561.5 nm, a trough at 643 nm reflecting its MLCT band, and the Soret band with $\lambda_{max} = 439$ nm and $\lambda_{min} = 400$ nm. Haem *d* displays an α-band at 629 nm, a trough at 740 nm (its MLCT band), and the Soret band with $\lambda_{max} = 430$ nm and $\lambda_{min} = 405$ nm. MLCT, metal-to-ligand charge transfer. Modified from Bloch *et al.* (32).

(in the E99L mutant), a large interaction potential (about −90 mV) between haem b_{558} and haem b_{595} is observed (32). The presence of haem d reduces the redox interaction between the two haems b by ca. three times.

In contrast, redox interaction between haem d and either b-type haems is weak. The latter apparently contradicts the fact that the distance between haems b_{558} and b_{595} is longer than that between haems d and b_{595} (281). However, a strong redox interaction between redox-active metal sites does not always mean a short distance between them. Lack of significant electrostatic interaction at short distance may be due to screening of the electron charge by the proton taken up on reduction (32). For instance, in cytochrome c oxidase, the distance between haem a_3 and Cu_B is much shorter than that between haem a_3 and haem a (154, 322). At the same time, redox interaction between haem a_3 and Cu_B was not reported, whereas the redox interaction between haems a and a_3 is significant (236). Notably, the redox interaction between haems a and a_3 in cytochrome c oxidase (−115 mV at pH 8.0) (128) is significantly larger than that in cytochrome bd-I.

This may be relevant to the proton pumping mechanism in cytochrome c oxidase (10, 196), although transient states occurring during the enzyme's catalytic cycle may not be accessible in equilibrium redox titrations (300). A possible redox interaction between semiquinone and the haems in cytochrome bd remains to be examined, although the midpoint potential of the bound quinone in cytochrome bd-I was reported (139).

Being high-spin pentacoordinate, haem d can bind not only the O_2 enzyme natural substrate but also exogenous ligands, such as CO (7, 34, 37, 38, 44, 50, 52, 54, 142, 143, 165–167, 169, 210, 232, 269, 302–304, 328), NO (34, 41–44, 148, 163, 167, 168), cyanide (34, 167, 177–179, 181, 198, 249, 262, 263, 277, 312, 313, 321), and H_2O_2 (35, 43, 49, 116, 155, 172, 209, 259). A marginal ligand reactivity of the haems b was also observed (34, 37, 52, 54, 143, 302). Detailed discussion of the reactions of cytochrome bd with the exogenous ligands is beyond the scope of this review but can be found in Borisov *et al.* (48) and Junemann (163).

V. Catalytic Cycle

Whereas the superfamily of haem/copper oxidases comprises both quinol and cytochrome c oxidases, the bd-type oxidases characterized thus far are all quinol oxidases. Unlike cytochromes c, quinols are two-electron-donating substrates. Yet, they are oxidized by cytochrome bd through sequential one-electron transfer steps, with O_2 acting as the electron acceptor (36, 48, 163). Three quinol types with distinct structural differences can act as physiological substrates for cytochrome bd: ubiquinol (UQH_2), menaquinol (MQH_2), and plastoquinol.

The nature of the quinol substrate can be species-specific or dependent on growth conditions. For instance, mycobacterial and cyanobacterial bd enzymes utilize MQH_2 and plastoquinol, respectively (24, 25, 73, 246), while *E. coli* cytochrome bd can use UQH_2 or MQH_2 depending on O_2 availability (24, 25, 246, 323). Interestingly, some cytochromes bd were found to copurify with tightly bound quinols (19, 20), and a structural role in dimer stabilization was proposed for the UQ8 molecule detected in the recently solved structure of *E. coli* cytochrome bd-I (280).

The primary acceptor of electrons donated by the quinol substrate is haem b_{558} (Fig. 13). From there, electrons are transferred intramolecularly to the haems b_{595} and d, but it is unclear which of the two other haems is reduced first upon oxidation of haem b_{558}. The structure of the *G. thermodenitrificans* enzyme (281), with the haems b_{558} and d significantly closer to each other than the two b-type haems (edge-to-edge distance of 5.9 *vs.* 8.5 Å, and Fe-Fe distance of 15.2 *vs.* 19.4 Å), points to a direct electron transfer from haem b_{558} to haem d.

Conversely, the recently solved structure of *E. coli bd*-I enzyme (280) with the same triangular arrangement of cofactors and similar interhaem distances, but interchanged haems b_{595} and d, suggests that electron transfer proceeds along the pathway haem $b_{558} \rightarrow$ haem $b_{595} \rightarrow$ haem d (Fig. 13). Despite this uncertainty, in both structures the haems b_{595} and d, without forming a binuclear site with their Fe atoms, are in van der Waals contact (edge-to-edge distances of 3.5 and 3.8 Å in the *G. thermodenitrificans* and *E. coli* enzyme, respectively). Therefore, regardless of which haem acts as the primary acceptor for electrons donated by

FIG. 13. Overview of electrogenic pathways in cytochrome *bd*. The oxidase comprises two major subunits (CydA, CydB) and a smaller subunit (CydS in *G. thermodenitrificans*, CydX in *E. coli*). An additional previously unknown accessory subunit (CydH) was recently revealed in the *E. coli* enzyme (280). Electrons donated by the quinol substrate (QH_2) are transferred to haem b_{558} and from there to the haems b_{595} and d, which are in fast redox equilibrium. Midpoint potentials of the haems of cytochrome bd from *E. coli* (32) and *G. thermodenitrificans* (280) are reported in mV near the haems. In Safarian *et al.* (280), the b haems of the enzyme from *G. thermodenitrificans* are not assigned but termed haem b^{N1} (+50 mV) and haem b^{N2} (+155 mV) here, respectively, assigned to haem b_{558} and haem b_{595}. The electron pathway may vary between the *G. thermodenitrificans* and the *E. coli* enzyme, as they display a similar haem arrangement, but with exchanged haems b_{595} and d (280, 281). The O_2 reduction to H_2O takes place at haem d. The reaction is electrogenic because protons deriving from quinol oxidation are released into the periplasm, whereas protons required for the O_2 chemistry are taken up from the cytoplasm.

haem b_{558}, electron equilibration between the haems b_{595} and d is expected to be very rapid.

The intramolecular electron transfer processes taking place inside cytochrome bd are not coupled to a proton pumping activity (267). Nevertheless (see section III.A), electron transfer is electrogenic and leads to generation of a transmembrane electric potential; its existence has been demonstrated for the enzymes from *E. coli* and *A. vinelandii* with diverse experimental approaches (19, 20, 26, 38, 51, 155, 183, 186, 187, 223, 224, 267). Generation of the transmembrane electric potential occurs as the electrons are transferred from haem b_{558} to the haems b_{595} and d (19, 20, 38, 155).

The potential arises from uptake and release of protons during electron transfer, but not from the electron transfer itself, in line with the information that the three haems are located at relatively similar depths inside the membrane. Experimental evidence suggests that the transmembrane electric potential results from the combined release into the periplasmic space and uptake from the cytoplasmic space of protons, respectively, associated with quinol oxidation and intramolecular reduction of haems b_{595} and d (19, 20, 38, 155) (Fig. 13). Thus, in the absence of a true redox-coupled proton pumping activity, combination of these events accounts for a vectorial proton transfer across the membrane, thereby contributing to the electric potential buildup.

Cytochrome bd in turnover conditions processes O_2 to H_2O with a very high affinity for O_2. For the *E. coli bd*-I and *bd*-II oxidases, low $K_{m(O2)}$ values were determined, respectively, in the 0.003–0.3 and 0.24–2.0 μM range, depending on the experimental approach used (16, 88, 156, 217). An usual feature of cytochrome bd among terminal oxidases is that in the single-electron reduced state ($\mathbf{R}^{1,\dagger}$), it can bind O_2 at reduced haem d to give a stable and spectroscopically distinct globin-like ferrous-oxy adduct ($\mathbf{A}^1$), first identified by Poole *et al.* (257). O_2 binds reduced haem d in the $\mathbf{R}^1$ state with high affinity [O_2 dissociation constant $K_{d(O2)}$ of 0.28 and 0.5 μM for the *E. coli* and *A. vinelandii* enzyme, respectively (17, 18)], accounting, at least in part, for the low $K_{m(O2)}$ values displayed by cytochrome bd in turnover [see Junemann *et al.* (164) and reference therein].

Interestingly, the single-electron ($\mathbf{R}^1$) and three-electron ($\mathbf{R}^3$) reduced states of the enzyme were found to bind O_2 at reduced haem d with remarkably different kinetics (17). Whereas O_2 binding to the $\mathbf{R}^3$ enzyme occurs with rates proportional to $[O_2]$, in the case of $\mathbf{R}^1$, a hyperbolic dependence of O_2 binding rates on $[O_2]$ was documented and proposed to result from an equilibrium between two conformations (called "open" and "closed") with different accessibility of O_2 to reduced haem d (17). This finding suggests that the reactivity of reduced haem d toward gaseous ligands is modulated by the redox state of haem b_{558} and/or haem b_{595}. Consistently, CO was found to bind and dissociate from haem d in the $\mathbf{R}^1$ enzyme more slowly than in the $\mathbf{R}^3$ enzyme, and a higher k_{off} of NO was reported for the $\mathbf{R}^3$ enzyme compared with the $\mathbf{R}^1$ enzyme (44, 142, 169, 269).

Binding of O_2 to the fully reduced enzyme leads to the four-electron reduction of O_2 to $2H_2O$ *via* several catalytic intermediates, which are similar in nature to those populated

---

†The superscript number denotes the total number of electrons in the enzyme species.

in the O_2 reaction with haem/copper oxidases. A scheme of the catalytic cycle is presented in Figure 14. In flow-flash experiments coupled with spectroscopic or electrometric measurements, it was found that haem d in the $\mathbf{R}^3$ enzyme binds O_2 very rapidly [$k_{on} \sim 2 \times 10^9 \ M^{-1} \ s^{-1}$ (17, 19, 142)] and forms a ferrous-oxy species ($\mathbf{A}^3$) without generating electric potential (19, 155). The same species can be observed immediately after photolysis of the CO-ligated ferrous species at temperatures below $-100°C$ (257). At room temperatures, this is followed by a rapid ($\tau = 4.5 \ \mu s$) nonelectrogenic transfer of three or four electrons to the bound O_2, respectively, resulting in the formation of either a true peroxy intermediate ["$\mathbf{P}$," (19, 38)] or a ferryl species with a radical on an amino acid or the haem porphyrin [$\mathbf{F}^*$, (242)].

Although the detailed chemical nature of this intermediate remains uncertain, it was noted that the recently solved structure of the *E. coli* enzyme does not rule out the occurrence of a true $\mathbf{P}$ intermediate (280). Regardless of its chemical identity, this intermediate (whether $\mathbf{P}$ or $\mathbf{F}^*$) is rapidly ($\tau = 47 \ \mu s$) and electrogenically converted into a nonradical ferryl $\mathbf{F}$ intermediate upon transfer of an additional electron from haem b_{558} (19, 20, 38, 155). In the presence of quinol(s) tightly bound to the enzyme, one or two electrons can be further transferred rapidly ($\tau = 0.6$–1.1 ms) to the O_2 binding site, respectively, converting the $\mathbf{F}$ intermediate into either a fully oxidized ($\mathbf{O}$) or a single-electron reduced oxygenated species ($\mathbf{A}^1$), further contributing to generation of the electric potential (19, 20).

In stopped-flow multiwavelength spectrophotometric experiments, the steady-state level of the catalytic O_2 intermediates of cytochrome bd was measured in turnover conditions sustained with excess dithiothreitol and Q_1. Under these conditions, at steady state, the mostly populated intermediates proved to be the ferryl ($\mathbf{F}$) and oxy-ferrous ($\mathbf{A}$) species, whereas only a minor portion of the enzyme was found to be in the $\mathbf{O}^1$ state with the electron residing on haem b_{558} (45), in accordance with the proposal that the fully oxidized $\mathbf{O}$ species does not take part in the catalytic mechanism (233, 343).

VI. Physiological Functions

The core functions of terminal oxidases are oxygen reduction, generally to water, reductant consumption (in this case ubiquinol), and proton movements across the membrane, either by proton pumping mechanisms (as in the case of the haem/copper superfamily) or balanced proton extrusion to the outside (periplasm) and uptake from the inside (cytoplasm), as in the case of cytochrome bd (Fig. 15). However, in the case of cytochrome bd, we can discern extra physiological functions or attributes of great interest. These are summarized at the foot of Figure 15 and described in detail in the following sections.

A. Respiratory protection of nitrogenase

In addition to its unique structure, characteristic modes of expression, oxygen kinetics, and resistance to inhibitors (sections C and VII), cytochrome bd is unusual in being implicated in a physiological mechanism termed respiratory protection. This is the maintenance of function of bacterial nitrogenase, an oxygen-labile enzyme, even under aerobic
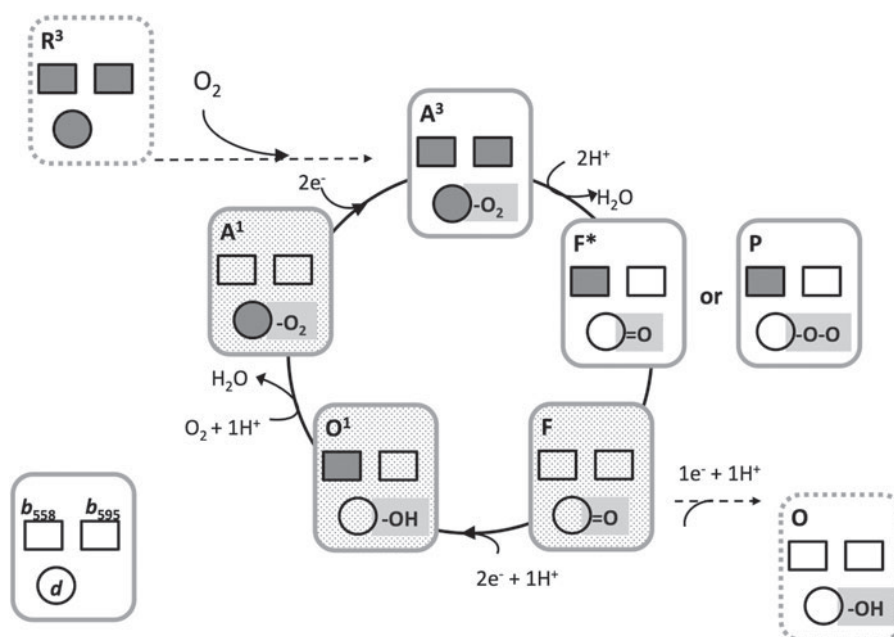
FIG. 14. Intermediates generated in the catalytic cycle of cytochrome *bd*. For each intermediate, the superscript number indicates the total number of electrons in the enzyme. Oxidized and reduced haems are, respectively, in *white* and *gray*. Bound O_2 and its derivatives are in *yellow*. The intermediates are denoted as follows: $\mathbf{R^3}$, fully (three-electron) reduced; $\mathbf{A^3}$, fully reduced with O_2 bound at ferrous haem *d*; $\mathbf{A^1}$, single-electron reduced with O_2 bound at ferrous haem *d*; $\mathbf{O^1}$, single-electron reduced with ferrous haem b_{558}; $\mathbf{O}$, fully oxidized; $\mathbf{P}$, peroxy. $\mathbf{F}$ and $\mathbf{F^*}$ are both ferryl intermediates, the *asterisk* denoting a radical on the haem *d* porphyrin ring. The shadowed intermediates are those detected at steady state in Borisov *et al.* (45).
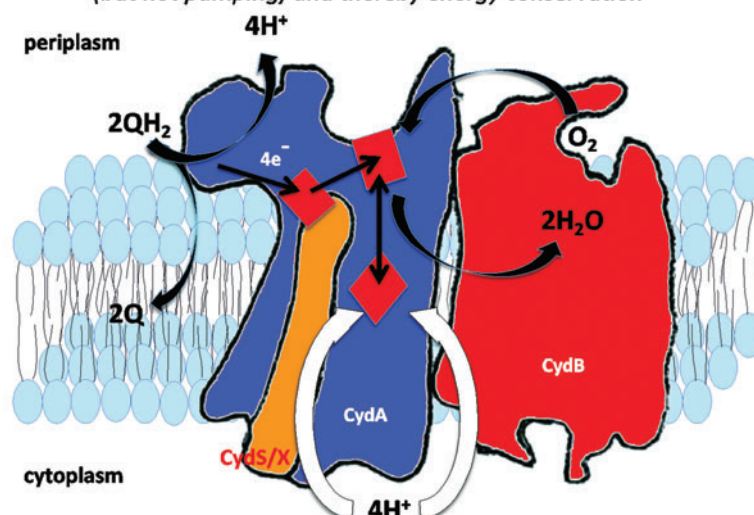
conditions, this being attributed to the phenomenal capacity of cytochrome *bd* for rapid oxygen consumption.

The free-living obligate aerobe *Azotobacter* can fix dinitrogen over a wide range of oxygen concentrations, despite the notoriously oxygen-sensitive activity of its nitrogenase.

Azotobacter adapts its respiratory rate in response to changing oxygen tensions (101) and, when fixing nitrogen, has one of the highest rates of respiration known (256). Dalton and Postgate proposed that ''uncoupled'' respiratory activity might prevent oxygen inhibition of nitrogenase activity (90).

FIG. 15. Overview of the structure and functions of the cytochrome *bd* class of terminal oxidases. The simplified structure of a three-subunit, three-haem complex in the membrane bilayer is drawn schematically, showing ubiquinol oxidation, electron transfers, oxygen reduction, and proton translocation. Key functions are shown above the scheme. Below the scheme are three major classes of additional attributes that, collectively, render cytochrome *bd* an important target for therapeutic interventions against bacteria. The fourth small subunit CydH/Y discovered in the *E. coli* cytochrome *bd*-I (280, 317) is not shown for simplicity. Color images are available online.

17

The evidence that this involves cytochrome *bd* is manifold: (i) the level of the oxidase increases when oxygen supply increases (*e.g.*, Moshiri *et al.* (230), but not in *E. coli*, where *cydAB* is expressed maximally at low O_2 tensions; see section II.D); (ii) consumption of carbon and energy sources is partially uncoupled from anabolism, specifically *via* cytochrome *bd*; and (iii) critically, Cyd⁻ mutants cannot fix nitrogen in air (180). However, a cytochrome *bo₃* mutant is aerotolerant during nitrogen fixation (203). The Fnr-like transcription factor CydR (338, 339) controls the expression of both cytochrome *bd* and the uncoupled NADH-ubiquinol dehydrogenase (Ndh) (27), which is thought to supply electrons to cytochrome *bd*-I and is also essential for aerotolerant nitrogen fixation (28).

The conclusion that cytochrome *bd* affords respiratory protection is supported by genetic studies of other bacteria. In *Azorhizobium caulinodans*, both cytochrome *bd* and cytochrome *cbb₃* contribute equally to nitrogen fixation in root nodule symbiosis; the double mutant totally lacked symbiotic N_2 fixation (175). In *Klebsiella pneumoniae*, N_2-fixing ability was severely impaired in a *cyd* mutant even at low oxygen concentrations (170).

The hypothesis of respiratory protection, specifically by cytochrome *bd*, is widely accepted and the genetic evidence (*i.e.*, that Cyd⁻ mutants cannot fix nitrogen in air) is viewed as the most convincing (238). Nevertheless, objections have been raised. One of these is that *total* respiratory oxygen consumption is not elevated above 70 μM O_2, where protection should be most important. However, *A. vinelandii* possesses, based on genome interrogation (293), five terminal oxidases: cytochrome *c* oxidase (Cdt), cytochrome *o* (Cox), cytochrome *bd* copy I (CydAB I), cytochrome *bd* copy II (CydAB II), and cytochrome *cbb₃* (Cco).

Note that the mutagenesis approach in Kelly *et al.* (180), which is taken as the best evidence for respiratory protection, was targeted at cytochrome *bd*-I. The presence of multiple oxidases allows flux through different branches, only one of which terminates in cytochrome *bd*-I, to be redistributed during protection of nitrogenase without elevation of total respiratory rates. A second concern is that the efficiency of respiration in protection may be insignificant because the rate of consumption is too low to prevent diffusion of O_2 into cells. However, the location of the O_2-reducing site deep within the oxidase structure may block O_2 access to the cytoplasm.

Clearly though, unanswered questions remain regarding the details of the mechanisms, and other factors (intracellular redox state, ATP provision for nitrogenase, and O_2 control of nitrogenase) might be important. Note, however, that "uncoupled" respiration (*i.e.*, respiration that is not coupled to PMF generation) is not an essential requirement of the proposed mechanism, which is only that cytochrome *bd*-supported oxygen uptake uniquely provides the protection. Other mechanisms probably play roles: thus, the alginate capsule of *A. vinelandii* is affected by oxygen tension and could create a barrier to the entry of oxygen (279). However, the genetic data do appear to provide the evidence required by Oelze (238) for the hypothesis of respiratory protection.

B. An oxygen-reactive oxidase in anaerobes?

Anaerobic microbes are sometimes defined as those that cannot grow at dissolved oxygen concentrations greater than 5 μM; however, many "anaerobes" survive at such levels. *B. fragilis* colonizes the colon, even in the absence of facultative anaerobes that could maintain low oxygen concentrations, and grows at oxygen concentrations around 300 nM. *B. fragilis* encodes a cytochrome *bd*-type oxidase and consumes oxygen at appreciable rates, but a $\Delta cydAB$ mutant was defective in oxygen uptake (13). In this organism, and in many prokaryotes that have been classified as strict anaerobes, *cyd* genes are widely distributed; these bacteria include *Methanosarcina*, *Archaeoglobus*, *Moorella*, and *Geobacter* species (13, 92, 205). The term "nanaerobes" has been coined to describe such bacteria that can benefit from, but do not require, oxygen for growth (13).

In the case of facultative anaerobes such as *E. coli*, survival in low-oxygen environments, such as the mammalian intestine, depends on the organism's respiratory flexibility and in particular the presence of cytochrome *bd*. Mutants lacking cytochrome *bd* fail to colonize (159, 160). Expression of genes in *E. coli* that encode the oxidases and other respiratory chain complexes has been widely studied, and recently in the context of systems biology [for reviews see Bettenbrock *et al.* (30) and Ederer *et al.* (104)].

In brief, there occurs a progressive switch to aerobic respiratory metabolism and a remodeling of the cell envelope as oxygen availability increases (276, 319). Maximal levels of cytochrome *bd* occur at intermediate levels of oxygen supply, that is, at a point approximately midway between anaerobiosis and the onset of aerobic metabolism as inferred from acetate excretion during glucose metabolism (276). In contrast, the *cyoABCDE* operon was maximally expressed under fully aerobic conditions: changes in abundance of the *cydAB* and *cyoA–E* transcripts were reflected cellular contents of cytochrome *bd* and cytochrome *bo₃*, respectively, consistent with the previously measured oxygen affinities. Cytochrome *bd*-II is also operative under limiting oxygen conditions (309).

Oxygen reduction is widespread in sulfur-reducing bacteria including some *Desulfovibrio* species (91) and supports chemiosmotic energy conservation (100). Although classified as an anaerobe, *D. gigas* contains a functional membrane-bound respiratory chain, including a canonical cytochrome *bd* quinol oxidase as its terminal enzyme (202, 215). Lemos *et al.* (202) demonstrated that membranes from *D. gigas* reduce oxygen to water and isolated a two-subunit oxidase of the cytochrome *bd* family, with spectral properties similar to other such oxidases. With NADH or succinate as electron donors, specific oxygen uptake activities were comparable with those of aerobes. Surprisingly, the expression levels of the oxidase were unaffected by 60 μM O_2, but modest upregulation was noted in the presence of 150 μM NO (215).

Other established anaerobes such as *D. vulgaris* respond to 0.1% oxygen exposure at the transcriptomic and proteomic levels (231). The genome sequence (140) indicates the presence of two oxidases: a cytochrome *c* oxidase and cytochrome *bd*. Both were confirmed by hybridization experiments with CoxA and CydA probes and further sequence analysis (288). The presence of *cydAB* genes in *D. vulgaris* was later confirmed and this oxidase shown to be more highly expressed than the *cox* operon encoding a *cc(o/b)o₃*-type oxidase (199). The oxygen affinity of the *bd*-type oxidase ($K_m = 600$ nM) was measured polarographically (268); however, such measurements probably overestimate the K_m value (88).

What are the roles of such oxidases in "anaerobes"? Plausible hypotheses include the following: (i) scavenging of O_2 for protection against the damaging effects of oxygen, (ii) ATP gain for survival aerobically in changeable habitats, and (iii) catalyzing a rapid, "uncoupled" electron transfer and burning excess reducing substrates. These functions may have long histories: phylogenetic analyses suggest that the Aquificae phylum is one of the earliest diverging phyla of Eubacteria for which sequence data are available and indicate that cytochrome *bd* was present in the most ancient Eubacteria (13). This is consistent with the view that sufficient oxygen to support respiration predated the photosynthesis-derived appearance of abundant oxygen on Earth.

C. Environmental stressors and their relationships with cytochrome bd

1. Peroxide. Cytochrome *bd* may contribute to protection against H_2O_2-induced stress. Mutant *E. coli* cells lacking cytochrome *bd* (126, 206, 329) showed high susceptibility to H_2O_2, and the same was shown for some pathogenic bacteria (14, 295). Consistently, addition of exogenous H_2O_2 (206) or endogenous production of ROS increased cytochrome *bd* expression (67). This protective role of cytochrome *bd* is not exclusive to *E. coli* [see Giuffrè *et al.* (124) and references therein]. Hypersensitivity to H_2O_2 or enhanced ROS production has been described also for other bacteria deficient in this oxidase (106, 340), including bacterial pathogens that inhabit microaerobic environments and are exposed to the ROS produced by the host immune system (107, 201, 212) or as a result of antibiotic treatments (212).

Accordingly, upon exposure to H_2O_2, an upregulation of cytochrome *bd* was documented in *Staphylococcus aureus* (66) and in *Mycobacterium tuberculosis*, where a catalase-independent hyper-resistance to H_2O_2 was also observed (305). When anaerobic cultures of an *E. coli* strain devoid of the antioxidant enzymes KatG, KatE, and Ahp are abruptly aerated, cytochrome *bd* is able to reduce intracellular H_2O_2 production (191), suggesting that the oxidase serves as an electron sink by diverting electrons from a fumarate reductase, a major H_2O_2-generator.

Moreover, *E. coli* cytochrome *bd*-I was shown to be capable of detoxifying H_2O_2 directly (Fig. 16). A high catalase activity was observed in both the isolated untagged *bd*-I enzyme and in catalase-deficient cells overexpressing cytochrome *bd*-I (40, 114). Cytochrome *bd*-I also shows peroxidase activity (1, 39, 182), particularly in the His-tagged enzyme with decyl-ubiquinol as the electron donor (1). The latter preparation, however, displays no catalase activity (1). The issue is discussed in Forte *et al.* (117). It remains to be established whether the H_2O_2-metabolizing ability is unique to the *E. coli* enzyme or is a common property of *bd*-type oxidases.

2. NO and ONOO⁻. NO and the product of its reaction with superoxide radical ($O_2^{•−}$), ONOO⁻, are produced by the host as part of the immune response to kill invading microbes. Cytochrome *bd* is involved in protection of bacteria against stress caused by these RNS. Transcriptional upregulation of genes encoding cytochrome *bd* has been observed in response to NO exposure in *E. coli* (150, 265) and in other bacteria (215, 229, 273, 296). NO induces greater growth inhibition in cytochrome *bd*-deficient *E. coli* strains, compared with cy-
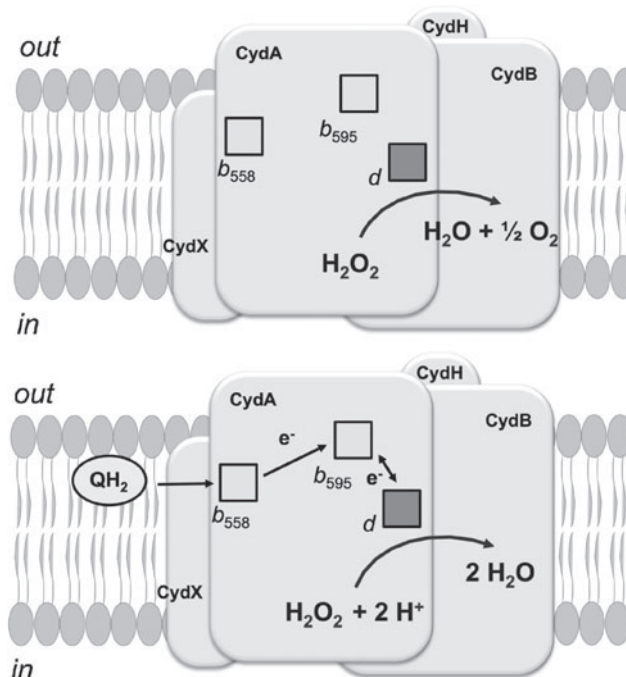

FIG. 16. *E. coli* **cytochrome *bd*-I is proposed to have catalase [(40),** *top***] or quinol peroxidase activity [(1),** *bottom***].**

tochrome bo_3-deleted mutants (217). The effect is observed in mutants of both the cytochrome *bd*-encoding *cydAB* genes and the *cydDC* genes (146).

Similar observations were made in cytochrome *bd* mutants of uropathogenic *E. coli* (14, 295). Cytochrome *bd* also protects *Salmonella enterica* against NO toxicity thereby enhancing its virulence (161). Like cytochrome *c* oxidase (289, 290), cytochrome *bd* is potently but reversibly inhibited by NO [$IC_{50} \sim 0.1 \, \mu M$ NO at $70 \, \mu M \, O_2$ (42)]. Such inhibition was shown both with *E. coli* cells (217, 310) and with cytochrome *bd* isolated from *E. coli* or *A. vinelandii* (42). NO reacts with haem *d*: when haem *d* is ferrous, oxy-ferrous, or ferric, the end-product is nitrosyl (41, 42, 44), whereas reaction of the ferryl haem *d* with NO yields nitrite (43) (Fig. 17). Due to an unprecedentedly high off-rate of NO from the ferrous haem *d*, reversal of cytochrome *bd* inhibition is much faster than with cytochrome *c* oxidase (42, 44, 217), explaining why cytochrome *bd* confers NO resistance to bacteria.

A further reason could be that ferryl cytochrome *bd*, a highly populated intermediate in turnover (45), converts NO into less toxic nitrite at a rate ~ 10 times higher than that of the analogous reaction of the ferryl cytochrome *c* oxidase (43).

ONOO⁻ was reported to irreversibly inhibit cytochrome *c* oxidase (294), whereas *E. coli* cytochrome *bd*-I is highly resistant to inhibition (47). Furthermore, cytochrome *bd*-I can metabolize this harmful RNS with an apparent turnover rate of ~ 10 mol ONOO⁻ (mol enzyme)$^{-1}$ s^{-1}, thereby playing a protective role against ONOO⁻ damage.

3. Sulfide. Sulfide potently inhibits cytochrome *c* oxidase, leading to energy depletion and cell death (76, 235, 244, 315). As many bacteria synthesize H_2S and inhabit sulfide-rich environments, such as the human colon, they may be endowed with a sulfide-insensitive oxidase, other than
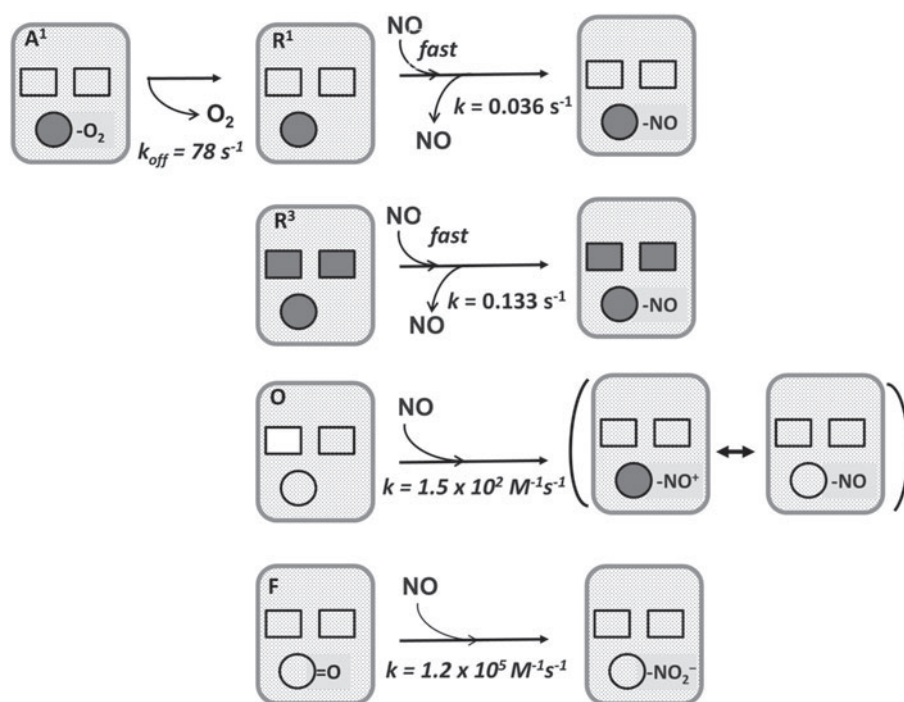
FIG. 17. **Reactions of cytochrome *bd* species with NO. A^1 reacts with NO after O_2 displacement yielding the single-electron reduced species (R^1).** The reaction with the A^1 intermediate is thus rate limited by O_2 dissociation. The R^1 and R^3 species react with NO quickly, yielding a nitrosyl ferrous (Fe^{2+}–NO) adduct. NO dissociates from R^3 species fourfold faster than from R^1. The **O** species reacts with NO, yielding a nitrosyl ferric (Fe^{3+}–NO $\leftrightarrow Fe^{2+}$–NO^+) adduct. The reaction of **F** with NO yields a nitrite–ferric (Fe^{3+}–NO_2^-) derivative. NO, nitric oxide.

cytochrome *c* oxidase. This hypothesis was tested on *E. coli* reaching the conclusion that such an oxidase is cytochrome *bd* (115, 192). Forte *et al.* found that whereas sulfide is a potent inhibitor of cytochrome bo_3 ($IC_{50} \sim 1.1 \, \mu M$), both cytochrome *bd*-I and cytochrome *bd*-II of *E. coli* are insensitive to sulfide up to 58 μM (115).

Furthermore, in *E. coli* mutants, O_2 respiration and growth are impaired by sulfide when respiration is sustained by cytochrome bo_3 alone, but unaffected by up to 200 μM sulfide when *bd*-I or *bd*-II acts as the only terminal oxidase. Similarly, Korshunov *et al.* reported that in a cytochrome *bd*-deficient mutant, both O_2 respiration and growth are inhibited by sulfide, exogenously administered or endogenously generated from cysteine (192). The sulfide insensitivity of cytochrome *bd* is possibly due to the lack of a copper site, since inhibition of cytochrome *c* oxidase by sulfide is thought to involve a transient binding of H_2S to Cu_B (235).

Based on these data, it was postulated that the sulfide tolerance provided by cytochrome *bd* can play a role in shaping the composition of human intestinal microbiota, thus impacting human physiology and pathophysiology (62). Interestingly, upregulation of the cytochrome *bd*-I and *bd*-II genes was observed in *E. coli* cells following addition of an H_2S donor, alone or in combination with the antibiotic ampicillin, indicating that expression of the sulfide-insensitive oxidases enables bacterial respiration under antibiotic-induced oxidative stress (298). Indeed, *E. coli* mutant strains lacking *bd*-type oxidase fail to colonize the mouse intestine, contrary to those lacking bo_3-type oxidase (159).

4. Chromate. Cytochrome *bd* has been recently shown to contribute to chromate resistance in *Alishewanella* sp. WH16-1 (340), a facultative anaerobic bacterium isolated from the soil of a copper and iron mine. This strain efficiently reduces sulfate to sulfide and the toxic hexavalent chromate Cr(VI) to the much less toxic Cr(III), thus showing a great potential for chromate bioremediation. Cr(VI), mainly produced by human activities, is considered a severe pollutant and a serious threat to human health, being mutagenic and carcinogenic. The high toxicity of Cr(VI) is linked to its ability to enter the cells and exert a strong oxidizing power. The structural similarity with sulfate allows Cr(VI) to cross the cellular membrane *via* sulfate transporters (80, 326) and, once in the cell, to generate ROS (306, 326).

Cytochrome *bd* confers bacterial resistance to chromate by decreasing chromate-induced cellular oxidative stress and allowing sulfide-dependent chromate reduction (340). In *Alishewanella* sp. WH16 WT and cytochrome *bd* mutant strains, the addition of millimolar K_2CrO_4 resulted in a higher H_2O_2 production in cytochrome *bd*-deficient cells compared with the WT or the cytochrome *bd*-complemented strain, suggesting a role for *Alishewanella* cytochrome *bd* in H_2O_2 detoxification, as also shown for the *E. coli* oxidase (1, 40).

Furthermore, in H_2O_2 inhibition zone tests, the mutant strain was more sensitive to exogenous H_2O_2 than was the WT. Since sulfide can be used as a reductant to reduce chromate to less toxic forms, the effect of Na_2S on cell growth was also investigated. Whereas growth of the WT cells was unaffected by the presence of 200 μM sulfide in the culture medium, the cytochrome *bd*-deficient strain was completely inhibited under these conditions. Thus, the cytochromes *bd* of both *Alishewanella* Sp. WH16-1 and *E. coli* (115) contribute to resistance to sulfide and, indirectly, also to chromate. Summing up, cytochrome *bd* contributes to the remarkably lower minimum inhibition concentration (MIC) for chromate, as well as the ability of WT strains to reduce chromate to less poisonous forms (340).

VII. Antibiotics and Antimicrobial Agents

A. Cationic amphiphilic peptides with antimicrobial activities

Cationic amphiphilic peptides with antimicrobial activities can be divided into two major classes: nonribosomally and

ribosomally synthesized peptides (134, 237). Both classes typically further undergo maturation and chemical modifications. Nonribosomally synthesized peptides are produced only in bacteria and fungi. The biosynthesis of these peptides proceeds on multifunctional peptide synthetases in an RNA-independent manner following the multiple carrier thiotemplate mechanism (308). The synthetases have a modular organization, and these modules interact in an ordered manner to produce the peptide product (327). Gene-encoded ribosomally synthesized peptides are produced by all species and can be further subdivided into bacteriocins (produced by bacteria), archaeocins (produced by Archaea), and antimicrobial peptides (produced by eukaryotes) (216, 237).

Bacteria use cationic amphiphilic peptides to kill or limit the growth of competitors that occupy the same ecological niche. In higher organisms, antimicrobial peptides are part of the innate immune response. The peptides are thought to kill bacteria primarily due to their interaction with bacterial membranes or cell walls. Permeabilization of the microbial membrane lipid bilayer is a commonly accepted mechanism of their action, since the peptides usually have a net positive charge and a high ratio of hydrophobic amino acids. These properties enable the peptides to selectively bind to negatively charged bacterial membranes leading to nonenzymatic membrane disruption (347).

However, a growing body of evidence suggests that cationic amphiphilic peptides can have other molecular targets. One such target could be a *bd*-type terminal oxidase. Indeed, *E. coli* cytochrome *bd*-I is targeted by several peptides tested, such as gramicidin S, cathelicidin LL-37, and microcin J25 (MccJ25) (Fig. 18). Thus, cytochrome *bd*-I would hardly contribute to bacterial defense against these peptides but rather serves as a mediator of their action.

1. Gramicidin S. Gramicidin S ("Soviet") is non-ribosomally produced by the gram-positive soil bacterium *An-*
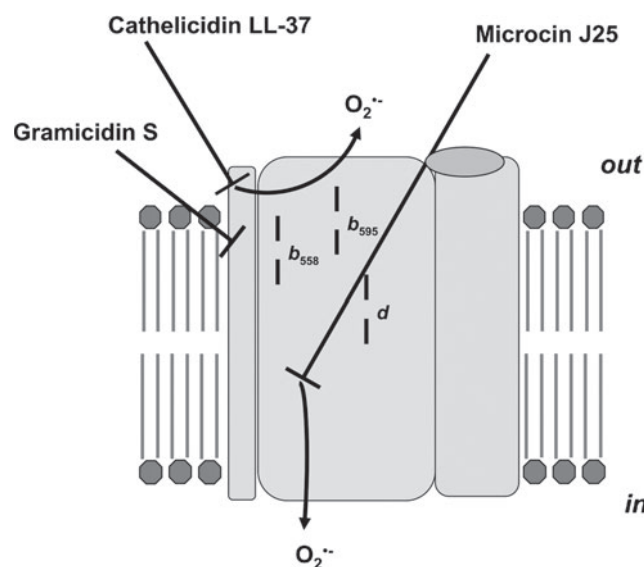

FIG. 18. Possible effects of cationic amphiphilic peptides with antimicrobial activities on *E. coli* cytochrome *bd*-I. Gramicidin S, microcin J25, and possibly cathelicidin LL-37 inhibit cytochrome *bd*-I. In addition, microcin J25 and cathelicidin LL-37 make cytochrome *bd*-I a site of superoxide ($O_2^{\bullet-}$) production (69, 118, 119, 228).

eurinibacillus migulanus. This is a cationic cyclic decapeptide made up of two identical pentapeptides joined head-to-tail with the primary structure [cyclo-(Val-Orn-Leu-D-Phe-Pro)$_2$]. The peptide has an antiparallel β-sheet arrangement stabilized by two type II′ β-turns and four intramolecular hydrogen bonds (149). Such a secondary structure makes the molecule amphiphilic that is probably essential for bioactivity. Gramicidin S at μM concentrations is active against gram-negative and gram-positive bacteria, fungi, viruses, and single-cell pathogenic eukaryotes (189). While the mechanism of cytotoxic activity of gramicidin S is still a matter of debate, the primary mode of its action is thought to be disruption of the integrity of the plasma membrane phospholipid bilayer. This leads to the increase in membrane permeability, dissipation of the membrane potential, and cell death (109).

It was shown recently that gramicidin S is a potent inhibitor of both membrane-bound and purified *E. coli* cytochrome *bd*-I (228). On the contrary, the naturally produced mixture of gramicidins A, B, and C, denoted collectively as gramicidin D, which are linear pentadecapeptides forming dimeric cationic channels, does not inhibit cytochrome *bd*. *E. coli* cytochrome *bo$_3$* and cyanide-insensitive quinol oxidase (CioAB) from *Gluconobacter oxydans* appeared to be one-order of magnitude less sensitive to gramicidin S. Although submicromolar concentrations of gramicidin S moderately stimulate the ubiquinol-1 oxidase activity of cytochrome *bd*-I, at higher peptide concentrations, cytochrome *bd*-I is inhibited. Upon preincubation of cytochrome *bd*-I with gramicidin S, IC_{50} values are in the range of 2.6–5.4 μM.

These values are consistent with the minimum inhibitory concentration (MIC) of *E. coli* cells (4–16 μM) (190), as well as IC_{50} values for 2-heptyl-4-hydroxyquinoline *N*-oxide (1 μM), antimycin A (5 μM), and piericidin A (10 μM), quinol oxidation site inhibitors (227, 228). This is thought to be mixed-type inhibition, decreasing the apparent V_{max} and the affinity for substrates (228). Gramicidin S does not affect the spectral properties of cytochrome *bd*-I in the air-oxidized and fully reduced states. The authors conclude that the *E. coli* cytochrome *bd*-I is a bacterial membrane target for the peptide, whereas according to current thinking, the principal target of gramicidin S is the lipid bilayer rather than any membrane protein. The underlying mechanism of inhibition may be an alteration of the cytochrome *bd*-I structure *via* binding to its hydrophobic surface.

2. Cathelicidin LL-37. Cathelicidins, along with defensins, are the two main families of ribosomally synthesized antimicrobial peptides, effector molecules of the innate immunity of mammals (318). Cathelicidins have a highly conserved N-terminal cathelin domain and a variable C-terminal antimicrobial domain. The latter can be released from the precursor peptide after protease cleavage. LL-37 is an active 37-residue α-helical C-terminal domain of the only human cathelicidin identified to date. The primary structure of LL-37 is LLGDFFRKSKEKIGKEFKRIVQRIKDFLRNLVPRTES (158). This 18-kDa propeptide is denoted as hCAP-18 (human cationic antimicrobial protein).

Recently, it was reported that cathelicidin LL-37 shows a fourfold lower MIC against *E. coli* in aerobic growth compared with under anaerobic or fermentation conditions (4 *vs.* 16 μM) (69). Thus, the MIC data suggest that the inhibition of *E. coli* growth by LL-37 is mediated by oxygen. In aerobic

growth conditions, LL-37 induces oxidative stress within seconds of contact with *E. coli*. To monitor oxidative stress, real-time, single-cell fluorescence imaging with the dyes CellROX Green and Amplex Red was used. ROS formation occurs after entry of LL-37 into the periplasm, but before permeabilization of the cytoplasmic membrane. Entry of the peptide into the periplasm gives it access to the outer leaflet of the cytoplasmic membrane and to external surfaces of cytoplasmic membrane proteins. Strong oxidative signals require a robust transmembrane potential and correlates with the lower MIC in aerobic, compared with anaerobic, growth conditions.

These observations imply that LL-37 affects the aerobic respiratory chain, disrupting electron flow. In aerobic *E. coli* cultures, the peptide-induced oxidative signals are attenuated in the cytochrome *bd*-I mutant but not in a cytochrome *bo₃* mutant (69). This suggests that LL-37 targets cytochrome *bd*-I, but not cytochrome *bo₃*, leading to release of ROS, most likely $O_2^{\bullet-}$, into the periplasmic space. The LL-37 action may be based on its direct interaction with cytochrome *bd*-I, for instance, due to electrostatic binding. Alternatively, being polycationic (net charge +6), LL-37 may impair cytochrome *bd*-I function indirectly by perturbation of the lipid environment, for example, *via* strong interaction with the annular anionic phospholipids such as cardiolipin or phosphatidylglycerol. The authors (69) propose that the host can use the degree of tissue aeration for selective control of the potency of LL-37 and possibly other antimicrobial peptides.

3. Microcin J25. Microcins are ribosomally synthesized bacteriocins produced by *E. coli* and related enterobacteria. MccJ25 belongs to class I microcins. This is a plasmid-encoded, posttranslationally modified, 21-residue lasso-peptide. The peptide is composed of the N-terminal macrolactam ring and the C-terminal tail. The ring consisting of eight amino acid residues is formed by a lactam bond between the first and eighth amino acids. The ring is threaded and trapped by the C-terminal tail of 13 residues forming a lasso (271). MccJ25 targets essentially foodborne pathogens, such as *E. coli*, *Shigella flexneri*, and *Salmonella enterica* serotypes Newport, Enteritidis, Heidelberg, and Paratyphi B (118).

To cross the outer membrane of a sensitive bacterium, MccJ25 uses the Trojan horse strategy. The peptide is thought to hijack FhuA, an outer-membrane transporter for Fe^{3+} chelated to the siderophore ferrichrome (285). The process requires a PMF that is transduced to FhuA by the inner membrane-anchored TonB–ExbB–ExbD complex. When in the periplasmic space, MccJ25 is proposed to interact with the inner membrane protein SbmA to cross the inner membrane (286). Once in the cytoplasm, MccJ25 inhibits bacterial transcription *via* interaction with RNA polymerase (RNAP). The peptide binds to the RNAP secondary channel that directs ribonucleotide precursors toward the active site, thereby blocking its operation in a cork in-the-bottle manner (271).

The other targets of MccJ25 are respiratory chains of sensitive bacteria. Although the inhibition mechanism is not yet completely clear, it was reported that the peptide can inhibit the activity of respiratory chain complexes and enhance $O_2^{\bullet-}$ production (21).

Recently, Galvan *et al.* examined the effect of MccJ25 on the properties of the *E. coli* terminal oxidases using bacterial cells, membranes (119), and the isolated enzymes (118). It was shown that *E. coli* mutant strains lacking cytochrome *bd*-I or cytochrome *bo₃*, in which the entry of MccJ25 is facilitated by overexpressing FhuA, are less sensitive to MccJ25 than the WT (119). The MIC of MccJ25-GA (a variant of MccJ25 in which the C-terminal carboxyl group is blocked with an L-glycine methyl ester that leads to the loss of its ability to interact with RNAP) for an *E. coli* cytochrome *bd*-I mutant increases 16-fold compared with WT. In the presence of MccJ25, membranes of the *E. coli* mutant expressing cytochrome *bd*-I as the only respiratory oxidase show significant ROS overproduction. The ROS overproduction observed with the membranes, however, is not seen with whole cells, possibly because detoxifying enzymes in the cytosol rapidly quench the ROS produced.

Membranes of the *E. coli* mutant expressing cytochrome *bo₃* as the only respiratory oxidase show no ROS overproduction in the presence of MccJ25. Galvan *et al.* concluded that MccJ25 affects *E. coli* cytochrome *bd*-I making it a major site of $O_2^{\bullet-}$ production. Interestingly, while the Δ*bo₃* and Δ*bd*-I mutants become less sensitive to the peptide compared with the WT, in the Δ*bo₃*/Δ*bd*-II and Δ*bd*-I/Δ*bd*-II double mutants, recovery of the original, WT-like sensitivity to MccJ25 and MccJ25-GA is observed. This observation allowed the authors to suggest that *E. coli* cytochrome *bd*-II may protect the cell from the deleterious effects of MccJ25 and MccJ25-GA (119). The protection could be achieved by ROS detoxification, but further investigation is required.

The inhibitory action of MccJ25 on enzymatic oxygen consumption was studied in detail with the isolated *E. coli* quinol oxidases, *bd*-I and *bo₃* (118). MccJ25 was found to inhibit the ubiquinol-1 oxidase activity of cytochrome *bd*-I with an IC_{50} of 76 μM. This is accompanied by a decrease in V_{max}, but K_m for ubiquinol-1 does not change significantly. Based on these effects of the peptide on the kinetic parameters, the authors proposed that MccJ25 inhibits cytochrome *bd*-I in a noncompetitive way (118). The influence of MccJ25-GA on the cytochrome *bd*-I activity appears to be similar to that of MccJ25. In contrast, the cytochrome *bo₃* activity is not affected by MccJ25, and V_{max} and K_m for ubiquinol-1 with and without peptide are not significantly different. When the isolated cytochrome *bd*-I is treated with MccJ25 or MccJ25-GA, ROS generation initiated by the addition of ubiquinol-1 increases by 39% or 31%, respectively.

Since superoxide dismutase suppresses ROS production, it was concluded that the generated species is $O_2^{\bullet-}$. Neither MccJ25 nor MccJ25-GA increases ROS production by the isolated cytochrome *bo₃*. The addition of MccJ25 to the air-oxidized cytochrome *bd*-I in the presence of 6 mM KCN induces absorption changes corresponding to the reduction of haem b_{558} and the displacement of bound O_2 from haem d^{2+}. Treatment of cytochrome *bo₃* with MccJ25 and cyanide causes no spectral change. Thus, the peptide can reduce cytochrome *bd*-I. This is consistent with the fact that MccJ25 is a redox-active peptide capable of forming a long-lived tyrosyl (Tyr9) radical (64).

However, it is still not clear whether the peptide-induced change in the oxidation state of cytochrome *bd*-I is related to its inhibitory action. It is possible that the binding of MccJ25 to the *bd*-I oxidase slows the rate of intraprotein electron transfer, for instance, by affecting quinol oxidation *via* conformational change in the protein. This could lead to the release of $O_2^{\bullet-}$, fast enough to compete with electron transfer to the oxygen-reducing site to form H_2O. It is clear, however,

that to have a significant inhibitory effect on both RNAP and the respiratory chain, the peptide should accumulate to high levels in the sensitive bacterial cell.

B. Other antimicrobial compounds

Cytochrome *bd* appears to be involved in the defense of mycobacteria against antibiotic-induced stress. Targeting the respiratory chain enzymes is now considered a new promising strategy for fighting multidrug-resistant, extensively drug-resistant, and totally drug-resistant strains of *Mycobacterium tuberculosis* (11, 72, 136). As for most bacteria, *M. tuberculosis* has a branched respiratory chain (71, 73). Electrons are transferred from the type II NDH or other dehydrogenases to the MQ pool, and then to O_2 through either the *bcc-aa₃* supercomplex, formed by cytochrome *bcc* (a variant of the *bc₁* complex) and cytochrome *aa₃*, or cytochrome *bd* (11, 72, 136, 152). The PMF thus generated powers of ATP synthesis by the ATP synthase.

1. Bedaquiline. Bedaquiline (BDQ; Sirturo™), a diarylquinoline compound (Fig. 19), was the first drug approved by the FDA and EMA that targets *M. tuberculosis* energy metabolism. It selectively inhibits the *M. tuberculosis* ATP synthase by binding to the c-ring rotor of its F_o subcomplex (4, 193, 261). As a result, ATP synthesis is inhibited and intracellular ATP levels decrease significantly (193, 194).

The inhibition mechanism is possibly based on the ability of BDQ, upon its localization at the ATP synthase, to create an uncoupled microenvironment by acting as an H^+/K^+ ionophore that causes dissipation of transmembrane pH and potassium gradients (137). The activity of BDQ appears to be specific for mycobacteria and is not observed with non-mycobacterial strains (4).

In mammalian cells, the compound affects neither the mitochondrial ATP synthase (133) nor the membrane potential (112). Killing of *M. tuberculosis* by BDQ is not concentration- but time-dependent, its bactericidal activity showing a delayed onset (195). The rate of *M. tuberculosis* H37Rv killing, however, is increased by 55% if cytochrome *bd* is mutated by replacing the *cydA* gene with a hygromycin cassette *via* specialized transduction (23).

While BDQ is bactericidal against *M. tuberculosis*, it is bacteriostatic against the nonpathogenic *M. smegmatis* (4). If the *cydA* gene is disrupted, susceptibility of *M. smegmatis* to BDQ increases (138) and the drug becomes bactericidal (212). Accordingly, both *M. tuberculosis* and *M. smegmatis* WT cells treated with BDQ show a marked increase in cytochrome *bd* expression levels (138, 195).

2. Clofazimine. Figure 19 shows the riminophenazine derivative clofazimine (CFZ) (12), a well-known antileprosy drug. The drug can also undergo reduction with NADH
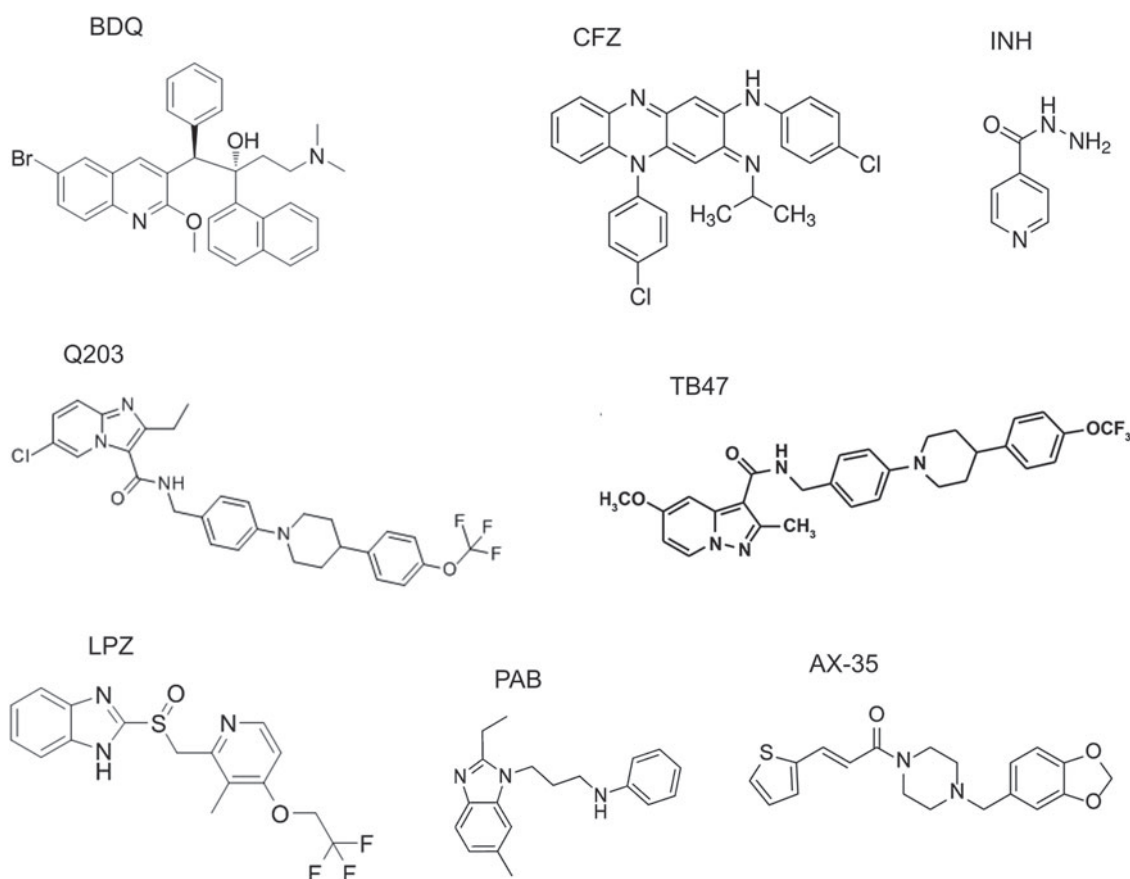

FIG. 19. Structures of antimicrobial compounds reported in section VII.B. Shown are BDQ (4), CFZ (12), INH (270), telacebec (Q203) (245), TB47 (213), LPZ (278), PAB compound 54 (65), and arylvinylpiperazine amide compound AX-35 (113). BDQ, bedaquiline; CFZ, clofazimine; INH, isoniazid; LPZ, lansoprazole; PAB, phenoxyalkylbenzimidazole; TB47, pyrazolo[1,5-*a*]pyridine-3-carboxamide.

catalyzed by NDH-2. Reduced CFZ is unstable and spontaneously oxidized by O_2, producing ROS (344). As NADH is continually produced in the Krebs cycle and fatty acid β-oxidation, the redox cycling of CFZ will continually run. The viability of the *M. smegmatis cydA* mutant is strongly reduced in response to CFZ compared with WT strains (212).

3. Isoniazid. Isoniazid (INH) (Fig. 19) is a first-line bactericidal antituberculosis drug that inhibits the biosynthesis of mycolic acids, the core components of the mycobacterial cell wall (270). Its activity, however, is reduced significantly under stress conditions, such as low aeration (335) and nutrient starvation (31). This indicates that the bactericidal effects of INH may not be due only to inhibition of the known target. INH rapidly increases ATP levels and oxygen consumption, and dissipates membrane potential in *Mycobacterium bovis* BCG. The fact that Q203 and BDQ compromise INH-mediated ATP increase and bactericidal activity suggests that a killing mechanism of INH involves perturbation of the mycobacterial respiratory chain (346). Indeed, *M. tuberculosis* mutants defective in *cydC* essential for cytochrome *bd* assembly appeared to be more susceptible to INH in mice (99).

Accordingly, inhibition of cytochrome *bd* by aurachin D significantly reduces cell recovery in a culture settling model (346). This points to a contribution of cytochrome *bd* in protection against INH stresses such as hypoxia (346). Interestingly, the rate of ROS production increases in INH-treated mycobacterial cell extracts (297), and disruption of superoxide dismutase A increases INH sensitivity (103). If INH induces ROS by interacting with the respiratory chain, cytochrome *bd* could protect mycobacterial cells against the drug *via* ROS detoxification.

Thus, protection against CFZ, BDQ, and INH provided by cytochrome *bd* may be related to the ability of the oxidase to scavenge and/or prevent generation of ROS [*e.g.*, see Al-Attar *et al.* (1), Borisov *et al.* (39), Borisov *et al.* (40), Forte *et al.* (114)] induced by the drugs (Fig. 20).

4. Cytochrome *bd* protection of mycobacteria from compounds targeting cytochrome *bcc*. Another drug targeting the *M. tuberculosis* respiratory chain is Q203 (Fig. 19), now designated telacebec by its developer, Qurient Co., Ltd. This imidazopyridine amide (IPA) compound and a clinical-stage drug candidate inhibit cytochrome *bcc* by binding to the quinol oxidation site (Q_p) in the cytochrome *b* (QcrB) subunit (245). However, Q203 is only bacteriostatic and does not kill the drug-tolerant persisters because, following *bcc* inhibition, electron flow rerouting to cytochrome *bd* is sufficient to

support sufficiently high oxidative phosphorylation and prevent Q203-induced death (173). Accordingly, while the growth of most *M. tuberculosis* clinical strains is fully inhibited by IPAs, the laboratory-adapted strains H37Rv, CDC1551, and Erdman can overcome this growth inhibition by upregulating the *cydA* gene, whose deletion makes the H37Rv strain highly susceptible to IPAs (5). The potency of Q203 is modulated by carbon catabolism and the composition of the culture broth medium (174). It is alleviated by glycerol supplementation that correlates with the overexpression of the *cydABDC* operon. The *cydAB* deletion annuls the detrimental effect of glycerol on the efficacy of Q203.

A study in a mouse model of tuberculosis reveals a powerful synthetic lethal interaction between cytochrome *bcc* and cytochrome *bd* (173). A synthetic lethal interaction refers to a type of genetic interaction where the single inactivation of two genes affects cell viability only slightly, whereas their simultaneous inactivation causes lethality (349). This also includes the case when the combination of a mutation and treatment with a chemical compound results in cell death, while the mutation or compound treatment alone is nonlethal. Simultaneous inactivation of both mycobacterial respiratory oxidase complexes (*via* genetic deletion of the *cydAB* genes and chemical inhibition of cytochrome *bcc* by Q203) results in complete inhibition of respiration, killing of phenotypic drug-tolerant persisters, and rapid eradication of *M. tuberculosis* infection *in vivo* (173). Thus, at least in the mouse lung microenvironment, the ability of *M. tuberculosis* to multiply and persist is dependent on oxygen respiration.

Mycobacterium ulcerans is known to be the causative agent of Buruli ulcer, a chronic, necrotizing disease that affects the skin and sometimes bone leading to permanent disfigurement and long-term disability. Due to a nonsense mutation in the *cydA* gene, cytochrome *bd* is inactive in all classical *M. ulcerans* strains. This makes cytochrome *bcc* the only functional terminal electron acceptor in their respiratory chain. As a result, Q203 becomes bactericidal at low dose against these strains both *in vitro* and in a mouse model. The drug could thus simplify and shorten Buruli ulcer treatment (292).

Figure 19 also shows other compounds targeting QcrB of the *M. tuberculosis* cytochrome *bcc*. These are pyrazolo[1,5-a]pyridine-3-carboxamide (TB47) (213), lansoprazole (278), phenoxyalkylbenzimidazoles (29, 65), and the arylvinylpiperazine amide (AX) series AX-35 and four related analogues (AX-36 to AX-39) (113). The compounds are bacteriostatic rather than bactericidal in their action. This is probably due to switching mycobacterial respiration to cytochrome *bd* that can be upregulated upon compound
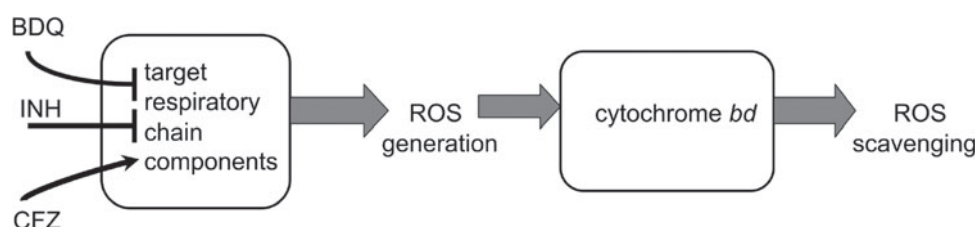

FIG. 20. Possible contribution of cytochrome *bd* to the defense of mycobacteria against antibiotic-induced stress *via* ROS detoxification. Protection of mycobacterial cells against CFZ, BDQ, and INH provided by the *bd* oxidase could be due to its ability to scavenge and/or prevent generation of ROS induced by the antimicrobial compounds. ROS, reactive oxygen species.
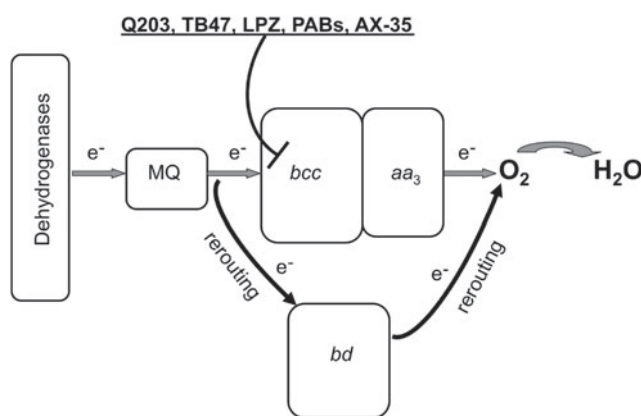
FIG. 21. Possible contribution of cytochrome *bd* to the protection of mycobacteria against cytochrome *bcc* inhibitors. The *bd* oxidase may provide an alternate respiratory route for electrons transferring from MQ to O_2 if cytochrome *bcc* is inhibited by telacebec (Q203), TB47, LPZ, PABs, and arylvinylpiperazine amide (AX-35). MQ, menaquinone.

treatment (113, 278). Accordingly, when cytochrome *bd* is disrupted, the compounds become bactericidal (29, 113, 213).

Thus, cytochrome *bd* seems to protect mycobacteria against cytochrome *bcc* inhibitors by providing an efficient alternative respiratory route (Fig. 21).

VIII. Cytochrome *bd* As a Potential Therapeutic Target

During host colonization, pathogenic bacteria face hostile environments, often characterized by harsh conditions, including severe O_2 limitation and abundance of harmful species, such as ROS and RNS produced by the host immune system, or high levels of H_2S produced by coexisting bacteria. Under these conditions, expression of cytochrome *bd* is potentially beneficial for pathogens, owing to the ability of this enzyme to function even under O_2-limiting conditions, due to its high O_2 affinity and resistance to cytotoxic species, such as H_2O_2, $ONOO^-$, NO, and H_2S. Therefore, it is not surprising that, as summarized below, cytochrome *bd* promotes virulence in several pathogenic bacteria.

In the case of *Shigella* sp., a well-known foodborne enteric pathogen, a markedly attenuated virulence was observed in mice models when CydAB expression was impaired by mutation of the *cydC* gene in the same operon. On the contrary, overexpression of CydAB in response to impaired synthesis of ubiquinone or riboflavin resulted in significantly higher bacterial virulence (334).

The role of cytochrome *bd* in bacterial virulence was also investigated in Group B *Streptococcus*, a common constituent of the vaginal microflora whose transmission to newborns during delivery can result in life-threatening sepsis. This pathogen, commonly assumed to have a strictly fermentative metabolism, was shown to adopt a quinone- and haem-dependent respiration-based metabolism requiring cytochrome *bd* (341). Inactivation of *cydA* in this pathogen was reported to result in reduced growth in human blood and, importantly, attenuated virulence in a neonatal rat sepsis model (341).

Another interesting case is represented by *S.* Typhimurium, a well-known foodborne pathogen responsible for a broad disease spectrum, ranging from self-limiting gastroenteritis to

acute systemic infection in susceptible patients. As in *E. coli*, this enteric pathogen encodes two *bd*-type oxidases: cytochrome *bd*-I and cytochrome *bd*-II, respectively, encoded by *cydAB* and *cyxAB*. Whereas cytochrome *bd*-II was found to be essential for intestinal colonization following antibiotic treatments depleting the gut of *Clostridia* species (275), cytochrome *bd*-I appears indispensable for sustaining tissue infection in mice models (85). Interestingly, the role of cytochrome *bd*-I in *S.* Typhimurium virulence was related to the ability of this oxidase to sustain bacterial energy metabolism under O_2-limiting conditions and to play a key role in the defence against nitrosative stress together with the NO-detoxifier flavohemoglobin (Hmp) (161).

The importance of cytochrome *bd* in affording NO-resistant respiration during the infection process was also demonstrated by Shepherd *et al.* (295) for uropathogenic *E. coli* (UPEC), a major cause of urinary tract infections, which are the most common nosocomial infections in developed countries. In this study, the relative contribution of the NO-detoxifying systems (Hmp, NorVW, NrfA), the iron/sulfur cluster repair protein YtfE, and the NO-tolerant cytochrome *bd*-I to UPEC growth and survival during infection was investigated. Cytochrome *bd*-I was shown not only to confer the highest resistance (together with Hmp) to an NO releaser but also to contribute to resistance to neutrophil-mediated killing and enable survival within macrophages. In addition, unlike the other defence systems (NorVW, Hmp, and YtfE), cytochrome *bd*-I was found to enhance UPEC survival in a mouse model after two days. On this basis, it was concluded that in UPEC, cytochrome *bd*-I is the main contributor to NO tolerance and host colonization under microaerobic conditions.

Cytochrome *bd* was also shown to play a role in the virulence of *Listeria monocytogenes* (77), another foodborne pathogen responsible for a number of life-threatening infections. This pathogen requires a special ability to adapt to varying O_2 levels. It encodes two respiratory terminal oxidases, a cytochrome *bd*-type (CydAB) and a cytochrome aa_3-type MQH_2 (QoxAB) oxidase. Both are used for respiration at different O_2 tensions and, importantly, have a role during infection, as mutation of either oxidase results in attenuated infection in mice. However, only the cytochrome *bd*-type oxidase is essential for aerobic respiration and bacterial replication in HeLa cells.

Less clear is the role played by cytochrome *bd* during the infection of *Brucella* spp., the pathogens responsible for brucellosis, a disease characterized by protracted recurrent fever in humans and abortion in ruminants. As a strategy to evade the host defence mechanisms, the *Brucella* spp. undergoes replication inside host macrophages, facing O_2-limiting and hyperoxidative conditions. In an early study on *B. abortus*, *cydB* mutants were found to display higher sensitivity to killing in murine macrophages and attenuated virulence in a mouse model, reverted by genes encoding superoxide dismutase or catalase (107). In a later report on *Brucella suis*, cytochrome *bd* was found to be the preferentially used terminal oxidase inside macrophages and to contribute to intracellular replication (208). However, in a subsequent study by the same group, lack of cytochrome *bd* was found to lead to bacterial hypervirulence (not attenuation) in a mouse model (157).

The role of cytochrome *bd* in microbial virulence was thoroughly investigated also in mycobacteria. *M. tuberculosis*

can survive, but not proliferate, under O_2-limiting conditions. As reviewed in Cook *et al.* (73), this pathogen has a versatile respiratory metabolism enabling bacterial survival at the significantly varying O_2 tensions encountered during host infection. The respiratory electron transfer chain is branched and terminates with two terminal oxidases: a *bd*-type oxidase (CydAB) and an aa_3-type cytochrome *c* oxidase that form a supercomplex with bc_1 (denoted as bc_1-aa_3). As revealed by investigating both *M. tuberculosis* (23) and the closely related nonpathogenic *M. smegmatis* (176), in the absence of stress factors, cytochrome *bd* is dispensable for growth in a rich medium. However, it appears to have a role in mycobacterial virulence, particularly at the transition between acute and chronic infection, when cytochrome *bd* and a nitrate transporter were shown to be transiently upregulated in a transcriptomic study on a murine infection model (296).

Mutation of *cydC* resulted in a lower bacterial burden in this transition phase, but not in the acute phase of infection, as observed in the same animal model (296). Although this observation was not reproduced in a later study (173), it is conceivable that cytochrome *bd* has a role during infection, when *M. tuberculosis* is expected to encounter several stresses, including limiting O_2 tensions, NO, and ROS/RNS produced by the host immune system. In line with this view, NO and hypoxic conditions were reported to enhance *cydAB* expression in *M. tuberculosis* and other mycobacteria (22, 33, 79, 127, 176, 296), and knockout of cytochrome *bd* was found to impair mycobacterial growth at low O_2 tensions (176, 296) and in the presence of H_2O_2 (212). Conversely, compared with the WT, a higher resistance to H_2O_2 was observed in an *M. tuberculosis* mutant strain with enhanced expression of cytochrome *bd* (305).

Altogether, the evidence reviewed above points to cytochrome *bd* as a prospective target for the development of next-generation antibiotics. However, a thorny path may await us. The flexibility of the Q-loop poses a problem to structure-driven design of quinone substrate-like inhibitors (280). For *bd*-type oxidases structurally similar to the *E. coli bd*-I, one could try to design hydrophobic compounds that would block the oxygen channel functioning. One more option is to develop quinol-like inhibitors that would compete with ubiquinol-8 for the CydB binding site, thereby preventing correct assembly of a CydAB core dimer (280).

IX. Possible Biotechnological Applications

Oxidases of the *bd* type have a broad potential application for biotechnology. This may relate to (i) the monitoring of parameters in biotechnological production processes, (ii) the creation of microbial fuel cells, (iii) the selection of industrial strains of microorganisms resistant to toxins and copper deprivation, (iv) various issues of bioremediation and wastewater treatment, and (v) the creation of conductive systems based on immobilized biofilms on the electrode. Some real and potential applications of cytochromes *bd* in industrial and medical biotechnology are illustrated by the following examples.

Forced aeration is one of the major energy consumption factors of bioleaching processes. The ability of cytochrome *bd* to be expressed under low oxygen conditions has been used for the identification and validation of genetic markers associated with oxygen availability in low-grade copper bioleaching systems (78).

Strains of *C. glutamicum* are used in the biotechnology industry for production of million tons of amino acids, mainly L-glutamate and L-lysine (95). In *C. glutamicum*, the respiratory chain, which includes cytochrome *bd*, was shown to be a target for improving amino acid production (171). These processes depend on aspects of respiration and how a cell responds to altered gene expression, including those encoding cytochrome *bd* (95, 184).

Extracellular electron transfer (EET), that is, electron movements outside the envelope of microbial cells, is highly relevant to the design of electrochemical systems, construction of fuel cells and biosensors, and understanding the physiology of the gut microbiota. Cytochrome *bd* activity was shown to attenuate EET in the gram-positive lactic acid bacterium *Enterococcus faecalis* through its effects on the redox status of the MQ pool. Wiring respiratory electron transfer from a bacterium such as *E. faecalis* to an electrode could be used as a sensor in screens for antimicrobial compounds acting by inhibition of cytochrome *bd* (240).

Mining, jewelry, and metal-processing industries use cyanide for extracting gold and other valuable metals, generating large amounts of highly toxic wastewater. There are microorganisms (*e.g.*, *Pseudomonas pseudoalcaligenes* CECT5344) that can grow under alkaline conditions using cyanide, cyanate, or different nitriles as the sole nitrogen source, and are able to remove cyanide from a jewelry industry wastewater. These bacteria will enable the development and optimization of improved strategies for biodegradation and bioremediation of industrial cyanide- and metal-containing effluents. As cyanide generally inhibits cellular aerobic respiration, bacteria possessing an alternative oxidase insensitive to cyanide, such as the quinol oxidase encoded by the *cioAB* genes, which belongs to the cytochrome *bd* family (60).

The study of *bd*-type oxidases also contributes to the development of means to combat biofilms in food and medical biotechnology. Cytochrome *bd*, a high-affinity quinol oxidase required for aerobic respiration under hypoxic conditions, is the most abundantly expressed respiratory complex in the biofilm community. It was shown recently that the cytochrome *bd*-expressing subpopulation is critical for biofilm development (14).

X. Conclusions

Cytochrome *bd* is found only in bacteria but is widely distributed among taxa and physiological types. However, its current importance and high profile were slow to be recognized: since its discovery by Keilin, Warburg and pioneers in respiratory metabolism in the 1930s (when it was named cytochrome a_2), publications on this oxidase accrued very slowly. Based on the Web of Science Core Collection, the number of articles has grown rapidly: in 1990, there was one article (searching for ''cytochrome AND bd''), but now that number is ~ 1500 per annum. The explosion of interest is a result of the recognition that cytochrome *bd* represents a novel class of oxidase and that its unique structure, catalytic capabilities, tolerance of stress, and importance to pathogens are worthy of detailed study.

Despite impressive advances, significant challenges remain. From the point of view of fundamental understanding of redox and antioxidant biology, the most pressing are a full description of electron flux through the three haems and the mechanisms of oxygen reduction. Since cytochrome *bd* is not a proton pump, although contributing to creation of a protonmotive force, accompanying proton movements are less problematic. However, the novel features of cytochrome *bd* pose additional challenges, particularly its ability to confer upon bacterial resistance to oxidative stress, NO and a number of important antimicrobial compounds. Its unique structure and function make it a profitable area of study for developing novel therapeutics, thereby contributing to overcoming the global scourge of resistance to established, and overused, antibiotics.

Funding Information

References

1. Al-Attar S, Yu Y, Pinkse M, Hoeser J, Friedrich T, Bald D, and de Vries S. Cytochrome *bd* displays significant quinol peroxidase activity. *Sci Rep* 6: 27631, 2016.

2. Alexeeva S, Hellingwerf K, and Teixeira de Mattos MJ. Quantitative assessment of oxygen availability: perceived aerobiosis and its effect on flux distribution in the respiratory chain of *Escherichia coli*. *J Bacteriol* 184: 1402–1406, 2002.

3. Allen RJ, Brenner EP, VanOrsdel CE, Hobson JJ, Hearn DJ, and Hemm MR. Conservation analysis of the CydX protein yields insights into small protein identification and evolution. *BMC Genomics* 15: 946, 2014.

4. Andries K, Verhasselt P, Guillemont J, Gohlmann HW, Neefs JM, Winkler H, Van Gestel J, Timmerman P, Zhu M, Lee E, Williams P, de Chaffoy D, Huitric E, Hoffner S, Cambau E, Truffot-Pernot C, Lounis N, and Jarlier V. A diarylquinoline drug active on the ATP synthase of *Mycobacterium tuberculosis*. *Science* 307: 223–227, 2005.

5. Arora K, Ochoa-Montano B, Tsang PS, Blundell TL, Dawes SS, Mizrahi V, Bayliss T, Mackenzie CJ, Cleghorn LA, Ray PC, Wyatt PG, Uh E, Lee J, Barry CE, 3rd, and Boshoff HI. Respiratory flexibility in response to inhibition of cytochrome *c* oxidase in *Mycobacterium tuberculosis*. *Antimicrob. Agents Chemother* 58: 6962–6965, 2014.

6. Arutyunyan AM, Borisov VB, Novoderezhkin VI, Ghaim J, Zhang J, Gennis RB, and Konstantinov AA. Strong excitonic interactions in the oxygen-reducing site of *bd*-type oxidase: the Fe-to-Fe distance between hemes *d* and b_{595} is 10 A. *Biochemistry* 47: 1752–1759, 2008.

7. Arutyunyan AM, Sakamoto J, Inadome M, Kabashima Y, and Borisov VB. Optical and magneto-optical activity of cytochrome *bd* from *Geobacillus thermodenitrificans*. *Biochim Biophys. Acta* 1817: 2087–2094, 2012.

8. Ashcroft JR and Haddock BA. Synthesis of alternative membrane-bound redox carriers during aerobic growth of *Escherichia coli* in the presence of potassium cyanide. *Biochem J* 148: 349–352, 1975.

9. Aung HL, Berney M, and Cook GM. Hypoxia-activated cytochrome *bd* expression in *Mycobacterium smegmatis* is cyclic AMP receptor protein dependent. *J. Bacteriol* 196: 3091–3097, 2014.

10. Babcock GT and Wikstrom M. Oxygen activation and the conservation of energy in cell respiration. *Nature* 356: 301–309, 1992.

11. Bald D, Villellas C, Lu P, and Koul A. Targeting energy metabolism in *Mycobacterium tuberculosis*, a new paradigm in antimycobacterial drug discovery. *mBio* 8: e00272-17, 2017.

12. Barry VC, Belton JG, Conalty ML, Denneny JM, Edward DW, O'Sullivan JF, Twomey D, and Winder F. A new series of phenazines (rimino-compounds) with high anti-tuberculosis activity. *Nature* 179: 1013–1015, 1957.

13. Baughn AD and Malamy MH. The strict anaerobe *Bacteroides fragilis* grows in and benefits from nanomolar concentrations of oxygen. *Nature* 427: 441–444, 2004.

14. Beebout CJ, Eberly AR, Werby SH, Reasoner SA, Brannon JR, De S, Fitzgerald MJ, Huggins MM, Clayton DB, Cegelski L, and Hadjifrangiskou M. Respiratory heterogeneity shapes biofilm formation and host colonization in uropathogenic *Escherichia coli*. *mBio* 10: e02400-18, 2019.

15. Bekker M, Alexeeva S, Laan W, Sawers G, Teixeira de Mattos J, and Hellingwerf K. The ArcBA two-component system of *Escherichia coli* is regulated by the redox state of both the ubiquinone and the menaquinone pool. *J Bacteriol* 192: 746–754, 2010.

16. Bekker M, de Vries S, Ter Beek A, Hellingwerf KJ, and de Mattos MJ. Respiration of *Escherichia coli* can be fully uncoupled via the nonelectrogenic terminal cytochrome *bd*-II oxidase. *J Bacteriol* 191: 5510–5517, 2009.

17. Belevich I, Borisov VB, Bloch DA, Konstantinov AA, and Verkhovsky MI. Cytochrome *bd* from *Azotobacter vinelandii*: evidence for high-affinity oxygen binding. *Biochemistry* 46: 11177–11184, 2007.

18. Belevich I, Borisov VB, Konstantinov AA, and Verkhovsky MI. Oxygenated complex of cytochrome *bd* from *Escherichia coli*: stability and photolability. *FEBS Lett* 579: 4567–4570, 2005.

19. Belevich I, Borisov VB, and Verkhovsky MI. Discovery of the true peroxy intermediate in the catalytic cycle of terminal oxidases by real-time measurement. *J Biol Chem* 282: 28514–28519, 2007.

20. Belevich I, Borisov VB, Zhang J, Yang K, Konstantinov AA, Gennis RB, and Verkhovsky MI. Time-resolved electrometric and optical studies on cytochrome *bd* suggest a mechanism of electron-proton coupling in the di-heme active site. *Proc Natl Acad Sci U S A* 102: 3657–3662, 2005.

21. Bellomio A, Vincent PA, de Arcuri BF, Farias RN, and Morero RD. Microcin J25 has dual and independent mechanisms of action in *Escherichia coli*: RNA polymerase inhibition and increased superoxide production. *J Bacteriol* 189: 4180–4186, 2007.

22. Berney M and Cook GM. Unique flexibility in energy metabolism allows mycobacteria to combat starvation and hypoxia. *PLoS One* 5: e8614, 2010.

23. Berney M, Hartman TE, and Jacobs WR, Jr. A *Mycobacterium tuberculosis* cytochrome *bd* oxidase mutant is hypersensitive to bedaquiline. *mBio* 5: e01275-14, 2014.

24. Berry S, Bolychevtseva YV, Rogner M, and Karapetyan NV. Photosynthetic and respiratory electron transport in the alkaliphilic cyanobacterium *Arthrospira* (*Spirulina*) *platensis Photosynth Res* 78: 67–76, 2003.

25. Berry S, Schneider D, Vermaas WF, and Rogner M. Electron transport routes in whole cells of *Synechocystis*

sp. strain PCC 6803: the role of the cytochrome *bd*-type oxidase. *Biochemistry* 41: 3422–3429, 2002.

26. Bertsova YV, Bogachev AV, and Skulachev VP. Generation of protonic potential by the *bd*-type quinol oxidase of *Azotobacter vinelandii*. *FEBS Lett* 414: 369–372, 1997.

27. Bertsova YV, Bogachev AV, and Skulachev VP. Two NADH:ubiquinone oxidoreductases of *Azotobacter vinelandii* and their role in the respiratory protection. *Biochim Biophys Acta* 1363: 125–133, 1998.

28. Bertsova YV, Bogachev AV, and Skulachev VP. Noncoupled NADH:ubiquinone oxidoreductase of *Azotobacter vinelandii* is required for diazotrophic growth at high oxygen concentrations. *J Bacteriol* 183: 6869–6874, 2001.

29. Berube BJ and Parish T. Combinations of respiratory chain inhibitors have enhanced bactericidal activity against *Mycobacterium tuberculosis*. *Antimicrob Agents Chemother* 62: e01677-17, 2018.

30. Bettenbrock K, Bai H, Ederer M, Green J, Hellingwerf KJ, Holcombe M, Kunz S, Rolfe MD, Sanguinetti G, Sawodny O, Sharma P, Steinsiek S, and Poole RK. Towards a systems level understanding of the oxygen response of *Escherichia coli*. *Adv Microb Physiol* 64: 65–114, 2014.

31. Betts JC, Lukey PT, Robb LC, McAdam RA, and Duncan K. Evaluation of a nutrient starvation model of *Mycobacterium tuberculosis* persistence by gene and protein expression profiling. *Mol Microbiol* 43: 717–731, 2002.

32. Bloch DA, Borisov VB, Mogi T, and Verkhovsky MI. Heme/heme redox interaction and resolution of individual optical absorption spectra of the hemes in cytochrome *bd* from *Escherichia coli*. *Biochim Biophys Acta* 1787: 1246–1253, 2009.

33. Boot M, Jim KK, Liu T, Commandeur S, Lu P, Verboom T, Lill H, Bitter W, and Bald D. A fluorescence-based reporter for monitoring expression of mycobacterial cytochrome *bd* in response to antibacterials and during infection. *Sci Rep* 7: 10665, 2017.

34. Borisov V, Arutyunyan AM, Osborne JP, Gennis RB, and Konstantinov AA. Magnetic circular dichroism used to examine the interaction of *Escherichia coli* cytochrome *bd* with ligands. *Biochemistry* 38: 740–750, 1999.

35. Borisov V, Gennis R, and Konstantinov AA. Peroxide complex of cytochrome *bd*: kinetics of generation and stability. *Biochem Mol Biol Int* 37: 975–982, 1995.

36. Borisov VB. Cytochrome *bd*: structure and properties. *Biochemistry (Mosc)* 61: 565–574, 1996.

37. Borisov VB. Interaction of *bd*-type quinol oxidase from *Escherichia coli* and carbon monoxide: heme *d* binds CO with high affinity. *Biochemistry (Mosc)* 73: 14–22, 2008.

38. Borisov VB, Belevich I, Bloch DA, Mogi T, and Verkhovsky MI. Glutamate 107 in subunit I of cytochrome *bd* from *Escherichia coli* is part of a transmembrane intraprotein pathway conducting protons from the cytoplasm to the heme b_{595}/heme *d* active site. *Biochemistry* 47: 7907–7914, 2008.

39. Borisov VB, Davletshin AI, and Konstantinov AA. Peroxidase activity of cytochrome *bd* from *Escherichia coli*. *Biochemistry (Mosc)* 75: 428–436, 2010.

40. Borisov VB, Forte E, Davletshin A, Mastronicola D, Sarti P, and Giuffre A. Cytochrome *bd* oxidase from *Escherichia coli* displays high catalase activity: an additional defense against oxidative stress. *FEBS Lett* 587: 2214–2218, 2013.

41. Borisov VB, Forte E, Giuffre A, Konstantinov A, and Sarti P. Reaction of nitric oxide with the oxidized di-heme and heme-copper oxygen-reducing centers of terminal oxidases: different reaction pathways and end-products. *J Inorg Biochem* 103: 1185–1187, 2009.

42. Borisov VB, Forte E, Konstantinov AA, Poole RK, Sarti P, and Giuffre A. Interaction of the bacterial terminal oxidase cytochrome *bd* with nitric oxide. *FEBS Lett* 576: 201–204, 2004.

43. Borisov VB, Forte E, Sarti P, Brunori M, Konstantinov AA, and Giuffre A. Nitric oxide reacts with the ferryl-oxo catalytic intermediate of the Cu_B-lacking cytochrome *bd* terminal oxidase. *FEBS Lett* 580: 4823–4826, 2006.

44. Borisov VB, Forte E, Sarti P, Brunori M, Konstantinov AA, and Giuffre A. Redox control of fast ligand dissociation from *Escherichia coli* cytochrome *bd*. *Biochem Biophys Res Commun* 355: 97–102, 2007.

45. Borisov VB, Forte E, Sarti P, and Giuffre A. Catalytic intermediates of cytochrome *bd* terminal oxidase at steady-state: ferryl and oxy-ferrous species dominate. *Biochim Biophys Acta* 1807: 503–509, 2011.

46. Borisov VB, Forte E, Siletsky SA, Arese M, Davletshin AI, Sarti P, and Giuffre A. Cytochrome *bd* protects bacteria against oxidative and nitrosative stress: a potential target for next-generation antimicrobial agents. *Biochemistry (Mosc)* 80: 565–575, 2015.

47. Borisov VB, Forte E, Siletsky SA, Sarti P, and Giuffre A. Cytochrome *bd* from *Escherichia coli* catalyzes peroxynitrite decomposition. *Biochim Biophys Acta* 1847: 182–188, 2015.

48. Borisov VB, Gennis RB, Hemp J, and Verkhovsky MI. The cytochrome *bd* respiratory oxygen reductases. *Biochim Biophys Acta* 1807: 1398–1413, 2011.

49. Borisov VB, Gennis RB, and Konstantinov AA. Interaction of cytochrome *bd* from *Escherichia coli* with hydrogen peroxide. *Biochemistry (Mosc)* 60: 231–239, 1995.

50. Borisov VB, Liebl U, Rappaport F, Martin JL, Zhang J, Gennis RB, Konstantinov AA, and Vos MH. Interactions between heme *d* and heme b_{595} in quinol oxidase *bd* from *Escherichia coli*: a photoselection study using femtosecond spectroscopy. *Biochemistry* 41: 1654–1662, 2002.

51. Borisov VB, Murali R, Verkhovskaya ML, Bloch DA, Han H, Gennis RB, and Verkhovsky MI. Aerobic respiratory chain of *Escherichia coli* is not allowed to work in fully uncoupled mode. *Proc Natl Acad Sci U S A* 108: 17320–17324, 2011.

52. Borisov VB, Sedelnikova SE, Poole RK, and Konstantinov AA. Interaction of cytochrome *bd* with carbon monoxide at low and room temperatures: evidence that only a small fraction of heme b_{595} reacts with CO. *J Biol Chem* 276: 22095–22099, 2001.

53. Borisov VB and Siletsky SA. Features of organization and mechanism of catalysis of two families of terminal oxidases: heme-copper and *bd*-type. *Biochemistry (Mosc)* 84: 1390–1402, 2019.

54. Borisov VB and Verkhovsky MI. Accommodation of CO in the di-heme active site of cytochrome *bd* terminal oxidase from *Escherichia coli*. *J Inorg Biochem* 118: 65–67, 2013.

55. Borisov VB and Verkhovsky MI. Oxygen as acceptor. *EcoSal Plus* 6, 2015. DOI: 10.1128/ecosalplus.ESP-0012-2015.

56. Brekasis D and Paget MS. A novel sensor of NADH/NAD^+ redox poise in *Streptomyces coelicolor* A3(2). *EMBO J* 22: 4856–4865, 2003.

57. Brochier-Armanet C, Talla E, and Gribaldo S. The multiple evolutionary histories of dioxygen reductases: implications for the origin and evolution of aerobic respiration. *Mol Biol Evol* 26: 285–297, 2009.

58. Brunori M, Giuffre A, and Sarti P. Cytochrome *c* oxidase, ligands and electrons. *J Inorg Biochem* 99: 324–336, 2005.

59. Brzezinski P and Gennis RB. Cytochrome *c* oxidase: exciting progress and remaining mysteries. *J Bioenerg Biomembr* 40: 521–531, 2008.

60. Cabello P, Luque-Almagro VM, Olaya-Abril A, Saez LP, Moreno-Vivian C, and Roldan MD. Assimilation of cyanide and cyano-derivatives by *Pseudomonas pseudoalcaligenes* CECT5344: from omic approaches to biotechnological applications. *FEMS Microbiol Lett* 365: fny032, 2018.

61. Calhoun MW, Newton G, and Gennis RB. *E. coli* map. Physical map locations of genes encoding components of the aerobic respiratory chain of *Escherichia coli*. *J Bacteriol* 173: 1569–1570, 1991.

62. Carbonero F, Benefiel AC, Alizadeh-Ghamsari AH, and Gaskins HR. Microbial pathways in colonic sulfur metabolism and links with health and disease. *Front Physiol* 3: 448, 2012.

63. Castresana J. Comparative genomics and bioenergetics. *Biochim Biophys Acta* 1506: 147–162, 2001.

64. Chalon MC, Wilke N, Pedersen J, Rufini S, Morero RD, Cortez L, Chehin RN, Farias RN, and Vincent PA. Redox-active tyrosine residue in the microcin J25 molecule. *Biochem Biophys Res Commun* 406: 366–370, 2011.

65. Chandrasekera NS, Berube BJ, Shetye G, Chettiar S, O'Malley T, Manning A, Flint L, Awasthi D, Ioerger TR, Sacchettini J, Masquelin T, Hipskind PA, Odingo J, and Parish T. Improved phenoxyalkylbenzimidazoles with activity against *Mycobacterium tuberculosis* appear to target QcrB. *ACS Infect Dis* 3: 898–916, 2017.

66. Chang W, Small DA, Toghrol F, and Bentley WE. Global transcriptome analysis of *Staphylococcus aureus* response to hydrogen peroxide. *J Bacteriol* 188: 1648–1659, 2006.

67. Charbon G, Campion C, Chan SH, Bjorn L, Weimann A, da Silva LC, Jensen PR, and Lobner-Olesen A. Re-wiring of energy metabolism promotes viability during hyperreplication stress in *E. coli*. *PLoS Genet* 13: e1006590, 2017.

68. Chen H, Luo Q, Yin J, Gao T, and Gao H. Evidence for requirement of CydX in function but not assembly of the cytochrome *bd* oxidase in *Shewanella oneidensis*. *Biochim Biophys Acta* 1850: 318–328, 2015.

69. Choi H, Yang Z, and Weisshaar JC. Oxidative stress induced in *E. coli* by the human antimicrobial peptide LL-37. *PLoS Pathog* 13: e1006481, 2017.

70. Ciccarelli FD, Doerks T, von Mering C, Creevey CJ, Snel B, and Bork P. Toward automatic reconstruction of a highly resolved tree of life. *Science* 311: 1283–1287, 2006.

71. Cook GM, Greening C, Hards K, and Berney M. Energetics of pathogenic bacteria and opportunities for drug development. *Adv Microb Physiol* 65: 1–62, 2014.

72. Cook GM, Hards K, Dunn E, Heikal A, Nakatani Y, Greening C, Crick DC, Fontes FL, Pethe K, Hasenoehrl E, and Berney M. Oxidative phosphorylation as a target space for tuberculosis: success, caution, and future directions. *Microbiol Spectr* 5, 2017. DOI: 10.1128/microbiolspec.TBTB2-0014-2016.

73. Cook GM, Hards K, Vilcheze C, Hartman T, and Berney M. Energetics of respiration and oxidative phosphorylation in mycobacteria. *Microbiol Spectr* 2: MGM2-0015-2013, 2014.

74. Cook GM and Poole RK. Oxidase and periplasmic cytochrome assembly in *Escherichia coli* K-12: CydDC and CcmAB are not required for haem-membrane association. *Microbiology* 146 (Pt 2): 527–536, 2000.

75. Cook GM and Poole RK. A bacterial oxidase like no other? *Science* 352: 518–519, 2016.

76. Cooper CE and Brown GC. The inhibition of mitochondrial cytochrome oxidase by the gases carbon monoxide, nitric oxide, hydrogen cyanide and hydrogen sulfide: chemical mechanism and physiological significance. *J Bioenerg Biomembr* 40: 533–539, 2008.

77. Corbett D, Goldrick M, Fernandes VE, Davidge K, Poole RK, Andrew PW, Cavet J, and Roberts IS. *Listeria monocytogenes* has both a *bd*-type and an *aa₃*-type terminal oxidase which allow growth in different oxygen levels and both are important in infection. *Infect Immun* 85: e00354-17, 2017.

78. Cortes M, Marin S, Galleguillos P, Cautivo D, and Demergasso C. Validation of genetic markers associated to oxygen availability in low-grade copper bioleaching systems: an industrial application. *Front Microbiol* 10: 1841, 2019.

79. Cortes T, Schubert OT, Banaei-Esfahani A, Collins BC, Aebersold R, and Young DB. Delayed effects of transcriptional responses in *Mycobacterium tuberculosis* exposed to nitric oxide suggest other mechanisms involved in survival. *Sci Rep* 7: 8208, 2017.

80. Costa M. Toxicity and carcinogenicity of Cr(VI) in animal models and humans. *Crit Rev Toxicol* 27: 431–442, 1997.

81. Cotter PA and Gunsalus RP. Contribution of the *fnr* and *arc*A gene products in coordinate regulation of cytochrome *o* and *d* oxidase (*cyoABCDE* and *cydAB*) genes in *Escherichia coli*. *FEMS Microbiol Lett* 91: 31–36, 1992.

82. Cotter PA, Melville SB, Albrecht JA, and Gunsalus RP. Aerobic regulation of cytochrome *d* oxidase (cydAB) operon expression in *Escherichia coli*: roles of Fnr and ArcA in repression and activation. *Mol Microbiol* 25: 605–615, 1997.

83. Crack JC, Green J, Hutchings MI, Thomson AJ, and Le Brun NE. Bacterial iron-sulfur regulatory proteins as biological sensor-switches. *Antioxid Redox Signal* 17: 1215–1231, 2012.

84. Crack JC, Stapleton MR, Green J, Thomson AJ, and Le Brun NE. Mechanism of [4Fe-4S](Cys)₄ cluster nitrosylation is conserved among NO-responsive regulators. *J Biol Chem* 288: 11492–11502, 2013.

85. Craig M, Sadik AY, Golubeva YA, Tidhar A, and Slauch JM. Twin-arginine translocation system (*tat*) mutants of *Salmonella* are attenuated due to envelope defects, not respiratory defects. *Mol Microbiol* 89: 887–902, 2013.

86. Cruz-Ramos H, Cook GM, Wu G, Cleeter MW, and Poole RK. Membrane topology and mutational analysis of *Escherichia coli* CydDC, an ABC-type cysteine exporter required for cytochrome assembly. *Microbiology* 150: 3415–3427, 2004.

87. Cruz-Ramos H, Crack J, Wu G, Hughes MN, Scott C, Thomson AJ, Green J, and Poole RK. NO sensing by FNR: regulation of the *Escherichia coli* NO-detoxifying flavohaemoglobin, Hmp. *EMBO J* 21: 3235–3244, 2002.

88. D'mello R, Hill S, and Poole RK. The cytochrome *bd* quinol oxidase in *Escherichia coli* has an extremely high oxygen affinity and two-oxygen-binding haems: implicaitons for regulation of activity *in vivo* by oxygen inihibition. *Microbiology* 142: 755–763, 1996.

89. Dailey FE and Berg HC. Mutants in disulfide bond formation that disrupt flagellar assembly in *Escherichia coli*. *Proc Natl Acad Sci U S A* 90: 1043–1047, 1993.

90. Dalton H and Postgate JR. Effect of oxygen on growth of *Azotobacter chroococcum* in batch and continuous cultures. *J Gen Microbiol* 54: 463–473, 1968.

91. Dannenberg S, Kroder M, Dilling W, and Cypionka H. Oxidation of H_2, organic compounds and inorganic sulfur compounds coupled to reduction of O_2 or nitrate by sulfate-reducing bacteria. *Arch Microbiol* 158: 93–99, 1992.

92. Das A, Silaghi-Dumitrescu R, Ljungdahl LG, and Kurtz DM, Jr. Cytochrome *bd* oxidase, oxidative stress, and dioxygen tolerance of the strictly anaerobic bacterium *Moorella thermoacetica*. *J Bacteriol* 187: 2020–2029, 2005.

93. Dassa J, Fsihi H, Marck C, Dion M, Kieffer-Bontemps M, and Boquet PL. A new oxygen-regulated operon in *Escherichia coli* comprises the genes for a putative third cytochrome oxidase and for pH 2.5 acid phosphatase (*app*A). *Mol Gen Genet* 229: 341–352, 1991.

94. Davidge KS, Sanguinetti G, Yee CH, Cox AG, McLeod CW, Monk CE, Mann BE, Motterlini R, and Poole RK. Carbon monoxide-releasing antibacterial molecules target respiration and global transcriptional regulators. *J Biol Chem* 284: 4516–4524, 2009.

95. Davoudi CF, Ramp P, Baumgart M, and Bott M. Identification of Surf1 as an assembly factor of the cytochrome bc_1-aa_3 supercomplex of *Actinobacteria*. *Biochim Biophys Acta* 1860: 148033, 2019.

96. Degli Esposti M, Rosas-Perez T, Servin-Garciduenas LE, Bolanos LM, Rosenblueth M, and Martinez-Romero E. Molecular evolution of cytochrome *bd* oxidases across proteobacterial genomes. *Genome Biol Evol* 7: 801–820, 2015.

97. Delaney JM and Georgopoulos C. Physical map locations of the *trxB*, *htrD*, *cydC*, and *cydD* genes of *Escherichia coli*. *J Bacteriol* 174: 3824–3825, 1992.

98. Delaney JM, Wall D, and Georgopoulos C. Molecular characterization of the *Escherichia coli htr*D gene: cloning, sequence, regulation, and involvement with cytochrome *d* oxidase. *J Bacteriol* 175: 166–175, 1993.

99. Dhar N and McKinney JD. *Mycobacterium tuberculosis* persistence mutants identified by screening in isoniazid-treated mice. *Proc Natl Acad Sci U S A* 107: 12275–12280, 2010.

100. Dilling W and Cypionka H. Aerobic respiration in sulfate-reducing bacteria. *FEMS Microbiol Lett* 71: 123–127, 1990.

101. Drozd J and Postgate JR. Effect of oxygen on acetylene reduction, cytochrome content and respiratory activity of *Azotobacter chroococcum*. *J Gen Microbiol* 63: 63–73, 1970.

102. Duc KM, Kang BG, Lee C, Park HJ, Park YM, Joung YH, and Bang IS. The small protein CydX is required for cytochrome *bd* quinol oxidase stability and function in *Salmonella* Typhimurium: a phenotypic study. *J Bacteriol* 202: e00348-19, 2020 .

103. Dussurget O, Rodriguez M, and Smith I. Protective role of the *Mycobacterium smegmatis* IdeR against reactive oxygen species and isoniazid toxicity. *Tuber Lung Dis* 79: 99–106, 1998.

104. Ederer M, Steinsiek S, Stagge S, Rolfe MD, Ter Beek A, Knies D, Teixeira de Mattos MJ, Sauter T, Green J, Poole RK, Bettenbrock K, and Sawodny O. A mathematical model of metabolism and regulation provides a systems-level view of how *Escherichia coli* responds to oxygen. *Front Microbiol* 5: 124, 2014.

105. Edgar RC. MUSCLE: multiple sequence alignment with high accuracy and high throughput. *Nucleic Acids Res* 32: 1792–1797, 2004.

106. Edwards SE, Loder CS, Wu G, Corker H, Bainbridge BW, Hill S, and Poole RK. Mutation of cytochrome *bd* quinol oxidase results in reduced stationary phase survival, iron deprivation, metal toxicity and oxidative stress in *Azotobacter vinelandii*. *FEMS Microbiol Lett* 185: 71–77, 2000.

107. Endley S, McMurray D, and Ficht TA. Interruption of the *cydB* locus in *Brucella abortus* attenuates intracellular survival and virulence in the mouse model of infection. *J Bacteriol* 183: 2454–2462, 2001.

108. Eng T, Demling P, Herbert RA, Chen Y, Benites V, Martin J, Lipzen A, Baidoo EEK, Blank LM, Petzold CJ, and Mukhopadhyay A. Restoration of biofuel production levels and increased tolerance under ionic liquid stress is enabled by a mutation in the essential *Escherichia coli* gene *cydC*. *Microb Cell Fact* 17: 159, 2018.

109. Epand RM and Vogel HJ. Diversity of antimicrobial peptides and their mechanisms of action. *Biochim Biophys Acta* 1462: 11–28, 1999.

110. Eser M, Masip L, Kadokura H, Georgiou G, and Beckwith J. Disulfide bond formation by exported glutaredoxin indicates glutathione's presence in the *E. coli* periplasm. *Proc Natl Acad Sci U S A* 106: 1572–1577, 2009.

111. Estes AM, Hearn DJ, Snell-Rood EC, Feindler M, Feeser K, Abebe T, Dunning Hotopp JC, and Moczek AP. Brood ball-mediated transmission of microbiome members in the dung beetle, *Onthophagus taurus* (Coleoptera: Scarabaeidae). *PLoS One* 8: e79061, 2013.

112. Feng X, Zhu W, Schurig-Briccio LA, Lindert S, Shoen C, Hitchings R, Li J, Wang Y, Baig N, Zhou T, Kim BK, Crick DC, Cynamon M, McCammon JA, Gennis RB, and Oldfield E. Antiinfectives targeting enzymes and the proton motive force. *Proc Natl Acad Sci U S A* 112: E7073–E7082, 2015.

113. Foo CS, Lupien A, Kienle M, Vocat A, Benjak A, Sommer R, Lamprecht DA, Steyn AJC, Pethe K, Piton J, Altmann KH, and Cole ST. Arylvinylpiperazine amides, a new class of potent inhibitors targeting QcrB of *Mycobacterium tuberculosis*. *MBio* 9: e01276-18, 2018.

114. Forte E, Borisov VB, Davletshin A, Mastronicola D, Sarti P, and Giuffre A. Cytochrome *bd* oxidase and hydrogen peroxide resistance in *Mycobacterium tuberculosis*. *MBio* 4: e01006-13, 2013.

115. Forte E, Borisov VB, Falabella M, Colaco HG, Tinajero-Trejo M, Poole RK, Vicente JB, Sarti P, and Giuffre A. The terminal oxidase cytochrome *bd* promotes sulfide-resistant bacterial respiration and growth. *Sci Rep* 6: 23788, 2016.

116. Forte E, Borisov VB, Siletsky SA, Petrosino M, and Giuffre A. In the respiratory chain of *Escherichia coli* cytochromes *bd*-I and *bd*-II are more sensitive to carbon

monoxide inhibition than cytochrome bo_3. *Biochim Biophys Acta Bioenerg* 1860: 148088, 2019.

117. Forte E, Borisov VB, Vicente JB, and Giuffre A. Cytochrome *bd* and gaseous ligands in bacterial physiology. *Adv Microb Physiol* 71: 171–234, 2017.

118. Galvan AE, Chalon MC, Rios Colombo NS, Schurig-Briccio LA, Sosa-Padilla B, Gennis RB, and Bellomio A. Microcin J25 inhibits ubiquinol oxidase activity of purified cytochrome *bd*-I from *Escherichia coli*. *Biochimie* 160: 141–147, 2019.

119. Galvan AE, Chalon MC, Schurig-Briccio LA, Salomon RA, Minahk CJ, Gennis RB, and Bellomio A. Cytochromes *bd*-I and bo_3 are essential for the bactericidal effect of microcin J25 on *Escherichia coli* cells. *Biochim Biophys Acta* 1859: 110–118, 2018.

120. Georgellis D, Kwon O, De Wulf P, and Lin EC. Signal decay through a reverse phosphorelay in the Arc two-component signal transduction system. *J Biol Chem* 273: 32864–32869, 1998.

121. Georgellis D, Kwon O, and Lin EC. Amplification of signaling activity of the arc two-component system of *Escherichia coli* by anaerobic metabolites. An in vitro study with different protein modules. *J Biol Chem* 274: 35950–35954, 1999.

122. Georgellis D, Kwon O, and Lin EC. Quinones as the redox signal for the arc two-component system of bacteria. *Science* 292: 2314–2316, 2001.

123. Georgiou CD, Fang H, and Gennis RB. Identification of the *cyd*C locus required for the expression of the functional form of the cytochrome *d* terminal oxidase complex in *Escherichia coli*. *J Bacteriol* 169: 2107–2112, 1987.

124. Giuffre A, Borisov VB, Arese M, Sarti P, and Forte E. Cytochrome *bd* oxidase and bacterial tolerance to oxidative and nitrosative stress. *Biochim Biophys Acta* 1837: 1178–1187, 2014.

125. Giuffre A, Borisov VB, Mastronicola D, Sarti P, and Forte E. Cytochrome *bd* oxidase and nitric oxide: from reaction mechanisms to bacterial physiology. *FEBS Lett* 586: 622–629, 2012.

126. Goldman BS, Gabbert KK, and Kranz RG. The temperature-sensitive growth and survival phenotypes of *Escherichia coli cydDC* and *cydAB* strains are due to deficiencies in cytochrome *bd* and are corrected by exogenous catalase and reducing agents. *J Bacteriol* 178: 6348–6351, 1996.

127. Gopinath V, Raghunandanan S, Gomez RL, Jose L, Surendran A, Ramachandran R, Pushparajan AR, Mundayoor S, Jaleel A, and Kumar RA. Profiling the proteome of *Mycobacterium tuberculosis* during dormancy and reactivation. *Mol Cell Proteomics* 14: 2160–2176, 2015.

128. Gorbikova EA, Vuorilehto K, Wikstrom M, and Verkhovsky MI. Redox titration of all electron carriers of cytochrome *c* oxidase by Fourier transform infrared spectroscopy. *Biochemistry* 45: 5641–5649, 2006.

129. Govantes F, Albrecht JA, and Gunsalus RP. Oxygen regulation of the *Escherichia coli* cytochrome *d* oxidase (*cyd*AB) operon: roles of multiple promoters and the Fnr-1 and Fnr-2 binding sites. *Mol Microbiol* 37: 1456–1469, 2000.

130. Govantes F, Orjalo AV, and Gunsalus RP. Interplay between three global regulatory proteins mediates oxygen regulation of the *Escherichia coli* cytochrome *d* oxidase (*cyd*AB) operon. *Mol Microbiol* 38: 1061–1073, 2000.

131. Green GN, Fang H, Lin R-J, Newton G, Mather M, Georgiou CD, and Gennis RB. The nucleotide sequence of the *cyd* locus encoding the two subunits of the cytochrome *d* terminal oxidase complex of *Escherichia coli*. *J Biol Chem* 263: 13138–13143, 1988.

132. Green J, Scott C, and Guest JR. Functional versatility in the CRP-FNR superfamily of transcription factors: FNR and FLP. *Adv Microb Physiol* 44: 1–34, 2001.

133. Haagsma AC, Abdillahi-Ibrahim R, Wagner MJ, Krab K, Vergauwen K, Guillemont J, Andries K, Lill H, Koul A, and Bald D. Selectivity of TMC207 towards mycobacterial ATP synthase compared with that towards the eukaryotic homologue. *Antimicrob Agents Chemother* 53: 1290–1292, 2009.

134. Hancock RE and Chapple DS. Peptide antibiotics. *Antimicrob Agents Chemother* 43: 1317–1323, 1999.

135. Hao W and Golding GB. Asymmetrical evolution of cytochrome *bd* subunits. *J Mol Evol* 62: 132–142, 2006.

136. Hards K and Cook GM. Targeting bacterial energetics to produce new antimicrobials. *Drug Resist Updat* 36: 1–12, 2018.

137. Hards K, McMillan DGG, Schurig-Briccio LA, Gennis RB, Lill H, Bald D, and Cook GM. Ionophoric effects of the antitubercular drug bedaquiline. *Proc Natl Acad Sci U S A* 115: 7326–7331, 2018.

138. Hards K, Robson JR, Berney M, Shaw L, Bald D, Koul A, Andries K, and Cook GM. Bactericidal mode of action of bedaquiline. *J Antimicrob Chemother* 70: 2028–2037, 2015.

139. Hastings SF, Kaysser TM, Jiang F, Salerno JC, Gennis RB, and Ingledew WJ. Identification of a stable semiquinone intermediate in the purified and membrane bound ubiquinol oxidase-cytochrome *bd* from *Escherichia coli*. *Eur J Biochem* 255: 317–323, 1998.

140. Heidelberg JF, Seshadri R, Haveman SA, Hemme CL, Paulsen IT, Kolonay JF, Eisen JA, Ward N, Methe B, Brinkac LM, Daugherty SC, Deboy RT, Dodson RJ, Durkin AS, Madupu R, Nelson WC, Sullivan SA, Fouts D, Haft DH, Selengut J, Peterson JD, Davidsen TM, Zafar N, Zhou L, Radune D, Dimitrov G, Hance M, Tran K, Khouri H, Gill J, Utterback TR, Feldblyum TV, Wall JD, Voordouw G, and Fraser CM. The genome sequence of the anaerobic, sulfate-reducing bacterium *Desulfovibrio vulgaris* Hildenborough. *Nat Biotechnol* 22: 554–559, 2004.

141. Heintz D, Gallien S, Wischgoll S, Ullmann AK, Schaeffer C, Kretzschmar AK, van Dorsselaer A, and Boll M. Differential membrane proteome analysis reveals novel proteins involved in the degradation of aromatic compounds in *Geobacter metallireducens*. *Mol Cell Proteomics* 8: 2159–2169, 2009.

142. Hill BC, Hill JJ, and Gennis RB. The room temperature reaction of carbon monoxide and oxygen with the cytochrome *bd* quinol oxidase from *Escherichia coli*. *Biochemistry* 33: 15110–15115, 1994.

143. Hill JJ, Alben JO, and Gennis RB. Spectroscopic evidence for a heme-heme binuclear center in the cytochrome *bd* ubiquinol oxidase from *Escherichia coli*. *Proc Natl Acad Sci U S A* 90: 5863–5867, 1993.

144. Hobson JJ, Gallegos AS, Atha BW, 3rd, Kelly JP, Lein CD, VanOrsdel CE, Weldon JE, and Hemm MR. Investigation of amino acid specificity in the CydX small protein shows sequence plasticity at the functional level. *PLoS One* 13: e0198699, 2018.

145. Hoeser J, Hong S, Gehmann G, Gennis RB, and Friedrich T. Subunit CydX of *Escherichia coli* cytochrome *bd* ubiquinol oxidase is essential for assembly and stability of the di-heme active site. *FEBS Lett* 588: 1537–1541, 2014.

146. Holyoake LV, Hunt S, Sanguinetti G, Cook GM, Howard MJ, Rowe ML, Poole RK, and Shepherd M. CydDC-mediated reductant export in *Escherichia coli* controls the transcriptional wiring of energy metabolism and combats nitrosative stress. *Biochem J* 473: 693–701, 2016.

147. Hoogewijs D, Geuens E, Dewilde S, Moens L, Vierstraete A, Vinogradov S, and Vanfleteren J. Genome-wide analysis of the globin gene family of *C. elegans*. *IUBMB Life* 56: 697–702, 2004.

148. Hori H, Tsubaki M, Mogi T, and Anraku Y. EPR study of NO complex of *bd*-type ubiquinol oxidase from *Escherichia coli*. *J Biol Chem* 271: 9254–9258, 1996.

149. Hull SE, Karlsson R, Main P, Woolfson MM, and Dodson EJ. The crystal structure of a hydrated gramicidin S–urea complex. *Nature* 275: 206–207, 1978.

150. Hyduke DR, Jarboe LR, Tran LM, Chou KJ, and Liao JC. Integrated network analysis identifies nitric oxide response networks and dihydroxyacid dehydratase as a crucial target in *Escherichia coli*. *Proc Natl Acad Sci U S A* 104: 8484–8489, 2007.

151. Ingledew WJ and Poole RK. The respiratory chains of *Escherichia coli*. *Microbiol Rev* 48: 222–271, 1984.

152. Iqbal IK, Bajeli S, Akela AK, and Kumar A. Bioenergetics of Mycobacterium: an emerging landscape for drug discovery. *Pathogens* 7: 24, 2018.

153. Iuchi S, Chepuri V, Fu HA, Gennis RB, and Lin EC. Requirement for terminal cytochromes in generation of the aerobic signal for the *arc* regulatory system in *Escherichia coli*: study utilizing deletions and *lac* fusions of *cyo* and *cyd*. *J Bacteriol* 172: 6020–6025, 1990.

154. Iwata S, Ostermeier C, Ludwig B, and Michel H. Structure at 2.8 A resolution of cytochrome *c* oxidase from *Paracoccus denitrificans*. *Nature* 376: 660–669, 1995.

155. Jasaitis A, Borisov VB, Belevich NP, Morgan JE, Konstantinov AA, and Verkhovsky MI. Electrogenic reactions of cytochrome *bd*. *Biochemistry* 39: 13800–13809, 2000.

156. Jesse HE, Nye TL, McLean S, Green J, Mann BE, and Poole RK. Cytochrome *bd*-I in *Escherichia coli* is less sensitive than cytochromes *bd*-II or *bo′′* to inhibition by the carbon monoxide-releasing molecule, CORM-3: N-acetylcysteine reduces CO-RM uptake and inhibition of respiration. *Biochim Biophys Acta* 1834: 1693–1703, 2013.

157. Jimenez de Bagues MP, Loisel-Meyer S, Liautard JP, and Jubier-Maurin V. Different roles of the two high-oxygen-affinity terminal oxidases of *Brucella suis*: cytochrome *c* oxidase, but not ubiquinol oxidase, is required for persistence in mice. *Infect Immun* 75: 531–535, 2007.

158. Johansson J, Gudmundsson GH, Rottenberg ME, Berndt KD, and Agerberth B. Conformation-dependent antibacterial activity of the naturally occurring human peptide LL-37. *J Biol Chem* 273: 3718–3724, 1998.

159. Jones SA, Chowdhury FZ, Fabich AJ, Anderson A, Schreiner DM, House AL, Autieri SM, Leatham MP, Lins JJ, Jorgensen M, Cohen PS, and Conway T. Respiration of *Escherichia coli* in the mouse intestine. *Infect Immun* 75: 4891–4899, 2007.

160. Jones SA, Gibson T, Maltby RC, Chowdhury FZ, Stewart V, Cohen PS, and Conway T. Anaerobic respiration of *Escherichia coli* in the mouse intestine. *Infect Immun* 79: 4218–4226, 2011.

161. Jones-Carson J, Husain M, Liu L, Orlicky DJ, and Vazquez-Torres A. Cytochrome *bd*-dependent bioenergetics and antinitrosative defenses in *Salmonella* pathogenesis. *mBio* 7: e02052-16, 2016.

162. Jormakka M, Yokoyama K, Yano T, Tamakoshi M, Akimoto S, Shimamura T, Curmi P, and Iwata S. Molecular mechanism of energy conservation in polysulfide respiration. *Nat Struct Mol Biol* 15: 730–737, 2008.

163. Junemann S. Cytochrome *bd* terminal oxidase. *Biochim Biophys Acta* 1321: 107–127, 1997.

164. Junemann S, Butterworth PJ, and Wrigglesworth JM. A suggested mechanism for the catalytic cycle of cytochrome *bd* terminal oxidase based on kinetic analysis. *Biochemistry* 34: 14861–14867, 1995.

165. Junemann S, Rich PR, and Wrigglesworth JM. CO flash photolysis of cytochrome *bd* from *Azotobacter vinelandii*. *Biochem Soc Trans* 23: 157S, 1995.

166. Junemann S and Wrigglesworth JM. Stoichiometry of CO binding to the cytochrome *bd* complex of *Azotobacter vinelandii*. *Biochem Soc Trans* 21: 345S, 1993.

167. Junemann S and Wrigglesworth JM. Cytochrome *bd* oxidase from *Azotobacter vinelandii*. Purification and quantitation of ligand binding to the oxygen reduction site. *J Biol Chem* 270: 16213–16220, 1995.

168. Junemann S and Wrigglesworth JM. Binding of NO to the oxygen reaction site of cytochrome *bd* from *Azotobacter vinelandii*. *Biochem Soc Trans* 24: 38S, 1996.

169. Junemann S, Wrigglesworth JM, and Rich PR. Effects of *decyl*-aurachin D and reversed electron transfer in cytochrome *bd*. *Biochemistry* 36: 9323–9331, 1997.

170. Juty NS, Moshiri F, Merrick M, Anthony C, and Hill S. The *Klebsiella pneumoniae* cytochrome *bd′* terminal oxidase complex and its role in microaerobic nitrogen fixation. *Microbiology* 143: 2673–2683, 1997.

171. Kabus A, Niebisch A, and Bott M. Role of cytochrome *bd* oxidase from *Corynebacterium glutamicum* in growth and lysine production. *Appl Environ Microbiol* 73: 861–868, 2007.

172. Kahlow MA, Zuberi TM, Gennis RB, and Loehr TM. Identification of a ferryl intermediate of *Escherichia coli* cytochrome *d* terminal oxidase by Resonance Raman spectroscopy. *Biochemistry* 30: 11485–11489, 1991.

173. Kalia NP, Hasenoehrl EJ, Ab Rahman NB, Koh VH, Ang MLT, Sajorda DR, Hards K, Gruber G, Alonso S, Cook GM, Berney M, and Pethe K. Exploiting the synthetic lethality between terminal respiratory oxidases to kill *Mycobacterium tuberculosis* and clear host infection. *Proc Natl Acad Sci U S A* 114: 7426–7431, 2017.

174. Kalia NP, Shi Lee B, Ab Rahman NB, Moraski GC, Miller MJ, and Pethe K. Carbon metabolism modulates the efficacy of drugs targeting the cytochrome $bc_1:aa_3$ in *Mycobacterium tuberculosis*. *Sci Rep* 9: 8608, 2019.

175. Kaminski PA, Kitts CL, Zimmerman Z, and Ludwig RA. *Azorhizobium caulinodans* uses both cytochrome *bd* (quinol) and cytochrome cbb_3 (cytochrome *c*) terminal oxidases for symbiotic N_2 fixation. *J Bacteriol* 178: 5989–5994, 1996.

176. Kana BD, Weinstein EA, Avarbock D, Dawes SS, Rubin H, and Mizrahi V. Characterization of the *cydAB*-encoded cytochrome *bd* oxidase from *Mycobacterium smegmatis*. *J Bacteriol* 183: 7076–7086, 2001.

177. Kauffman HF, DerVartanian DV, van Gelder BF, and Wampler J. EPR studies on cytochrome components in phosphorylating particles of *Azotobacter vinelandii*. *J Bioenerg* 7: 215–222, 1975.

178. Kauffman HF and Van Gelder BF. The respiratory chain of *Azotobacter vinelandii*. II. The effect of cyanide on cytochrome *d*. *Biochim Biophys Acta* 314: 276–283, 1973.

179. Kauffman HF and Van Gelder BF. The respiratory chain of *Azotobacter vinelandii*. III. The effect of cyanide in the presence of substrates. *Biochim Biophys Acta* 333: 218–227, 1974.

180. Kelly MJS, Poole RK, Yates MG, and Kennedy C. Cloning and mutagenesis of genes encoding the cytochrome *bd* terminal oxidase complex in *Azotobacter vinelandii*: mutants deficient in the cytochrome *d* complex are unable to fix nitrogen in air. *J Bacteriol* 172: 6010–6019, 1990.

181. Keyhani E and Minai-Tehrani D. The binding of cyanide to cytochrome *d* in intact cells, spheroplasts, membrane fragments and solubilized enzyme from *Salmonella typhimurium*. *Biochim Biophys Acta* 1506: 1–11, 2001.

182. Khademian M and Imlay JA. *Escherichia coli* cytochrome *c* peroxidase is a respiratory oxidase that enables the use of hydrogen peroxide as a terminal electron acceptor. *Proc Natl Acad Sci U S A* 114: E6922–E6931, 2017.

183. Kita K, Konishi K, and Anraku Y. Terminal oxidases of *Escherichia coli* aerobic respiratory chain. II. Purification and properties of cytochrome b_{558}-*d* complex from cells grown with limited oxygen and evidence of branched electron-carrying systems. *J Biol Chem* 259: 3375–3381, 1984.

184. Koch-Koerfges A, Pfelzer N, Platzen L, Oldiges M, and Bott M. Conversion of *Corynebacterium glutamicum* from an aerobic respiring to an aerobic fermenting bacterium by inactivation of the respiratory chain. *Biochim Biophys Acta* 1827: 699–708, 2013.

185. Koland JG, Miller MJ, and Gennis RB. Potentiometric analysis of the purified cytochrome *d* terminal oxidase complex from *Escherichia coli*. *Biochemistry* 23: 1051–1056, 1984.

186. Koland JG, Miller MJ, and Gennis RB. Reconstitution of the membrane-bound, ubiquinone-dependent pyruvate oxidase respiratory chain of *Escherichia coli* with the cytochrome *d* terminal oxidase. *Biochemistry* 23: 445–453, 1984.

187. Kolonay JF, Jr. and Maier RJ. Formation of pH and potential gradients by the reconstituted *Azotobacter vinelandii* cytochrome *bd* respiratory protection oxidase. *J Bacteriol* 179: 3813–3817, 1997.

188. Komine Y, Adachi T, Inokuchi H, and Ozeki H. Genomic organization and physical mapping of the transfer RNA genes in *Escherichia coli* K12. *J Mol Biol* 212: 579–598, 1990.

189. Kondejewski LH, Farmer SW, Wishart DS, Hancock RE, and Hodges RS. Gramicidin S is active against both gram-positive and gram-negative bacteria. *Int J Pept Protein Res* 47: 460–466, 1996.

190. Kondejewski LH, Farmer SW, Wishart DS, Kay CM, Hancock RE, and Hodges RS. Modulation of structure and antibacterial and hemolytic activity by ring size in cyclic gramicidin S analogs. *J Biol Chem* 271: 25261–25268, 1996.

191. Korshunov S and Imlay JA. Two sources of endogenous hydrogen peroxide in *Escherichia coli*. *Mol Microbiol* 75: 1389–1401, 2010.

192. Korshunov S, Imlay KR, and Imlay JA. The cytochrome *bd* oxidase of *Escherichia coli* prevents respiratory inhibition by endogenous and exogenous hydrogen sulfide. *Mol Microbiol* 101: 62–77, 2016.

193. Koul A, Dendouga N, Vergauwen K, Molenberghs B, Vranckx L, Willebrords R, Ristic Z, Lill H, Dorange I, Guillemont J, Bald D, and Andries K. Diarylquinolines target subunit c of mycobacterial ATP synthase. *Nat Chem Biol* 3: 323–324, 2007.

194. Koul A, Vranckx L, Dendouga N, Balemans W, Van den Wyngaert I, Vergauwen K, Gohlmann HW, Willebrords R, Poncelet A, Guillemont J, Bald D, and Andries K. Diarylquinolines are bactericidal for dormant mycobacteria as a result of disturbed ATP homeostasis. *J Biol Chem* 283: 25273–25280, 2008.

195. Koul A, Vranckx L, Dhar N, Gohlmann HW, Ozdemir E, Neefs JM, Schulz M, Lu P, Mortz E, McKinney JD, Andries K, and Bald D. Delayed bactericidal response of *Mycobacterium tuberculosis* to bedaquiline involves remodelling of bacterial metabolism. *Nat Commun* 5: 3369, 2014.

196. Krab K and Wikstrom M. Principles of coupling between electron transfer and proton translocation with special reference to proton-translocation mechanisms in cytochrome oxidase. *Biochim Biophys Acta* 895: 25–39, 1987.

197. Kranz RG, Beckett CS, and Goldman BS. Genomic analyses of bacterial respiratory and cytochrome *c* assembly systems: *Bordetella* as a model for the system II cytochrome *c* biogenesis pathway. *Res Microbiol* 153: 1–6, 2002.

198. Krasnoselskaya I, Arutjunjan AM, Smirnova I, Gennis R, and Konstantinov AA. Cyanide-reactive sites in cytochrome *bd* complex from *E. coli*. *FEBS Lett* 327: 279–283, 1993.

199. Lamrabet O, Pieulle L, Aubert C, Mouhamar F, Stocker P, Dolla A, and Brasseur G. Oxygen reduction in the strict anaerobe *Desulfovibrio vulgaris* Hildenborough: characterization of two membrane-bound oxygen reductases. *Microbiology* 157: 2720–2732, 2011.

200. Larsson JT, Rogstam A, and von Wachenfeldt C. Coordinated patterns of cytochrome *bd* and lactate dehydrogenase expression in *Bacillus subtilis*. *Microbiology* 151: 3323–3335, 2005.

201. Leclerc J, Rosenfeld E, Trainini M, Martin B, Meuric V, Bonnaure-Mallet M, and Baysse C. The cytochrome *bd* oxidase of *Porphyromonas gingivalis* contributes to oxidative stress resistance and dioxygen tolerance. *PLoS One* 10: e0143808, 2015.

202. Lemos RS, Gomes CM, Santana M, LeGall J, Xavier AV, and Teixeira M. The 'strict' anaerobe *Desulfovibrio gigas* contains a membrane-bound oxygen-reducing respiratory chain. *FEBS Lett* 496: 40–43, 2001.

203. Leung D, van der Oost J, Kelly M, Saraste M, Hill S, and Poole RK. Mutagenesis of a gene encoding a cytochrome *o*-like terminal oxidase of *Azotobacter vinelandii*: a cytochrome *o* mutant is aero-tolerant during nitrogen fixation. *FEMS Microbiol Lett* 119: 351–357, 1994.

204. Li H, Jubelirer S, Garcia Costas AM, Frigaard NU, and Bryant DA. Multiple antioxidant proteins protect *Chlorobaculum tepidum* against oxygen and reactive oxygen species. *Arch Microbiol* 191: 853–867, 2009.

205. Lin WC, Coppi MV, and Lovley DR. *Geobacter sulfurreducens* can grow with oxygen as a terminal electron acceptor. *Appl Environ Microbiol* 70: 2525–2528, 2004.

206. Lindqvist A, Membrillo-Hernandez J, Poole RK, and Cook GM. Roles of respiratory oxidases in protecting *Escherichia coli* K12 from oxidative stress. *Antonie Van Leeuwenhoek* 78: 23–31, 2000.

207. Liu X, Cheng Y, Lyu M, Wen Y, Song Y, Chen Z, and Li J. Redox-sensing regulator Rex regulates aerobic metabolism, morphological differentiation, and avermectin production in *Streptomyces avermitilis*. *Sci Rep* 7: 44567, 2017.

208. Loisel-Meyer S, Jimenez de Bagues MP, Kohler S, Liautard JP, and Jubier-Maurin V. Differential use of the two high-oxygen-affinity terminal oxidases of *Brucella suis* for in vitro and intramacrophagic multiplication. *Infect Immun* 73: 7768–7771, 2005.

209. Lorence RM and Gennis RB. Spectroscopic and quantitative analysis of the oxygenated and peroxy states of the purified cytochrome *d* complex of *Escherichia coli*. *J Biol Chem* 264: 7135–7140, 1989.

210. Lorence RM, Koland JG, and Gennis RB. Coulometric and spectroscopic analysis of the purified cytochrome *d* complex of *Escherichia coli*: evidence for the identification of ''cytochrome a_1'' as cytochrome b_{595}. *Biochemistry* 25: 2314–2321, 1986.

211. Lorence RM, Miller MJ, Borochov A, Faiman-Weinberg R, and Gennis RB. Effects of pH and detergent on the kinetic and electrochemical properties of the purified cytochrome *d* terminal oxidase complex of *Escherichia coli*. *Biochim Biophys Acta* 790: 148–153, 1984.

212. Lu P, Heineke MH, Koul A, Andries K, Cook GM, Lill H, van Spanning R, and Bald D. The cytochrome *bd*-type quinol oxidase is important for survival of *Mycobacterium smegmatis* under peroxide and antibiotic-induced stress. *Sci Rep* 5: 10333, 2015.

213. Lu X, Williams Z, Hards K, Tang J, Cheung CY, Aung HL, Wang B, Liu Z, Hu X, Lenaerts A, Woolhiser L, Hastings C, Zhang X, Wang Z, Rhee K, Ding K, Zhang T, and Cook GM. Pyrazolo[1,5-*a*]pyridine inhibitor of the respiratory cytochrome *bcc* complex for the treatment of drug-resistant tuberculosis. *ACS Infect Dis* 5: 239–249, 2019.

214. Lynch AS and Lin EC. Transcriptional control mediated by the ArcA two-component response regulator protein of Escherichia coli: characterization of DNA binding at target promoters. *J Bacteriol* 178: 6238–6249, 1996.

215. Machado P, Felix R, Rodrigues R, Oliveira S, and Rodrigues-Pousada C. Characterization and expression analysis of the cytochrome *bd* oxidase operon from *Desulfovibrio gigas*. *Curr Microbiol* 52: 274–281, 2006.

216. Makarova KS, Wolf YI, Karamycheva S, Zhang D, Aravind L, and Koonin EV. Antimicrobial peptides, polymorphic toxins, and self-nonself recognition systems in archaea: an untapped armory for intermicrobial conflicts. *MBio* 10: e00715-19, 2019.

217. Mason MG, Shepherd M, Nicholls P, Dobbin PS, Dodsworth KS, Poole RK, and Cooper CE. Cytochrome *bd* confers nitric oxide resistance to *Escherichia coli*. *Nat Chem Biol* 5: 94–96, 2009.

218. Matsumoto Y, Murai M, Fujita D, Sakamoto K, Miyoshi H, Yoshida M, and Mogi T. Mass spectrometric analysis of the ubiquinol-binding site in cytochrome *bd* from *Escherichia coli*. *J Biol Chem* 281: 1905–1912, 2006.

219. McDonald AG, Boyce S, and Tipton KF. ExplorEnz: the primary source of the IUBMB enzyme list (https://www.enzyme-database.org). *Nucleic Acids Res* 37: D593–D597, 2009.

220. Meinhardt SW, Gennis RB, and Ohnishi T. EPR studies of the cytochrome-*d* complex of *Escherichia coli*. *Biochim Biophys Acta* 975: 175–184, 1989.

221. Meunier B, Madgwick SA, Reil E, Oettmeier W, and Rich PR. New inhibitors of the quinol oxidation sites of bacterial cytochromes *bo* and *bd*. *Biochemistry* 34: 1076–1083, 1995.

222. Miller MJ and Gennis RB. The purification and characterization of the cytochrome *d* terminal oxidase complex of the *Escherichia coli* aerobic respiratory chain. *J Biol Chem* 258: 9159–9165, 1983.

223. Miller MJ and Gennis RB. The cytochrome *d* complex is a coupling site in the aerobic respiratory chain of *Escherichia coli*. *J Biol Chem* 260: 14003–14008, 1985.

224. Miller MJ, Hermodson M, and Gennis RB. The active form of the cytochrome *d* terminal oxidase complex of *Escherichia coli* is a heterodimer containing one copy of each of the two subunits. *J Biol Chem* 263: 5235–5240, 1988.

225. Milse J, Petri K, Ruckert C, and Kalinowski J. Transcriptional response of *Corynebacterium glutamicum* ATCC 13032 to hydrogen peroxide stress and characterization of the OxyR regulon. *J Biotechnol* 190: 40–54, 2014.

226. Mogi T, Akimoto S, Endou S, Watanabe-Nakayama T, Mizuochi-Asai E, and Miyoshi H. Probing the ubiquinol-binding site in cytochrome *bd* by site-directed mutagenesis. *Biochemistry* 45: 7924–7930, 2006.

227. Mogi T and Kita K. Gramicidin S and polymyxins: the revival of cationic cyclic peptide antibiotics. *Cell Mol Life Sci* 66: 3821–3826, 2009.

228. Mogi T, Ui H, Shiomi K, Omura S, and Kita K. Gramicidin S identified as a potent inhibitor for cytochrome *bd*-type quinol oxidase. *FEBS Lett* 582: 2299–2302, 2008.

229. Moore CM, Nakano MM, Wang T, Ye RW, and Helmann JD. Response of *Bacillus subtilis* to nitric oxide and the nitrosating agent sodium nitroprusside. *J Bacteriol* 186: 4655–4664, 2004.

230. Moshiri F, Smith EG, Taormino JP, and Maier RJ. Transcriptional regulation of cytochrome *d* in nitrogen-fixing *Azotobacter vinelandii*. Evidence that up-regulation during N_2 fixation is independent of nifA but dependent on ntrA. *J Biol Chem* 266: 23169–23174, 1991.

231. Mukhopadhyay A, Redding AM, Joachimiak MP, Arkin AP, Borglin SE, Dehal PS, Chakraborty R, Geller JT, Hazen TC, He Q, Joyner DC, Martin VJ, Wall JD, Yang ZK, Zhou J, and Keasling JD. Cell-wide responses to low-oxygen exposure in *Desulfovibrio vulgaris* Hildenborough. *J Bacteriol* 189: 5996–6010, 2007.

232. Muntyan MS, Bloch DA, Drachev LA, and Skulachev VP. Kinetics of CO binding to putative Na^+-motive oxidases of the *o*-type from *Bacillus FTU* and of the *d*-type from *Escherichia coli*. *FEBS Lett* 327: 347–350, 1993.

233. Murali R and Gennis RB. Functional importance of Glutamate-445 and Glutamate-99 in proton-coupled electron transfer during oxygen reduction by cytochrome *bd* from *Escherichia coli*. *Biochim Biophys Acta* 1859: 577–590, 2018.

234. Narra HP, Schroeder CL, Sahni A, Rojas M, Khanipov K, Fofanov Y, and Sahni SK. Small regulatory RNAs of *Rickettsia conorii*. *Sci Rep* 6: 36728, 2016.

235. Nicholls P, Marshall DC, Cooper CE, and Wilson MT. Sulfide inhibition of and metabolism by cytochrome *c* oxidase. *Biochem Soc Trans* 41: 1312–1316, 2013.

236. Nicholls P and Petersen LC. Haem-haem interactions in cytochrome aa_3 during the anaerobic-aerobic transition. *Biochim Biophys Acta* 357: 462–467, 1974.

237. Ntwasa M. Cationic peptide interactions with biological macromolecules. In: *Binding Protein*, edited by Abdelmohsen K. London, England: IntechOpen, 2012, pp. 139–164.

238. Oelze J. Respiratory protection of nitrogenase in *Azotobacter* species: is a widely held hypothesis unequivocally supported by experimental evidence? *FEMS Microbiol Rev* 24: 321–333, 2000.

239. Osborne JP and Gennis RB. Sequence analysis of cytochrome *bd* oxidase suggests a revised topology for subunits I. *Biochim Biophys Acta* 1410: 32–50, 1999.

240. Pankratova G, Leech D, Gorton L, and Hederstedt L. Extracellular electron transfer by the gram-positive bacterium *Enterococcus faecalis*. *Biochemistry* 57: 4597–4603, 2018.

241. Parkhill J, Wren BW, Mungall K, Ketley JM, Churcher C, Basham D, Chillingworth T, Davies RM, Feltwell T, Holroyd S, Jagels K, Karlyshev AV, Moule S, Pallen MJ, Penn CW, Quail MA, Rajandream MA, Rutherford KM, van Vliet AH, Whitehead S, and Barrell BG. The genome sequence of the food-borne pathogen *Campylobacter jejuni* reveals hypervariable sequences. *Nature* 403: 665–668, 2000.

242. Paulus A, Rossius SG, Dijk M, and de Vries S. Oxoferryl-porphyrin radical catalytic intermediate in cytochrome *bd* oxidases protects cells from formation of reactive oxygen species. *J Biol Chem* 287: 8830–8838, 2012.

243. Pereira MM, Sousa FL, Verissimo AF, and Teixeira M. Looking for the minimum common denominator in haem-copper oxygen reductases: towards a unified catalytic mechanism. *Biochim Biophys Acta* 1777: 929–934, 2008.

244. Petersen LC. The effect of inhibitors on the oxygen kinetics of cytochrome *c* oxidase. *Biochim Biophys Acta* 460: 299–307, 1977.

245. Pethe K, Bifani P, Jang J, Kang S, Park S, Ahn S, Jiricek J, Jung J, Jeon HK, Cechetto J, Christophe T, Lee H, Kempf M, Jackson M, Lenaerts AJ, Pham H, Jones V, Seo MJ, Kim YM, Seo M, Seo JJ, Park D, Ko Y, Choi I, Kim R, Kim SY, Lim S, Yim SA, Nam J, Kang H, Kwon H, Oh CT, Cho Y, Jang Y, Kim J, Chua A, Tan BH, Nanjundappa MB, Rao SP, Barnes WS, Wintjens R, Walker JR, Alonso S, Lee S, Kim J, Oh S, Oh T, Nehrbass U, Han SJ, No Z, Lee J, Brodin P, Cho SN, Nam K, and Kim J. Discovery of Q203, a potent clinical candidate for the treatment of tuberculosis. *Nat Med* 19: 1157–1160, 2013.

246. Pils D and Schmetterer G. Characterization of three bioenergetically active respiratory terminal oxidases in the cyanobacterium *Synechocystis* sp. strain PCC 6803. *FEMS Microbiol Lett* 203: 217–222, 2001.

247. Pittman MS, Corker H, Wu G, Binet MB, Moir AJ, and Poole RK. Cysteine is exported from the *Escherichia coli* cytoplasm by CydDC, an ATP-binding cassette-type transporter required for cytochrome assembly. *J Biol Chem* 277: 49841–49849, 2002.

248. Pittman MS, Robinson HC, and Poole RK. A bacterial glutathione transporter (*Escherichia coli* CydDC) exports reductant to the periplasm. *J Biol Chem* 280: 32254–32261, 2005.

249. Poole RK. Bacterial cytochrome oxidases. In: *Bacterial Energy Transduction*, edited by Anthony C. London: Academic Press, 1988, pp. 231–291.

250. Poole RK, Blum H, Scott RI, Collinge A, and Ohnishi T. The orientation of cytochromes in membrane multilayers prepared from aerobically grown *Escherichia coli* K12. *J Gen Microbiol* 119: 145–154, 1980.

251. Poole RK and Chance B. Oxidase names: to '3' or not to '3'? *Microbiology* 141: 752–753, 1995.

252. Poole RK and Cook GM. Redundancy of aerobic respiratory chains in bacteria? Routes, reasons and regulation. *Adv Microb Physiol* 43: 165–224, 2000.

253. Poole RK, Cozens AG, and Shepherd M. The CydDC family of transporters. *Res Microbiol* 170: 407–416, 2019.

254. Poole RK, Gibson F, and Wu G. The *cyd*D gene product, component of a heterodimeric ABC transporter, is required for assembly of periplasmic cytochrome *c* and of cytochrome *bd* in *Escherichia coli*. *FEMS Microbiol Lett* 117: 217–224, 1994.

255. Poole RK, Hatch L, Cleeter MWJ, Gibson F, Cox GB, and Wu G. Cytochrome *bd* biosynthesis in *Escherichia coli*: the sequences of the *cydC* and *cydD* genes suggest that they encode the components of an ABC membrane transporter. *Mol Microbiol* 10: 421–430, 1993.

256. Poole RK and Hill S. Respiratory protection of nitrogenase activity in *Azotobacter vinelandii*—roles of the terminal oxidases. *Biosci Rep* 17: 307–317, 1997.

257. Poole RK, Kumar C, Salmon I, and Chance B. The 650 nm chromophore in *Escherichia coli* is an 'Oxy-' or oxygenated compound, not the oxidized form of cytochrome oxidase *d*: a hypothesis. *J Gen Microbiol* 129: 1335–1344, 1983.

258. Poole RK and Williams HD. Proposal that the function of the membrane-bound cytochrome a_1-like haemoprotein (cytochrome *b*-595) in *Escherichia coli* is a direct electron donation to cytochrome *d*. *FEBS Lett* 217: 49–52, 1987.

259. Poole RK and Williams HD. Formation of the 680-nm-absorbing form of the cytochrome *bd* oxidase complex of *Escherichia coli* by reaction of hydrogen peroxide with the ferric form. *FEBS Lett* 231: 243–246, 1988.

260. Poole RK, Williams HD, Downie JA, and Gibson F. Mutations affecting the cytochrome *d*-containing oxidase complex of *Escherichia coli* K12: identification and mapping of a fourth locus, *cydD*. *J Gen Microbiol* 135: 1865–1874, 1989.

261. Preiss L, Langer JD, Yildiz O, Eckhardt-Strelau L, Guillemont JE, Koul A, and Meier T. Structure of the mycobacterial ATP synthase F_o rotor ring in complex with the anti-TB drug bedaquiline. *Sci Adv* 1: e1500106, 2015.

262. Pudek MR and Bragg PD. Inhibition by cyanide of the respiratory chain oxidases of *Escherichia coli*. *Arch Biochem Biophys* 164: 682–693, 1974.

263. Pudek MR and Bragg PD. Reaction of cyanide with cytochrome *d* in respiratory particles from exponential phase *Escherichia coli*. *FEBS Lett* 50: 111–113, 1975.

264. Pudek MR and Bragg PD. Redox potentials of the cytochromes in the respiratory chain of aerobically grown *Escherichia coli*. *Arch Biochem Biophys* 174: 546–552, 1976.

265. Pullan ST, Gidley MD, Jones RA, Barrett J, Stevanin TM, Read RC, Green J, and Poole RK. Nitric oxide in chemostat-cultured *Escherichia coli* is sensed by Fnr and other global regulators: unaltered methionine

biosynthesis indicates lack of S nitrosation. *J Bacteriol* 189: 1845–1855, 2007.

266. Puri-Taneja A, Schau M, Chen Y, and Hulett FM. Regulators of the *Bacillus subtilis cydABCD* operon: identification of a negative regulator, CcpA, and a positive regulator, ResD. *J Bacteriol* 189: 3348–3358, 2007.

267. Puustinen A, Finel M, Haltia T, Gennis RB, and Wikstrom M. Properties of the two terminal oxidases of *Escherichia coli*. *Biochemistry* 30: 3936–3942, 1991.

268. Ramel F, Amrani A, Pieulle L, Lamrabet O, Voordouw G, Seddiki N, Brethes D, Company M, Dolla A, and Brasseur G. Membrane-bound oxygen reductases of the anaerobic sulfate-reducing *Desulfovibrio vulgaris* Hildenborough: roles in oxygen defense and electron link with the periplasmic hydrogen oxidation. *Microbiology* 159: 2663–2673, 2013.

269. Rappaport F, Zhang J, Vos MH, Gennis RB, and Borisov VB. Heme-heme and heme-ligand interactions in the di-heme oxygen-reducing site of cytochrome *bd* from *Escherichia coli* revealed by nanosecond absorption spectroscopy. *Biochim Biophys Acta* 1797: 1657–1664, 2010.

270. Rawat R, Whitty A, and Tonge PJ. The isoniazid-NAD adduct is a slow, tight-binding inhibitor of InhA, the *Mycobacterium tuberculosis* enoyl reductase: adduct affinity and drug resistance. *Proc Natl Acad Sci U S A* 100: 13881–13886, 2003.

271. Rebuffat S. Microcins in action: amazing defence strategies of Enterobacteria. *Biochem Soc Trans* 40: 1456–1462, 2012.

272. Rice CW and Hempfling WP. Oxygen-limited continuous culture and respiratory energy conservation in *Escherichia coli*. *J Bacteriol* 134: 115–124, 1978.

273. Richardson AR, Dunman PM, and Fang FC. The nitrosative stress response of *Staphylococcus aureus* is required for resistance to innate immunity. *Mol Microbiol* 61: 927–939, 2006.

274. Richter OM and Ludwig B. Electron transfer and energy transduction in the terminal part of the respiratory chain—lessons from bacterial model systems. *Biochim Biophys Acta* 1787: 626–634, 2009.

275. Rivera-Chavez F, Zhang LF, Faber F, Lopez CA, Byndloss MX, Olsan EE, Xu G, Velazquez EM, Lebrilla CB, Winter SE, and Baumler AJ. Depletion of butyrate-producing *Clostridia* from the gut microbiota drives an aerobic luminal expansion of *Salmonella*. *Cell Host Microbe* 19: 443–454, 2016.

276. Rolfe MD, Ter Beek A, Graham AI, Trotter EW, Asif HM, Sanguinetti G, de Mattos JT, Poole RK, and Green J. Transcript profiling and inference of *Escherichia coli* K-12 ArcA activity across the range of physiologically relevant oxygen concentrations. *J Biol Chem* 286: 10147–10154, 2011.

277. Rothery R and Ingledew WJ. The cytochromes of anaerobically grown *Escherichia coli*. *Biochem J* 262: 437–443, 1989.

278. Rybniker J, Vocat A, Sala C, Busso P, Pojer F, Benjak A, and Cole ST. Lansoprazole is an antituberculous prodrug targeting cytochrome bc_1. *Nat Commun* 6: 7659, 2015.

279. Sabra W, Zeng AP, Lunsdorf H, and Deckwer WD. Effect of oxygen on formation and structure of *Azotobacter vinelandii* alginate and its role in protecting nitrogenase. *Appl Environ Microbiol* 66: 4037–4044, 2000.

280. Safarian S, Hahn A, Mills DJ, Radloff M, Eisinger ML, Nikolaev A, Meier-Credo J, Melin F, Miyoshi H, Gennis RB, Sakamoto J, Langer JD, Hellwig P, Kuhlbrandt W, and Michel H. Active site rearrangement and structural divergence in prokaryotic respiratory oxidases. *Science* 366: 100–104, 2019.

281. Safarian S, Rajendran C, Muller H, Preu J, Langer JD, Ovchinnikov S, Hirose T, Kusumoto T, Sakamoto J, and Michel H. Structure of a bd oxidase indicates similar mechanisms for membrane-integrated oxygen reductases. *Science* 352: 583–586, 2016.

282. Sakamoto J, Koga E, Mizuta T, Sato C, Noguchi S, and Sone N. Gene structure and quinol oxidase activity of a cytochrome *bd*-type oxidase from *Bacillus stearothermophilus*. *Biochim Biophys Acta* 1411: 147–158, 1999.

283. Sakamoto J, Matsumoto A, Oobuchi K, and Sone N. Cytochrome *bd*-type quinol oxidase in a mutant of *Bacillus stearothermophilus* deficient in caa_3-type cytochrome *c* oxidase. *FEMS Microbiol Lett* 143: 151–158, 1996.

284. Salmon KA, Hung SP, Steffen NR, Krupp R, Baldi P, Hatfield GW, and Gunsalus RP. Global gene expression profiling in *Escherichia coli* K12: effects of oxygen availability and ArcA. *J Biol Chem* 280: 15084–15096, 2005.

285. Salomon RA and Farias RN. The FhuA protein is involved in microcin 25 uptake. *J Bacteriol* 175: 7741–7742, 1993.

286. Salomon RA and Farias RN. The peptide antibiotic microcin 25 is imported through the TonB pathway and the SbmA protein. *J Bacteriol* 177: 3323–3325, 1995.

287. Sanguinetti G, Lawrence ND, and Rattray M. Probabilistic inference of transcription factor concentrations and gene-specific regulatory activities. *Bioinformatics* 22: 2775–2781, 2006.

288. Santana M. Presence and expression of terminal oxygen reductases in strictly anaerobic sulfate-reducing bacteria isolated from salt-marsh sediments. *Anaerobe* 14: 145–156, 2008.

289. Sarti P, Arese M, Forte E, Giuffre A, and Mastronicola D. Mitochondria and nitric oxide: chemistry and pathophysiology. *Adv Exp Med Biol* 942: 75–92, 2012.

290. Sarti P, Forte E, Giuffre A, Mastronicola D, Magnifico MC, and Arese M. The chemical interplay between nitric oxide and mitochondrial cytochrome *c* oxidase: reactions, effectors and pathophysiology. *Int J Cell Biol* 2012: 571067, 2012.

291. Schau M, Chen Y, and Hulett FM. *Bacillus subtilis* YdiH is a direct negative regulator of the *cydABCD* operon. *J Bacteriol* 186: 4585–4595, 2004.

292. Scherr N, Bieri R, Thomas SS, Chauffour A, Kalia NP, Schneide P, Ruf MT, Lamelas A, Manimekalai MSS, Gruber G, Ishii N, Suzuki K, Tanner M, Moraski GC, Miller MJ, Witschel M, Jarlier V, Pluschke G, and Pethe K. Targeting the *Mycobacterium ulcerans* cytochrome $bc_1:aa_3$ for the treatment of Buruli ulcer. *Nat Commun* 9: 5370, 2018.

293. Setubal JC, dos Santos P, Goldman BS, Ertesvag H, Espin G, Rubio LM, Valla S, Almeida NF, Balasubramanian D, Cromes L, Curatti L, Du Z, Godsy E, Goodner B, Hellner-Burris K, Hernandez JA, Houmiel K, Imperial J, Kennedy C, Larson TJ, Latreille P, Ligon LS, Lu J, Maerk M, Miller NM, Norton S, O'Carroll IP, Paulsen I, Raulfs EC, Roemer R, Rosser J, Segura D, Slater S, Stricklin SL, Studholme DJ, Sun J, Viana CJ, Wallin E, Wang B, Wheeler C, Zhu H, Dean DR, Dixon R, and Wood D. Genome sequence of *Azotobacter vinelandii*, an obligate

aerobe specialized to support diverse anaerobic metabolic processes. *J Bacteriol* 191: 4534–4545, 2009.

294. Sharpe MA and Cooper CE. Interaction of peroxynitrite with mitochondrial cytochrome oxidase. Catalytic production of nitric oxide and irreversible inhibition of enzyme activity. *J Biol Chem* 273: 30961–30972, 1998.

295. Shepherd M, Achard ME, Idris A, Totsika M, Phan MD, Peters KM, Sarkar S, Ribeiro CA, Holyoake LV, Ladakis D, Ulett GC, Sweet MJ, Poole RK, McEwan AG, and Schembri MA. The cytochrome *bd*-I respiratory oxidase augments survival of multidrug-resistant *Escherichia coli* during infection. *Sci Rep* 6: 35285, 2016.

296. Shi L, Sohaskey CD, Kana BD, Dawes S, North RJ, Mizrahi V, and Gennaro ML. Changes in energy metabolism of *Mycobacterium tuberculosis* in mouse lung and under in vitro conditions affecting aerobic respiration. *Proc Natl Acad Sci U S A* 102: 15629–15634, 2005.

297. Shoeb HA, Bowman BU, Jr., Ottolenghi AC, and Merola AJ. Evidence for the generation of active oxygen by isoniazid treatment of extracts of *Mycobacterium tuberculosis* H37Ra. *Antimicrob Agents Chemother* 27: 404–407, 1985.

298. Shukla P, Khodade VS, SharathChandra M, Chauhan P, Mishra S, Siddaramappa S, Pradeep BE, Singh A, and Chakrapani H. "On demand" redox buffering by H_2S contributes to antibiotic resistance revealed by a bacteria-specific H_2S donor. *Chem Sci* 8: 4967–4972, 2017.

299. Siegele DA, Imlay KR, and Imlay JA. The stationary-phase-exit defect of *cydC* (*surB*) mutants is due to the lack of a functional terminal cytochrome oxidase. *J Bacteriol* 178: 6091–6096, 1996.

300. Siletsky SA, Belevich I, Wikstrom M, Soulimane T, and Verkhovsky MI. Time-resolved O_H->E_H transition of the aberrant ba_3 oxidase from *Thermus thermophilus*. *Biochim Biophys Acta* 1787: 201–205, 2009.

301. Siletsky SA, Borisov VB, and Mamedov MD. Photosystem II and terminal respiratory oxidases: molecular machines operating in opposite directions. *Front Biosci (Landmark Ed)* 22: 1379–1426, 2017.

302. Siletsky SA, Dyuba AV, Elkina DA, Monakhova MV, and Borisov VB. Spectral-kinetic analysis of recombination reaction of heme centers of *bd*-type quinol oxidase from *Escherichia coli* with carbon monoxide. *Biochemistry (Mosc)* 82: 1354–1366, 2017.

303. Siletsky SA, Rappaport F, Poole RK, and Borisov VB. Evidence for fast electron transfer between the high-spin haems in cytochrome *bd*-I from *Escherichia coli*. *PLoS One* 11: e0155186, 2016.

304. Siletsky SA, Zaspa AA, Poole RK, and Borisov VB. Microsecond time-resolved absorption spectroscopy used to study CO compounds of cytochrome *bd* from *Escherichia coli*. *PLoS One* 9: e95617, 2014.

305. Small JL, Park SW, Kana BD, Ioerger TR, Sacchettini JC, and Ehrt S. Perturbation of cytochrome *c* maturation reveals adaptability of the respiratory chain in *Mycobacterium tuberculosis*. *mBio* 4: e00475-13, 2013.

306. Sobol Z and Schiestl RH. Intracellular and extracellular factors influencing Cr(VI) and Cr(III) genotoxicity. *Environ Mol Mutagen* 53: 94–100, 2012.

307. Sousa JS, Calisto F, Langer JD, Mills DJ, Refojo PN, Teixeira M, Kuhlbrandt W, Vonck J, and Pereira MM. Structural basis for energy transduction by respiratory alternative complex III. *Nat Commun* 9: 1728, 2018.

308. Stein T, Vater J, Kruft V, Otto A, Wittmann-Liebold B, Franke P, Panico M, McDowell R, and Morris HR. The multiple carrier model of nonribosomal peptide biosynthesis at modular multienzymatic templates. *J Biol Chem* 271: 15428–15435, 1996.

309. Steinsiek S, Stagge S, and Bettenbrock K. Analysis of *Escherichia coli* mutants with a linear respiratory chain. *PLoS One* 9: e87307, 2014.

310. Stevanin TM, Ioannidis N, Mills CE, Kim SO, Hughes MN, and Poole RK. Flavohemoglobin Hmp affords inducible protection for *Escherichia coli* respiration, catalyzed by cytochromes *bo'* or *bd*, from nitric oxide. *J Biol Chem* 275: 35868–35875, 2000.

311. Sun C, Benlekbir S, Venkatakrishnan P, Wang Y, Hong S, Hosler J, Tajkhorshid E, Rubinstein JL, and Gennis RB. Structure of the alternative complex III in a supercomplex with cytochrome oxidase. *Nature* 557: 123–126, 2018.

312. Sun J, Kahlow MA, Kaysser TM, Osborne JP, Hill JJ, Rohlfs RJ, Hille R, Gennis RB, and Loehr TM. Resonance Raman spectroscopic identification of a histidine ligand of b_{595} and the nature of the ligation of chlorin *d* in the fully reduced *Escherichia coli* cytochrome *bd* oxidase. *Biochemistry* 35: 2403–2412, 1996.

313. Sun J, Osborne JP, Kahlow MA, Kaysser TM, Gennis RB, and Loehr TM. Resonance Raman studies of *Escherichia coli* cytochrome *bd* oxidase. Selective enhancement of the three heme chromophores of the "as-isolated" enzyme and characterization of the cyanide adduct. *Biochemistry* 34: 12144–12151, 1995.

314. Sun YH, de Jong MF, den Hartigh AB, Roux CM, Rolan HG, and Tsolis RM. The small protein CydX is required for function of cytochrome *bd* oxidase in *Brucella abortus*. *Front Cell Infect Microbiol* 2: 47, 2012.

315. Szabo C, Ransy C, Modis K, Andriamihaja M, Murghes B, Coletta C, Olah G, Yanagi K, and Bouillaud F. Regulation of mitochondrial bioenergetic function by hydrogen sulfide. Part I. Biochemical and physiological mechanisms. *Br J Pharmacol* 171: 2099–2122, 2014.

316. Teramoto H, Inui M, and Yukawa H. OxyR acts as a transcriptional repressor of hydrogen peroxide-inducible antioxidant genes in *Corynebacterium glutamicum* R. *FEBS J* 280: 3298–3312, 2013.

317. Theßeling A, Rasmussen T, Burschel S, Wohlwend D, Kagi J, Muller R, Bottcher B, and Friedrich T. Homologous *bd* oxidases share the same architecture but differ in mechanism. *Nat Commun* 10: 5138, 2019.

318. Tjabringa GS, Rabe KF, and Hiemstra PS. The human cathelicidin LL-37: a multifunctional peptide involved in infection and inflammation in the lung. *Pulm Pharmacol Ther* 18: 321–327, 2005.

319. Trotter EW, Rolfe MD, Hounslow AM, Craven CJ, Williamson MP, Sanguinetti G, Poole RK, and Green J. Reprogramming of *Escherichia coli* K-12 metabolism during the initial phase of transition from an anaerobic to a micro-aerobic environment. *PLoS One* 6: e25501, 2011.

320. Tseng C-P, Albrecht J, and Gunsalus RP. Effect of microaerophilic cell growth conditions on expression of the aerobic (*cyo*ABCDE and *cyd*AB) and anaerobic (*nar*GHJI, *frd*ABCD, and *dms*ABC) respiratory pathway genes in *Escherichia coli*. *J Bacteriol* 178: 1094–1098, 1996.

321. Tsubaki M, Hori H, Mogi T, and Anraku Y. Cyanide-binding site of *bd*-type ubiquinol oxidase from *Escherichia coli*. *J Biol Chem* 270: 28565–28569, 1995.

322. Tsukihara T, Aoyama H, Yamashita E, Tomizaki T, Yamaguchi H, Shinzawa-Itoh K, Nakashima T, Yaono R, and Yoshikawa S. Structures of metal sites of oxidized bovine heart cytochrome *c* oxidase at 2.8 A. *Science* 269: 1069–1074, 1995.

323. Unden G and Bongaerts J. Alternative respiratory pathways of *Escherichia coli*: energetics and transcriptional regulation in response to electron acceptors. *Biochim Biophys Acta* 1320: 217–234, 1997.

324. VanOrsdel CE, Bhatt S, Allen RJ, Brenner EP, Hobson JJ, Jamil A, Haynes BM, Genson AM, and Hemm MR. The *Escherichia coli* CydX protein is a member of the CydAB cytochrome *bd* oxidase complex and is required for cytochrome *bd* oxidase activity. *J. Bacteriol* 195: 3640–3650, 2013.

325. Vinogradov SN, Tinajero-Trejo M, Poole RK, and Hoogewijs D. Bacterial and archaeal globins—a revised perspective. *Biochim Biophys Acta* 1834: 1789–1800, 2013.

326. Viti C, Marchi E, Decorosi F, and Giovannetti L. Molecular mechanisms of Cr(VI) resistance in bacteria and fungi. *FEMS Microbiol Rev* 38: 633–659, 2014.

327. von Dohren H, Keller U, Vater J, and Zocher R. Multifunctional peptide synthetases. *Chem Rev* 97: 2675–2706, 1997.

328. Vos MH, Borisov VB, Liebl U, Martin JL, and Konstantinov AA. Femtosecond resolution of ligand-heme interactions in the high-affinity quinol oxidase *bd*: A di-heme active site? *Proc Natl Acad Sci U S A* 97: 1554–1559, 2000.

329. Wall D, Delaney JM, Fayet O, Lipinska B, Yamamoto T, and Georgopoulos C. *arc*-Dependent thermal regulation and extragenic suppression of the *Escherichia coli* cytochrome *d* operon. *J Bacteriol* 174: 6554–6562, 1992.

330. Wan F, Shi M, and Gao H. Loss of OxyR reduces efficacy of oxygen respiration in *Shewanella oneidensis*. *Sci Rep* 7: 42609, 2017.

331. Wang E, Bauer MC, Rogstam A, Linse S, Logan DT, and von Wachenfeldt C. Structure and functional properties of the *Bacillus subtilis* transcriptional repressor Rex. *Mol Microbiol* 69: 466–478, 2008.

332. Wareham LK, Begg R, Jesse HE, Van Beilen JW, Ali S, Svistunenko D, McLean S, Hellingwerf KJ, Sanguinetti G, and Poole RK. Carbon monoxide gas is not inert, but global, in its consequences for bacterial gene expression, iron acquisition, and antibiotic resistance. *Antioxid Redox Signal* 24: 1013–1028, 2016.

333. Wareham LK, McLean S, Begg R, Rana N, Ali S, Kendall JJ, Sanguinetti G, Mann BE, and Poole RK. The broad-spectrum antimicrobial potential of [Mn(CO)$_4$(S$_2$CN-Me(CH$_2$CO$_2$H))], a water-soluble CO-releasing molecule (CORM-401): intracellular accumulation, transcriptomic and statistical analyses, and membrane polarization. *Antioxid Redox Signal* 28: 1286–1308, 2018.

334. Way SS, Sallustio S, Magliozzo RS, and Goldberg MB. Impact of either elevated or decreased levels of cytochrome *bd* expression on *Shigella flexneri* virulence. *J Bacteriol* 181: 1229–1237, 1999.

335. Wayne LG and Hayes LG. An in vitro model for sequential study of shiftdown of *Mycobacterium tuberculosis* through two stages of nonreplicating persistence. *Infect Immun* 64: 2062–2069, 1996.

336. Wikstrom M and Verkhovsky MI. Mechanism and energetics of proton translocation by the respiratory heme-copper oxidases. *Biochim Biophys Acta* 1767: 1200–1214, 2007.

337. Winstedt L, Yoshida K, Fujita Y, and von Wachenfeldt C. Cytochrome *bd* biosynthesis in *Bacillus subtilis*: characterization of the *cydABCD* operon. *J Bacteriol* 180: 6571–6580, 1998.

338. Wu G, Cruz-Ramos H, Hill S, Green J, Sawers G, and Poole RK. Regulation of cytochrome *bd* expression in the obligate aerobe *Azotobacter vinelandii* by CydR (Fnr). Sensitivity to oxygen, reactive oxygen species, and nitric oxide. *J Biol Chem* 275: 4679–4686, 2000.

339. Wu G, Hill S, Kelly MJ, Sawers G, and Poole RK. The cydR gene product, required for regulation of cytochrome *bd* expression in the obligate aerobe *Azotobacter vinelandii*, is an Fnr-like protein. *Microbiology* 143: 2197–2207, 1997.

340. Xia X, Wu S, Li L, Xu B, and Wang G. The cytochrome *bd* complex is essential for chromate and sulfide resistance and is regulated by a GbsR-type regulator, CydE, in *Alishewanella* sp. WH16-1. *Front Microbiol* 9: 1849, 2018.

341. Yamamoto Y, Poyart C, Trieu-Cuot P, Lamberet G, Gruss A, and Gaudu P. Respiration metabolism of Group B Streptococcus is activated by environmental haem and quinone and contributes to virulence. *Mol Microbiol* 56: 525–534, 2005.

342. Yamashita M, Shepherd M, Booth WI, Xie H, Postis V, Nyathi Y, Tzokov SB, Poole RK, Baldwin SA, and Bullough PA. Structure and function of the bacterial heterodimeric ABC transporter CydDC: stimulation of ATPase activity by thiol and heme compounds. *J Biol Chem* 289: 23177–23188, 2014.

343. Yang K, Borisov VB, Konstantinov AA, and Gennis RB. The fully oxidized form of the cytochrome *bd* quinol oxidase from *E. coli* does not participate in the catalytic cycle: direct evidence from rapid kinetics studies. *FEBS Lett* 582: 3705–3709, 2008.

344. Yano T, Kassovska-Bratinova S, Teh JS, Winkler J, Sullivan K, Isaacs A, Schechter NM, and Rubin H. Reduction of clofazimine by mycobacterial type 2 NADH:quinone oxidoreductase: a pathway for the generation of bactericidal levels of reactive oxygen species. *J Biol Chem* 286: 10276–10287, 2011.

345. Yaoi H and Tamiya H. On the respiratory pigment, cytochrome, in bacteria. *Proc Imp Acad Japan* 4: 436–439, 1928.

346. Zeng S, Soetaert K, Ravon F, Vandeput M, Bald D, Kauffmann JM, Mathys V, Wattiez R, and Fontaine V. Isoniazid bactericidal activity involves electron transport chain perturbation. *Antimicrob Agents Chemother* 63: e01841–18, 2019.

347. Zhang LJ and Gallo RL. Antimicrobial peptides. *Curr Biol* 26: R14–R19, 2016.

348. Zhang X, Xue C, Zhao F, Li D, Yin J, Zhang C, Caiyin Q, and Lu W. Suitable extracellular oxidoreduction potential inhibit *rex* regulation and effect central carbon and energy metabolism in *Saccharopolyspora spinosa*. *Microb Cell Fact* 13: 98, 2014.

349. Zimmermann GR, Lehar J, and Keith CT. Multi-target therapeutics: when the whole is greater than the sum of the parts. *Drug Discov Today* 12: 34–42, 2007.

Address correspondence to:
Prof. Robert K. Poole
Department of Molecular Biology and Biotechnology
The University of Sheffield
Firth Court
Western Bank
Sheffield S10 2TN
United Kingdom

E-mail: r.poole@sheffield.ac.uk

Abbreviations Used

τ = time constant, reciprocal of rate constant
A = cytochrome *bd* species with ferrous-oxy haem *d*
ABC = ATP-binding cassette
ATP = adenosine triphosphate
AX = arylvinylpiperazine amide
BDQ = bedaquiline
CFZ = clofazimine
CIO = cyanide-insensitive oxidase
CO = carbon monoxide
CORM = CO-releasing molecule
CRP = cAMP receptor protein
Cryo-EM = single-particle cryoelectron microscopy
DNA = deoxyribonucleic acid
EET = extracellular electron transfer
F = cytochrome *bd* species with ferryl haem *d*
FNR = ''fumarate nitrate reduction'' regulator
GSH = glutathione (L-γ-glutamylcysteinylglycine)
H_2O = water
H_2O_2 = hydrogen peroxide
H_2S = hydrogen sulfide
hCAP-18 = human cationic antimicrobial protein
Hmp = flavohemoglobin
IC_{50} = the half maximal inhibitory concentration

INH = isoniazid
IPA = imidazopyridine amide
K_d = dissociation constant
K_m = Michaelis/Menten constant
k_{off} = dissociation rate constant
k_{on} = binding rate constant
LPZ = lansoprazole
MccJ25 = microcin J25
MIC = minimum inhibition concentration
MLCT = metal-to-ligand charge transfer
MQ = menaquinone
MQH_2 = menaquinol
NADH = nicotinamide adenine dinucleotide (reduced form)
NO = nitric oxide
O = cytochrome *bd* species with ferric haem *d*
O_2 = dioxygen
$O_2^{\bullet-}$ = superoxide
$ONOO^-$ = peroxynitrite
P = cytochrome *bd* species with peroxy complex of haem *d*
PAB = phenoxyalkylbenzimidazole
PDB = Protein Data Bank
PMF = proton motive force
Q_1 = 2,3-dimethoxy-5-methyl-6-(3-methyl-2-butenyl)-1,4-benzoquinone
Q203 = telacebec
QH_2 = quinol
R = cytochrome *bd* species with ferrous uncomplexed haem *d*
RMSD = root mean square deviation
RNA = ribonucleic acid
RNAP = RNA polymerase
RNS = reactive nitrogen species
ROS = reactive oxygen species
TB47 = pyrazolo[1,5-*a*]pyridine-3-carboxamide
UPEC = uropathogenic *Escherichia coli*
UQ8 = ubiquinone-8
UQH_2 = ubiquinol
V_{max} = maximum rate
WT = wild type